Faunal dynamics across the Silurian–Devonian positive isotope excursions (δ^{13}C, δ^{18}O) in Podolia, Ukraine: Comparative analysis of the Ireviken and Klonk events

GRZEGORZ RACKI, ANDRZEJ BALIŃSKI, RYSZARD WRONA, KRZYSZTOF MAŁKOWSKI, DANIEL DRYGANT, and HUBERT SZANIAWSKI

Racki, G., Baliński, A., Wrona, R., Małkowski, K., Drygant, D., and Szaniawski, H. 2012. Faunal dynamics across the Silurian–Devonian positive isotope excursions (δ^{13}C, δ^{18}O) in Podolia, Ukraine: Comparative analysis of the Ireviken and Klonk events. *Acta Palaeontologica Polonica* 57 (4): 795–832.

Two global isotopic events, the early Sheinwoodian (early Wenlock) and that at the Silurian–Devonian transition, have been comprehensively studied in representative carbonate successions at Kytayhorod and Dnistrove, respectively, in Podolia, Ukraine, to compare geochemistry and biotic changes related correspondingly to the Ireviken and Klonk events. These two large-scale isotope excursions reveal different regional ecosystem tendencies. The well-defined increasing trend across the Llandovery–Wenlock boundary in siliciclastic input, redox states and, supposedly, bioproductivity, was without strict correlative relations to the major ^{13}C enrichment event. The environmental and biotic evolution was forced by eustatic sea-level fluctuations and two-step climate change toward a glaciation episode, but strongly modified by regional epeirogeny movements due to location near the mobile Teisseyre-Törnquist Fault Zone. Thus, the global early Sheinwoodian biogeochemical perturbation was of minor depositional significance in this epeiric sea, as in many other Laurussian domains. Conversely, the Podolian sedimentary record of the Klonk Event exhibits temporal links to the abrupt δ^{13}C anomaly, overprinted by a tectonically driven deepening pulse in the crucial S–D boundary interval. This carbon cycling turnover was reflected in the regional carbonate crisis and cooling episodes, paired with a tendency towards eutrophication and recurrent oxygen deficiency, but also with major storms and possible upwelling. Faunal responses in both Podolian sections follow some characters of the Silurian pattern worldwide, as manifested by conodont changeover prior to the major early Sheinwoodian isotopic/climatic anomaly. This contrasts with the relative brachiopod and chitinozoan resistances in the course of the Ireviken Event. Also, during the Klonk Event, a moderate faunal turnover, both in benthic and pelagic groups, occurred only near the very beginning of the prolonged ^{13}C-enriched timespan across the system boundary, possibly due to progressive dysoxia and temperature drop. The characters point to a peculiarity of the Klonk Event by comparison with the Silurian global events, and some similarity already to the succeeding Devonian transgressive/anoxic episodes.

Key words: Brachiopoda, Conodonta, Chitinozoa, carbon isotopes, oxygen isotopes, geochemistry, faunal dynamics, Ireviken Event, Klonk Event, Silurian, Podolia.

Grzegorz Racki [grzegorz.racki@us.edu.pl], Institute of Palaeobiology, Polish Academy of Sciences, ul. Twarda 51/55, 00-818 Warszawa, Poland; present address: Faculty of Earth Sciences, University of Silesia, ul. Będzińska 60, 41-200 Sosnowiec, Poland;
Andrzej Baliński [balinski@twarda.pan.pl], Ryszard Wrona [wrona@twarda.pan.pl], Krzysztof Małkowski, and Hubert Szaniawski [szaniaw@twarda.pan.pl], Institute of Palaeobiology, Polish Academy of Sciences, ul. Twarda 51/55, 00-818 Warszawa, Poland;
Daniel Drygant [drygant@museum.lviv.net], State Museum of Natural History, National Academy of Sciences of Ukraine, Teatralna 18, Lviv 79008, Ukraine.

Introduction

In contrast to previous views, the Silurian Period has recently been shown as a short mid-Palaeozoic time slice characterized by recurring changes of the global ecosystem following recovery from the end-Ordovician extinction (Calner 2008). Surprisingly large-amplitude positive carbon and oxygen stable isotope anomalies (up to 10‰ in the late Ludlow; Fig. 1) were episodes of profound environmental change ("oceanic events"; Jeppsson 1990, 1998) manifested by distinctive fa-
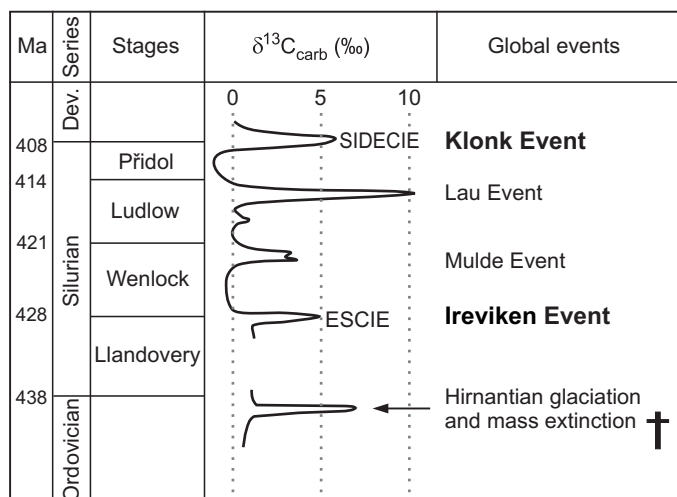
Fig. 1. Schematic compilation of positive δ¹³C excursions and global events in the Late Ordovician to Early Devonian interval (adapted from Stricanne et al. 2006: fig. 1; for more refined composite isotopic curve see Cramer et al. 2011a: fig. 3; for discussion of the Silurian timescale see Cramer et al. 2011b and Melchin et al. 2012). Abbreviations: Dev., Devonian; ESCIE, early Sheinwoodian carbon isotope excursion; SIDECIE, Silurian–Devonian carbon isotope excursion.

cies variation and associated stepwise extinctions both preceding plus coincident with the isotopic excursions (see summary in Munnecke et al. 2003, 2010; Calner 2008; and Melchin et al. 2012). Regular occurrences of teratological acritarchs record these high stress conditions (Munnecke et al. 2012). In general, pelagic communities were more strongly affected than shallow-water biota in the repeatedly pronounced oceanographic and climatic changes (see overviews in Kaljo et al. 1996; Jeppsson 1998; and Calner 2008; also e.g., Boucot 1990; Brett and Baird 1995; Porębska et al. 2004; Johnson 2006; Stricanne et al. 2006; Lehnert et al. 2007b, 2010; Loydell 2007; Eriksson et al. 2009; Nardin et al. 2011; Molloy and Simpson 2012; Manda et al. 2012; Noble et al. 2012). In fact, Silurian graptolites exhibit a very dynamic evolutionary history (Urbanek 1993; Štorch 1995; Sadler et al. 2011), contrary to the relatively stable Silurian reef biotas (Copper 2002b), and crinoid and brachiopod faunas (Talent et al. 1993; Kaljo et al. 1996; Ruban 2011). On the other hand, synchroneity of mass mortalities in graptolites, conodonts and, especially, the poorly known benthos is uncertain (e.g., Copper 2002b; Loydell 2007; Manda et al. 2012; Noble et al. 2012), and also separate terms have been proposed for the graptolite- and conodont-based crises (see Jeppsson 1990; 1998; Urbanek 1993; Štorch 1995; Kaljo et al. 1996). Conversely, some authors used terms coupling both biotic and geochemical aspects of global events (e.g., the Ireviken isotopic excursion; Cramer et al. 2011a; see also Buggisch and Joachimski 2006), even though the anomalously heavy δ¹³C values are roughly correlated with these medium-order biosphere perturbations (see Melchin et al. 2012: fig. 21.11).

Five distinct δ¹³C excursions have been identified in the "classical" Silurian to Lower Devonian low-latitude carbonate successions of Podolia, Ukraine (Azmy et al. 1998; Kaljo et al. 2007, 2012; Małkowski et al. 2009; Fig. 1). Biotic responses and ecological interactions are as yet poorly known from these key stratigraphical levels. Two of these biogeochemical perturbations, the early Sheinwoodian excursion (early Wenlock; ESCIE, cf. Lehnert et al. 2010) and the Silurian–Devonian passage excursion (SIDECIE = SIDE of Kaljo et al. 2012), approximately correlative with the major Ireviken (2nd order) and subordinate Klonk (5th order) biotic crises, respectively (see Kaljo et al. 1996; Jeppsson 1998), have been comprehensively studied by us in representative Podolian localities to compare geochemical and faunal trends in the epeiric domain. The goal is to present distributional and frequency patterns of benthic (brachiopods) and presumably pelagic (conodonts, chitinozoans) biota across these two δ¹³C anomalies, which are separated by a ca. 14 my interval (Melchin et al. 2012). The integrated event-stratigraphical analysis of biotic signals from very different ecologic groups, against stable isotope and inorganic geochemical proxies, provides an improved insight into concomitant ecosystem relationships in the rapidly evolving Silurian marine realm.

The responsibility of authors is as follows: GR and KM for geochemical data and interpretation; AB and RW for brachiopod and chitinozoan results, respectively; and DD and HS for regional and conodont aspects; the final discussion and conclusions are joint.

Institutional abbreviations.—ZPAL, Institute of Palaeobiology, Polish Academy of Sciences, Warszawa, Poland.

Other abbreviations.—ESCIE, early Sheinwoodian carbon isotope excursion; FAD, first appearance datum; GC–MS, Gas Chromatography–Mass Spectrometry; ICP, Inductively Coupled Plasma; S–D, Silurian–Devonian; SIDECIE, Silurian–Devonian carbon isotope excursion; SOIE, Sheinwoodian oxygen isotope excursion; TC, total carbon; TESZ, Trans-European Suture Zone; TIC, total inorganic carbon; TOC, total organic carbon; USGS, U.S. Geological Survey; V-PDB, Vienna-Pee Dee Belemnite Standard.

Geological setting

The extended middle Silurian to Lower Devonian marine succession of the Dniester Basin (Fig. 2) is considered as one of the most continuous successions of this age in the world, and have a long history of geological and palaeontological investigations (see Kozłowski 1929; Nikiforova et al. 1972; Tsegelnyuk et al. 1983; Koren et al. 1989; Uchman et al. 2004; Kaljo et al. 2007; Skompski et al. 2008; Małkowski et al. 2009; Krzemiński et al. 2010). The mostly carbonate deposits are well exposed in the escarpments of the Dniester valley and its tributaries, and form an internally conformable regressive unit with a total thickness of more than 900 m. The essentially undeformed Podolian sequence is strongly controlled by its location in the marginal belt of the East European Platform, near
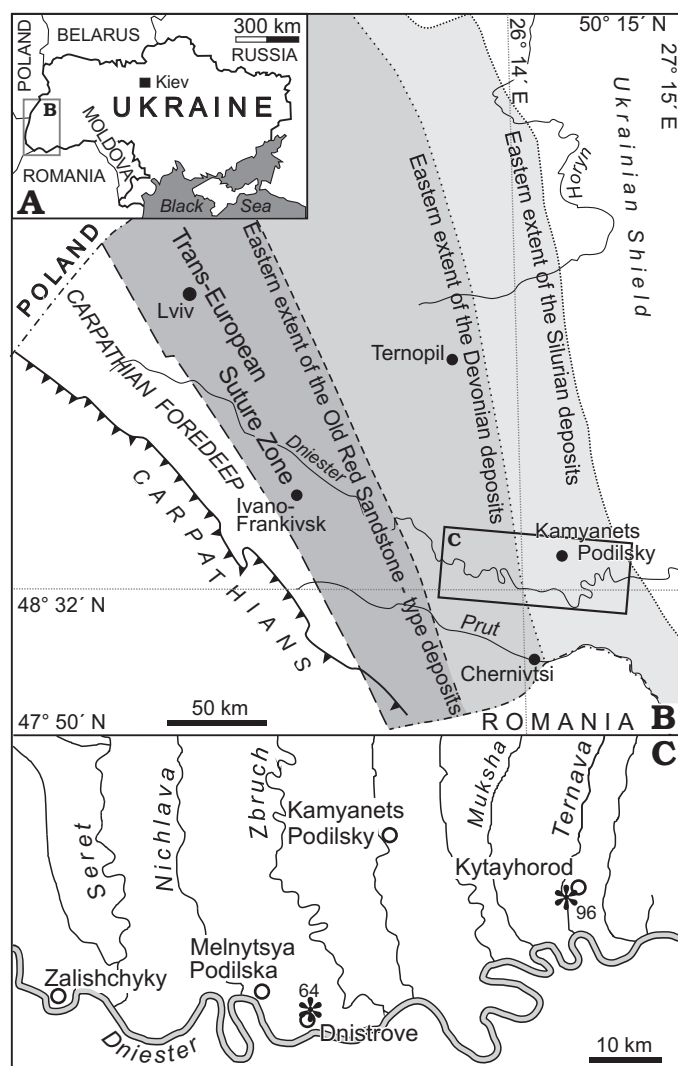
Fig. 2. **A**. General location of the study area in Ukraine. **B**. Distribution of the Silurian and Devonian deposits in Podolia, SW Ukraine, and geological setting of the study area. **C**. Location of two sampled outcrops (arrowed) in the vicinity of Dniester valley (modified from Małkowski et al. 2009: fig. 1). Section numbers after Nikiforova et al. (1972): Kytayhorod (96) and Dnistrove (64).

to the mobile Trans-European Suture Zone—the TESZ or Teisseyre-Törnquist Fault Zone (Fig. 2B; see Drygant 2000; Sliaupa et al. 2006; Krawczyk et al. 2008). The succession thickens toward the suture zone where the sedimentation rate was controlled by platform-margin faults and subsidence.

In the Silurian succession, which is more than 400 m thick, two depositional phases can be distinguished (Drygant 2003). The Wenlock and Ludlow phase of carbonate shelf sedimentation is characterized by numerous bioherms and biostromes (see Koren et al. 1989; Skompski et al. 2008; Łuczyński et al. 2009), and the Pridoli phase is characterized by rapid and differentiated sedimentation rates, especially in the vicinity of the platform margin. The Lower Devonian (Lochkovian) marine deposits, about 530 m thick, can be assigned to a third phase of continuous sedimentation (see Małkowski et al. 2009). The

phase is characterized by the flysch-like interbeds of limestone and shale with gradually increasing amounts of terrigenous material resulting for gradual regression and a simultaneous uniform but comparatively strong, subsidence regime (e.g., Uchman et al. 2004).

Facies evolution and analysed sections

The lower sampled interval (Fig. 3) includes open-shelf carbonate facies, very well naturally exposed in the Dniester River valley (Tarnava tributary) near the village of Kytayhorod (section no. 96 of Nikiforova et al. 1972; see Małkowski et al. 2009: fig. 3A; N48°32'16.9", E26°14'21.4"). The

Fig. 3. Stratigraphic scheme of the Silurian deposits of Podolia (after Nikiforova and Predtechensky 1968; Drygant 1984), and stratigraphic position of studied localities (see Fig. 2): Kytayhorod (96) and Dnistrove (64).
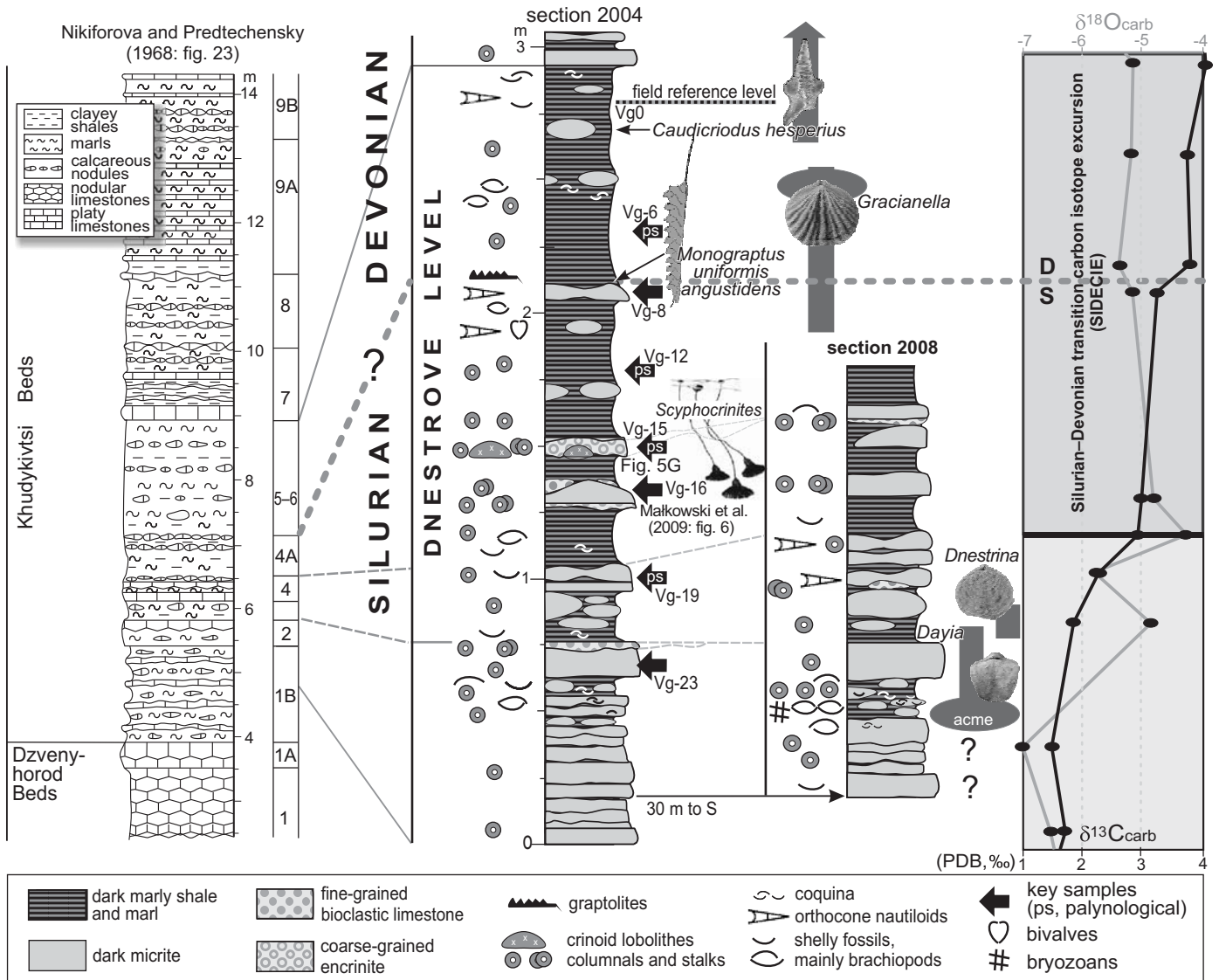
Fig. 4. Lithologic and faunal succession through the Silurian–Devonian boundary beds at Dnistrove in the early Klonk Event, with detail of newly proposed Dnistrove Level, against the secular pattern of δ^{13}C (black curve) and δ^{18}O (grey curve) values (after Małkowski and Racki 2009: table 2). Note that the system boundary is placed 0.7 m higher than the tentative positioning given in Małkowski et al. (2009: fig. 6). Onset of the carbon isotope anomaly (SIDECIE), first appearances of the index graptolite and conodont species are shown, as well as the key brachiopod distribution (Baliński 2012; see also Figs. 8, 19, 20), rapid lateral changes of crinoid accumulations, and selected samples.

late Llandovery to earliest Wenlock Restiv Beds (rhythmically alternating grey platy limestone and clayey shale beds) are succeeded in the section by Wenlock (Homerian) nodular limestone, with subordinate platy calcareous and clayey sets (Demshyn Beds). These fossiliferous strata pass upward into the more monotonous calcareous-nodular Maryanivka Beds. This succession has been studied in terms of its graptolite (Tsegelnyuk 1976; Tsegelnyuk et al. 1983) and conodont (Drygant 1984) zonation. Koren et al. (1989) claimed that the Llandovery–Wenlock boundary is located 2.2 m above the base of Restiv Beds, and is based on the first and only occurrence of *Cyrtograptus murchisoni* within the *Pterospathodus amorphognathoides* Conodont Zone (see Fig. 3 and below; compare the updated biostratigraphy in Cramer et al. 2010, 2011a; Kleffner and Barrick 2010; and Melchin et al. 2012).

The second succession studied is the partly trenched Dnistrove (former Volkovtsy, [64]; N48°38'19.1", E26°47' 18.6") section, which is a regional reference succession across the Silurian–Devonian (S–D) boundary, described in Małkowski et al. (2009; compare the Dnistrove-West locality in Kaljo et al. 2012). The Silurian sequence terminates with the Trubchyn (upper part of the former Rashkiv Beds) and Dzvenyhorod Beds of the upper part of the Skala Horizon (see Skompski et al. 2008: fig. 3). The strata are mostly calcareous, with dark, fossiliferous, nodular limestone predominating in the topmost interval. The S–D boundary is tentatively placed 3.2 m above this interval, in a succession of interbedded greenish-grey argillaceous shale and marl containing dark-grey limestone nodules. This unique, laterally differentiated and clay-enriched part of the lowermost Khudykivtsi Beds

(= units 3 to 6 of Nikiforova and Predtechenski 1968: fig. 23) is informally distinguished herein as "Dnistrove Level" (2.2 to 3.1 m thick; Fig. 4).

The boundary is based on the first and only occurrence of the index graptolite species *Monograptus uniformis angustidens* (Nikiforova et al. 1972; Nikiforova 1977), but some of the conodont species are also important. *Ozarkodina typica* and *Wurmiella excavata curvata* do not occur higher than 1.4 m below the boundary while *Parazieglerodina eosteinhornensis* disappears just below the boundary (Drygant and Szaniawski 2009). Forty cm below the S–D boundary *Zieglerodina remsheidensis* appears and 60 cm above the boundary is the first representative of the icriodonts, *Caudicriodus hesperius.* Mashkova (1971) reported first occurence of the icriodonts 1.5 m below the boundary but we can not confirm that. In the recently revised conodont zonation scheme, the Devonian system base is defined by first occurrence of *Caudicriodus hesperius* (= the bottom of "*hesperius* Zone" of Corradini and Corriga 2012 and "*hesperius–optima* Zone" of Slavík et al. 2012; see below). This system boundary can also be fixed by the first appearance of the chitinozoan index species *Eisenackitina bohemica*, and the last appearance datum of *Eisenackitina barrandei* and *Cingulochitina klonkensis*. These chitinozoan faunas provide potential for accurate correlation with the international stratotype at Klonk, Barrandian area, Czech Republic (Chlupač and Hladil 2000; Fatka et al. 2003; see also Wrona 1980; Nestor 1994; Paris et al. 2000).

The lower part of the Lochkovian Stage, the Khudykivtsi Beds of the Borshchiv Horizon (57 m thick), is developed in the form of marly limestone interbedded with shale. The higher fossil-rich, open-marine Lochkovian limestone and shale suite represents an uninterrupted continuation of the Silurian–Devonian deposition (Małkowski et al. 2009).

Material and methods

As stressed above, the two intervals selected for quantitative study are characterized by profound carbon and oxygen isotope anomalies (Fig. 1), against well constrained biostratigraphical and facies background information (see also Nikiforova et al. 1972; Kaljo et al. 2007, 2012). The present study utilized a variety of geochemical and quantitative ecological approaches.

Isotope geochemistry.—We comprehensively sampled the Kytayhorod succession (38.7 m thick) in 2008 and 2009, whereas the Dnistrove section had already been studied for stable isotopes, based on 28 samples from a 22.35 m thick interval by Małkowski et al. (2009). The samples were collected from fresh surfaces of marly and micritic limestone layers (see microfacies types in Fig. 5, based on 15 thin sections; for generalized mineralogy and petrography see Nikiforova et al. 1972 and Kaljo et al. 2007), with a stratigraphical spacing of decimetres to metres.

A total of 44 bulk-rock samples from Kytayhorod was analysed for carbon and oxygen stable isotopes in the Light Stable Isotopes Laboratory of the Institute of Geological Sciences and Institute of Palaeobiology, Polish Academy of Sciences, Warsaw (see SOM 1 in Supplementary Online Material available at http://app.pan.pl/SOM/app57-Racki_etal_SOM.pdf; and Małkowski et al. 2009). The carbonate powder for analysis was extracted with a microdrill and decomposed under vacuum in 100% H_3PO_4 (ortho-phosphoric acid) for 24 h at 25°C. Released CO_2, after freezing it out from the separation line, was analyzed on a Finnigan Mat delta plus gas mass-spectrometer. Every gas sample was introduced into the spectrometer in dual inlet mode and the measurement was repeated eight times, with the mean values treated as results. The standard error of the spectrometer measurements was 0.02‰. All carbon isotope values are reported in permil relative to V-PDB. The precision (reproducibility of replicate analyses) of both carbon and oxygen isotope analysis was usually better than ±0.1‰. Data are normalized to the V-PDB scale using National Bureau of Standards NBS-19 ($\delta^{18}O$ = -2.20‰ and $\delta^{13}C$ = 1.95‰).

In addition, 11 samples from Kytayhorod and 13 from Dnistrove (SOM 1 and 3) were studied for carbon isotopes in organic carbon in GeoZentrum Nordbayern, Erlangen, Germany. This analysis of organic matter was performed with an elemental analyser (Carlo-Erba 1110) connected online to a ThermoFinnigan Delta Plus mass-spectrometer. Accuracy and reproducibility of the analyses was checked by replicate analyses of international standards (USGS 40). Reproducibility was better than ±0.07‰.

Organic geochemistry.—Twelve samples from Kytayhorod and 16 from Dnistrove were measured for total carbon (TC) and total inorganic carbon (TIC) abundances at the Faculty of Earth Sciences, University of Silesia (SOM 1 and 3). TC and TIC contents were determined using an Eltra CS-500 IR-analyser with a TIC module. Total organic carbon (TOC) was calculated as the difference between total carbon and total inorganic carbon. Analytical precision and accuracy were better than ±2% for TC and ±3% for TIC. Four (from six) pilot samples from both sites (SOM 5) were sufficiently rich in extracted organic matter to be analysed by gas chromatography coupled with mass spectrometry (GC–MS) for biomarker characteristics at the Faculty of Earth Sciences, University of Silesia (for method details see Racka et al. 2010).

Inorganic bulk geochemistry.—Sixteen rock pulp samples from the Kytayhorod section and 27 samples from the Dnistrove outcrop (SOM 2 and 4); supplemented by extra 7 samples from Zalishchyky (upper Lochkovian Ivanie Beds; Małkowski et al. 2009; SOM 4), were analysed at the Acme Analytical Laboratories (Vancouver) Ltd, Canada. Total abundances of the major oxides and several minor elements were reported from a 0.2 g sample analysed by ICP-emission spectrometry following lithium metaborate/tetraborate fusion and dilute nitric digestion. Rare earth and refractory elements (e.g., Ba, Co, Sr, Th, U, V, Zr) were determined by ICP mass
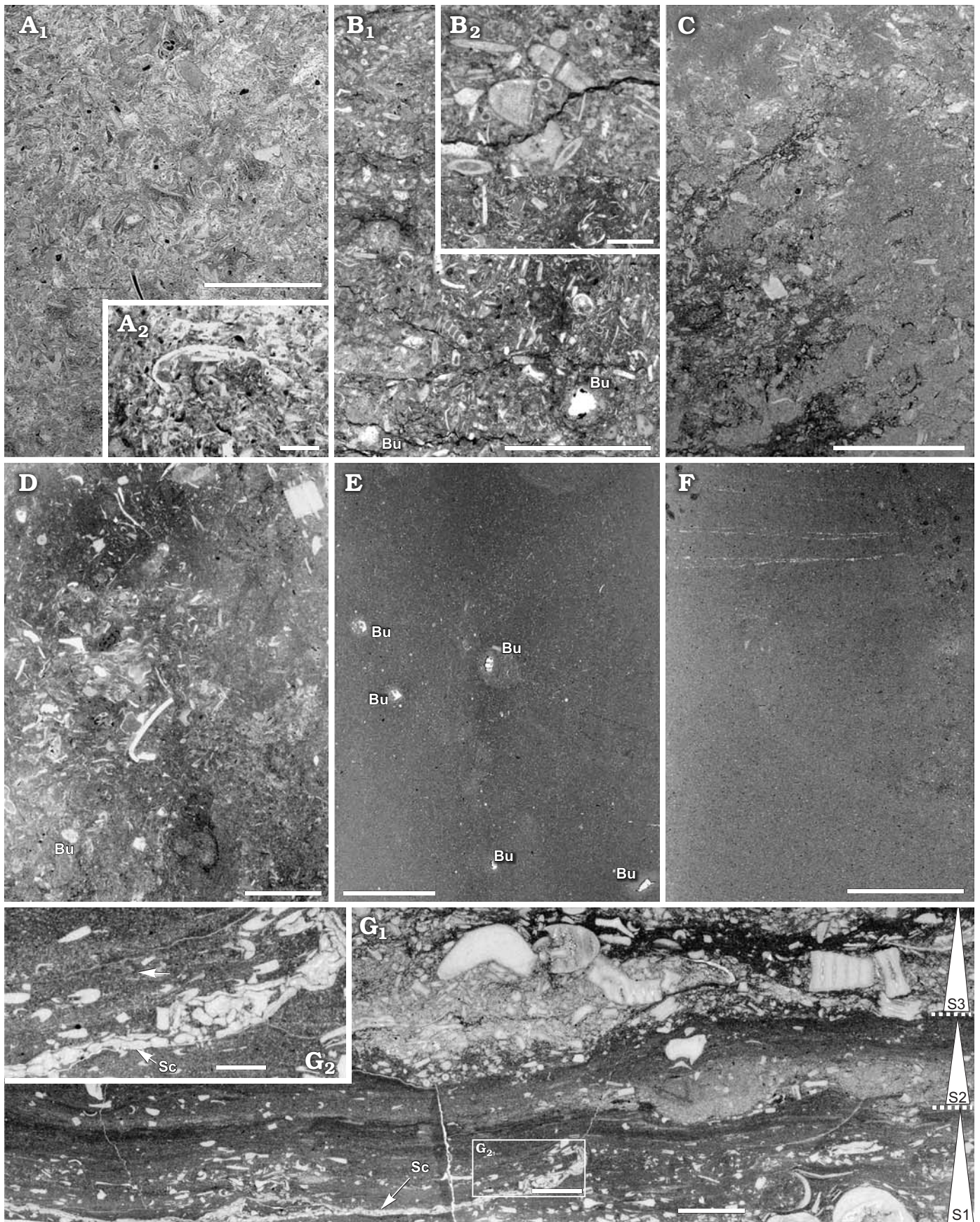
Table 1. Averaged, minimal and maximal Al/normalized concentrations of key elements in the Podolian sections under study against the average limestone and average shale Al/normalized abundance levels (based on Wedepohl 1971, 1991; Taylor and McLennan 1985), and averaged Al abundances (shaded).

Element	(Average limestone/Al) $\times 10^4$	(Average shale/Al) $\times 10^4$	(Average sample from Kytayhorod/Al) $\times 10^4$ [minimal value–maximal value]	(Average sample from Dnistrove/Al) $\times 10^4$ [minimal value–maximal value]
Ba	92.3	65	90 [45–303]	50 [33–165]
P	230.8	70	310 [20–790]	160 [59–413]
Mn	538.5	90	610 [160–50]	198 [47–469]
Zn	17.7	8.5	25.9 [5.8–170]	7.5* [4.6–19.4]
Pb	6.9	2	5.1 [1.8–13.4]	3.3 [0.6–30.8]
V	15.4	15	12.1 [7.7–17]	15.4** [10.6–23.3]
Cu	3.1	5	2.9 [0.5–10.1]	6.3 [2.4–15.6]
Co	1.5	2.3	2 [1.4–2.7]	2 [1.1–2.9]
Ni	11.5	5.5	5.2 [4.1–9.1]	5.2 [2.7–6.9]
Mo	0.3	0.1	0.26** [≥0.03–1.79]	0.1**[≥0.02–0.6]
U	1.6	0.3	0.8 [0.3–2.1]	0.8 [0.4–3.3]
Zr	14.6	21	29 [23.6–36.9]	26 [16.4–82.2]
Al (%)	1.3	10	2.2 [1.0–6.8]	2.6 [0.7–6.6]

* Excluding the abnormally enriched sample SD-27 (6543 ppm). **Approximated values based on maximal concentrations in the samples below the detection level.

spectrometry following the same decomposition method. A separate 0.5 g split was digested with 3 ml 2:2:2 HCl-HNO$_3$-H$_2$O and also analysed by ICP mass spectrometry for the precious and base metals (e.g., Mo, Cu, Pb, Zn, Ni, As, Cd). In addition, total carbon and sulphur analyses by Leco were supplied. The reliability of the results was examined by analyses of some international standard reference materials. Precision and accuracy of the results were better than ±0.9% (mostly ±0.4%) for the 11 major elements, and better than ±15% for the 45 trace elements, considered only in part in this study. When the concentrations of trace metals (especially Mo and Cr) were lower than the detection limits, the highest value below the suitable detection limit value was used in averaged abundance and proxy calculations (Table 1; SOM 2 and 4; see Racka et al. 2010 for further method details).

Palaeontological data.—Although various macrofossil groups are present, only the most abundant shelly component, brachiopods, has been quantitatively analyzed in frequency terms (ca. 1800 specimens). Nevertheless, occurrences of other groups were noted as well, and the distribution data have been compared with the faunal lists in Nikiforova and Predtechensky (1968), Nikiforova et al. (1972), and Koren et al. (1989).

Absolute and relative abundances have been estimated for two common acid-resistant microfossil groups in the both sections studied (SOM 6 and 7), derived from 33 samples for conodonts (17 from Kytayhorod and 16 from Dnistrove,) and 47 samples for chitinozoans (18 from Kytayhorod and 29 from Dnistrove; SOM 5). Conodonts were extracted by acetic acid digestion from mostly ca. 500–1000 grams of limestone, whilst about 100–150 grams of each sample were processed for chitinozoans. The samples for chitinozoans were processed using a standard palynological HCl-HF acids technique (see Miller 1996). The residues were sieved using 50 µm screens, but the relatively large amount of resistant residues obtained from the clay- and silt-rich marly samples was reduced about ten times for examination of chitinozoans.

Diversity indices were calculated utilizing a software package for paleontological data analysis PAST Version 1.94b (Hammer et al. 2001). The following statistics are presented (see also Hints et al. 2006):
– Frequency (absolute abundance): the number of specimens (n) per gram or kilogram of rock.
– Taxic diversity (S): the number of species or genera in a sample.
– Margalef's richness index: (S-1)/ln(n), where S is the total

← Fig. 5. Variety of microfacies from the Silurian to Lowermost Devonian of Podolia: bioturbated skeletal packstone to grainstone (**A**), bioturbated skeletal packstone (**B, C**), bioturbated skeletal wackestone to packstone (**D**), burrowed (**E**) to slightly bioturbated mudstone (**F**), and partly amalgamated crinoid packstone in three bioclastic, allegedly storm-generated intercalations (S1–S3), graded into non-fossiliferous shale (**G**; see also Małkowski et al. 2009: fig. 6). Demshyn (SD-36, D) and Maryanivka Beds at Kytayhorod (SD-50, A; SD-45, B); Dzvenyhorod Beds (SD-21, C), and lower (Vg-15, Dnistrove Level, G; see also Fig. 4) and upper (SD-20, E; SD-3, F) Khudykivtsi Beds at Dnistrove. Differently disarticulated and fragmented skeletal constituents dominated by shelly faunas (brachiopods; molluscs, see bivalve valve on A$_2$) and echinoderms (crinoids; rare echinoids), associated with frequent ostracods (A$_1$), dasycladacean algae (B$_1$; close-up in B$_2$) and trilobites. Note stylo-nodular fabric (C, lower left part), differently preserved burrows (Bu), partly with pellets (E), dispersed fine euhedral pyrite in micrite matrix (C–F), as well as *Scyphocrinites* lobolith arrowed in G$_1$ (close-up in G$_2$). Scale bars 5 mm except A$_1$, B$_1$ and G$_1$ 1 mm.

number of taxa, and $\ln(n)$ is the natural logarithm of the to-
tal number of the individuals n.

– Equitability: $-\text{sum}((n_i/n)\ln(n_i/n))/\ln S$, where n_i is number
of individuals of taxon i, and n is the total number of the in-
dividuals.

– Dominance: $\text{sum}((n_i/n)^2)$, where n_i is number of individu-
als of taxon i, and n is the total number of the individuals.

Geochemical evaluation of environmental factors

As reviewed by Cramer and Saltzman (2005, 2007b), Brand et
al. (2006), Loydell (2007), Calner (2008), Vecoli et al. (2009),
Munnecke et al. (2003, 2010), Kaljo et al. (2012) and Koz-
łowski and Sobień (2012), different scenarios have been postu-
lated to explain the Silurian worldwide $\delta^{13}C$ and $\delta^{18}O$ positive
anomalies. Saltzman (2005) indicated that so striking $\delta^{13}C$ vol-
atility was sustained by positive feedback between oxygen de-
ficiency and bioproductivity in the usually P-limited and
cooler-water Silurian oceans. Thus, one popular explanation
invokes elevated primary productivity and/or the increased
burial rate of organic matter, visible especially in black shale
deposition. The Silurian excursions, however, are usually not
synchronous with widespread black shale levels (with excep-
tion of the Middle Silurian Mulde Event, Calner 2008; in some
regions, also of the ESCIE and SIDECIE, Lüning et al. 2000;
Buggisch and Joachimski 2006; Loydell and Frýda 2007;
Vecoli et al. 2009; Noble et al. 2012). Therefore, following
"a weathering hypothesis" of Kump et al. (1999) for the Hir-
nantian glaciation as a trigger for the large-scale ecosystem ca-
tastrophe, enhanced weathering of exposed Silurian carbonate
terrains in a regressive episode has been postulated as well
(e.g., Loydell 2007; Noble et al. 2012). Eventually these led to
a drop in atmospheric pCO_2 and cooling (anti-greenhouse ef-
fect; e.g., Wenzel and Joachimski 1996; Kump and Arthur
1999; Małkowski and Racki 2009), as confirmed by reliable
oxygen isotope paleothermometry based on conodont apatite
data (Joachimski et al. 2009; Lehnert et al. 2010). In this study,
because no data in Podolian successions for substantial
changes in redox regimes, organic matter composition and
thermal overprint (see discussion in Cramer and Saltzman
2007a), the paired inorganic and organic carbon isotope curves
are used to estimate $\Delta^{13}C$ (= $\delta^{13}C_{carb} - \delta^{13}C_{org}$), to roughly track
changes in atmospheric pCO_2 (Kump and Arthur 1999).

The severe drop in primary productivity and plankton star-
vation has been considered as a main cause of the trophic web
instability and subsequent biotic crises (Jeppsson 1990, 1997,
2005; see also Porębska et al. 2004; Cramer and Saltzman
2007a). During the Ireviken Event, however, phytoplankton
data reveal most of the acritarch losses at the final of the biotic
overturn, without links to conodont demise steps (Gelsthorpe
2004). This timing of primary production collapse in the
Gotland succession, however, is questionable according to
Lehnert et al. (2010) because of major facies change. On

the other hand, the phytoplankton abundances analysed by
Stricanne et al. (2006) indicate, at least for the major Lau
(= Kozlowskii) Event, decreased bio-productivities during the
isotope excursion peak (see Noble et al. 2012) or perturbations
in nutrient composition and availability (Kozłowski and So-
bień 2012). If so, the large-scale ^{12}C sequestration may rather
be attributed to black shale deposition in restricted oceanic
and/or epeiric regions (e.g., Wenzel and Joachimski 1996;
Cramer and Saltzman 2005, 2007a, b), as exemplified by
northern Gondwanan hot shales since from Rhuddanian to
early Wenlock times (Lüning et al. 2000, Vecoli et al. 2009).
Advection of ^{13}C-enriched near-surface waters in stratified
ocean, attributed to onset of an antiestuarine shelf circulation
in more arid climate states, is an alternative hypothesis (e.g.,
Bickert et al. 1997; Munnecke et al. 2003; Jeppson 2005). In
fact, the recurring graptolite mass mortalities are seen as trig-
gered by regressive pulses and "oxic events" paired with vig-
orous thermohaline circulation and retreat of black shale or-
ganic-rich facies (e.g., Štorch 1995; Wenzel and Joachimski
1996; Porębska 2005; Johnson 2006). The most hospitable
graptolite habitats may have been located near the boundary
zone between oxic and denitrified, anoxic waters (= anoxi-
tropic niche sensu Berry et al. 1989).

These conjectural oligotrophic vs. eutrophic photic zone
conditions may potentially be tested by combined use of
several assumed palaeoproductivity proxies: organic matter
abundance (TOC) combined with inorganic tracers (P, Ba, and
Si; e.g., Pujol et al. 2006; Tribovillard et al. 2006; Calvert and
Pedersen 2007; Jenkyns 2010). As a micronutrient proxy the
authigenic fraction of Ni, Zn and Cu is also considered here, as
it is associated mostly with organic carbon (e.g., Brumsack
2006; Tribovillard et al. 2006; Śliwiński et al. 2012). Extreme
enrichment in some elements (particularly Zn, Cu, Sr, and Ba)
requires an additional external source, such as hydrothermal
activity (see Brumsack 2006; Tribovillard et al. 2006; Pujol et
al. 2006). Limited to a single sample (one-point) overabun-
dances, exemplified by the distinctive sulphide-enriched sam-
ple SD-27 from Dnistrove (S—0.38%, Zn—6543 ppm, Cd—
20 ppm; SOM 4), may suggest an episodic hydrothermal wa-
ter influxes to the Podolian sedimentary basin, or rather indi-
cate an imprint of post-depositional diagenetic and/or mineral-
izing magmatic-hydrothermal fluid signature (see Pujol et al.
2006; Tribovillard et al. 2006; Sindern et al. 2008). However,
the studied samples display typically depleted Al-normalized
abundances, and in infrequent cases only are distinctly higher
relative to the average limestone (e.g., Zr and Cu at Dnestrove,
see Table 1).

On the other hand, bottom-water oxygenation depletion
is tracked by increased abundances of redox-sensitive (e.g.,
Mo, U, V, As, Cr,) and/or sulphide-forming trace metals
(e.g., Co, Cu, Ni, Pb, Zn; see Brumsack 2006; Tribovillard et
al. 2006; Calvert and Pedersen 2007; Schröder and Grot-
zinger 2007; Ver Straeten et al. 2011; Śliwiński et al. 2012).
However, frequently used redox indices often suggest con-
tradictory conclusions (see e.g., Racka et al. 2010). Even if
Mo and U contents are mostly low (Table 1), the combined

use of Mo/Al and U/Th ratios appears to be the most useful to suggest oxygen-deficient conditions in the Podolian successions. Considering other markers, the time series of V/V+Ni ratio consistently imply far more extensive hypoxia, whereas the Ni/Co ratio variations manifest only oxic regimes in the both sections.

Al is well known as the key lithogenous compositional (i.e., aluminosilicate) standard, and dilution effects by carbonate and quartz were reduced by use of the element/Al ratios as weight-ratios (e.g., Sageman et al. 2003; Pujol et al. 2006; Calvert and Pedersen 2007; Sindern et al. 2008; Ver Straeten et al. 2011). Furthermore, if (i) the non-normalized element concentrations are at the best close to the average limestone contents, and paired with (ii) a good correlation between the element vs Al, this abundance cannot be considered as an environmental proxy; these two characters indicate clearly its dominance by terrigenous provenance and scarcity of the authigenic fraction (Tribovillard et al. 2006; Śliwiński et al. 2012; see Table 1 and examples below). For example, only Al-normalized phosphorus concentrations are more commonly useful in the bioproductivity context in Podolian samples (see below).

The total lithogenous fraction content, as an approximation of the siliciclastic input, is mirrored by Al concentration, whilst aeolian delivery to the outer-shelf Podolian basin can be detected using elemental indicators for sediment grain-size, such as Si/Al, Ti/Al, and Zr/Al ratios (Calvert and Pedersen 2007; Schröder and Grotzinger 2007; Ver Straeten et al. 2011). The applicability of quartz to aluminosilicate (clay) phase ratio is justified by the absence of biogenous silica in Podolian sites. For example, the larger average grain-size is tracked by elevated Zr/Al and Si/Al ratios, recording a proportionally increased content of zircon and quartz grains, respectively. Ver Straeten et al. (2011) designated a Si/Al ratio above 5 as a tracer for sand-dominated clastic supply. Wind-blown dust may also be compositionally influenced by volcanic input, reflected by high Zr abundance levels in fine-grained volcaniclastic admixture (e.g., Pujol et al. 2006), up to 260 ppm in Silurian ash levels of Podolia (Huff et al. 2000: table 1). Elsewhere, Kiipli et al. (2010) have interpreted Silurian sea level variations in a deep-shelf Latvian section by combined SiO_2/Al_2O_3 and K_2O/Al_2O_3 ratios, reflecting the contribution of quartz, and muscovite and K-feldspar, respectively, in siliciclastic material (see also Sageman et al. 2003; Sindern et al. 2008).

Geochemical trends across the Ireviken Event

The Kytayhorod succession is characterized by rather monotonous grey carbonate-marly lithologies evolving from planar bedded, rhythmic to unbedded, nodular varieties (Fig. 6A; for microfacies see Figs. 5A, B, D and 11; see also Nikiforova et al. 1972: figs. 31, 32, and 126). Calcium car-

bonate content (calculated from CaO) is mostly above 70%, with notable exceptions in the lower part, where this abundance drops to 20.8%. The Restiv Beds are distinguished by very high SiO_2 abundance in several layers, above 47% in the basal SD-42 sample, and Al_2O_3 content above 12% (Fig. 7; compare the basal transgressive sandy set of Nikiforova et al. 1972: 36, 132). In most samples, however, the quartz contribution is negligible (SiO_2 ranges between 9 and 17%), as also is that of the clay minerals (Al_2O_3 between 2 and 4%). Dolomitisation remains minor in the succession as MgO content is largely below 1.7%.

Carbon and oxygen isotopes.—As noted by Kaljo et al. (2007), the distinctive $\delta^{13}C_{carb}$ increase of 2.6‰ in the Kytayhorod section begins in the Restiv Beds, and reaches its peak value of 4.0‰ at the very base of the early Sheinwoodian Demshyn Beds. The isotopic highstand (slice E-2; Fig. 6A) is followed by stable but negative $\delta^{13}C$ values up to -0.9‰ in the upper parts (see coeval brachiopod calcite results in Azmy et al. 1998).

Our and Kaljo et al. (2007: fig. 4) $\delta^{13}C$ time series agree with the worldwide chemostratigraphical pattern in the Llandovery–Wenlock transition (e.g., Brand et al. 2006; Cramer et al. 2010; Noble et al. 2012), especially with Estonian $\delta^{13}C$ profiles, marked by an obscured slice of transient value decline (isotopic feature 2 of Cramer et al. 2010). The early Sheinwoodian excursion (ESCIE) amplitude approaches 4.5‰ if a -0.5% regional $\delta^{13}C_{carb}$ baseline is used (guided by E-4 interval; Fig. 6A). In addition, the C-isotopic event is clearly coupled with a positive $\delta^{18}O_{carb}$ excursion, evident also in the values in table 3 of Kaljo et al. (2007), but neglected by these authors as a probable diagenetic artifact in whole-rock carbonate samples (see also e.g., Martma et al. 2005). Their overall primary character is demonstrated, however, by comparable brachiopod calcite values from this site in Azmy et al. (1998; see also Wenzel and Joachimski 1996, Bickert et al. 1997, Heath et al. 1998; Munnecke et al. 2003; Cramer and Saltzman 2005; Brand et al. 2006) and, especially by a similar reliable chemostratigraphical $\delta^{18}O$ pattern (i.e., the SOIE excursion; see below) recognized in conodont apatites by Lehnert et al. (2010, see also discussion on the S–D transition signature in Małkowski et al. 2009). The $\delta^{18}O_{carb}$ shift begins with values between -5.2 to -6.2‰, increases up to -3.9‰ in the plateau interval of high $\delta^{13}C$ values, and very gradually diminishes by ca. 2‰ in the Maryanivka Beds (background E-4 interval; Fig. 5A).

The $\delta^{13}C_{carb}$ excursion is partly reflected also in the organic carbon data (based on few samples), but marked probably by a distinctly lower amplitude. The Podolian record of the ESCIE is associated in addition with an irregular $\Delta^{13}C$ rise by ca. 2‰; this highest value corresponds with the uppermost sample from the crucial E-2 slice (Fig. 7A).

Inorganic bulk geochemistry.—The detrital admixture exhibits two slightly fluctuating (particularly in the lowest interval;), but contrasting secular tendencies: (i) decreasing clay abundance tied with (ii) increased coarser clastic input indi-
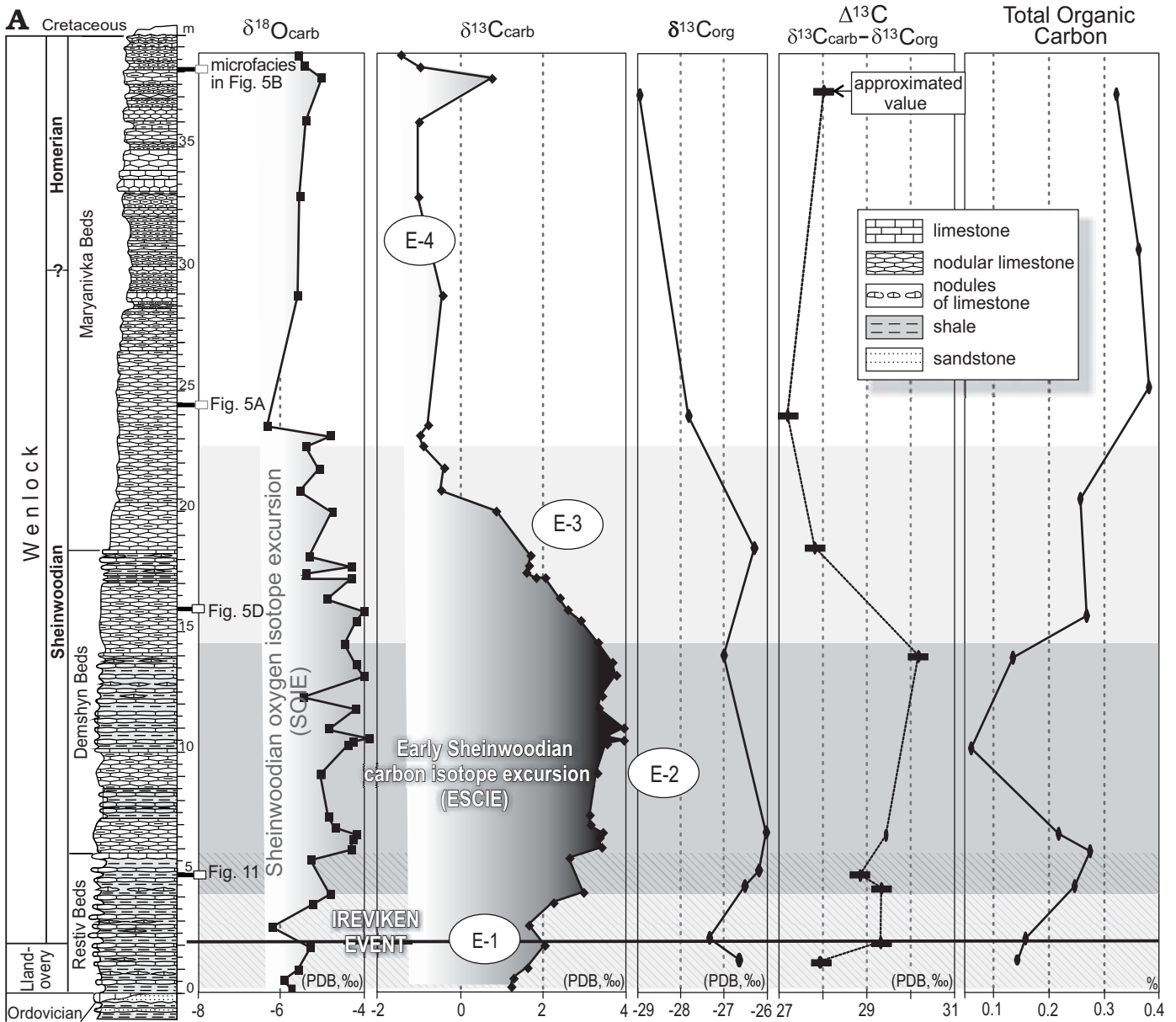
Fig. 6. **A**. Secular trends of $\delta^{13}C$ and $\delta^{18}O$ values in carbonate and organic matter, $\Delta^{13}C$ and total organic carbon from section 96 near Kytayhorod village (see SOM 1). Lithology after Nikiforova et al. (1972: fig. 82), modified. Three slices E-1 to E-3 (marked by shades of grey) denote of the early Shein-woodian (ESCIE) carbon isotope excursion: the interval E-2 corresponds to the isotopic highstand (see a widened excursion definition in Cramer et al. 2010, also Sadler 2012); E-1 and E-3 to the increasing and decreasing curve segments, respectively, and E-4 to the regional background. Note that the Ireviken bi-otic event (crossed band) correlates with the initial positive $\delta^{13}C$ shift slice (E-1); the lower event boundary corresponds the last occurrence of conodont *Pseudooneotodus tricornis*, and the upper boundary is questionably placed above the disappearance of chitinozoan *Eisenackitina* cf. *dolioliformis* (Figs. 15, 16; see Jeppsson 1997; Nestor et al. 2002;). Approximated $\Delta^{13}C$ levels are calculated for $\delta^{13}C_{carb}$ values averaged for two stratigraphically adjacent samples, as shown also by a dotted line of the curve. The microfacies illustrated are marked as rectangles. **B**. General view of the natural outcrop in the Dniester River valley (Tarnawa tributary) near Kytayhorod village; arrow indicates the main sampled site.
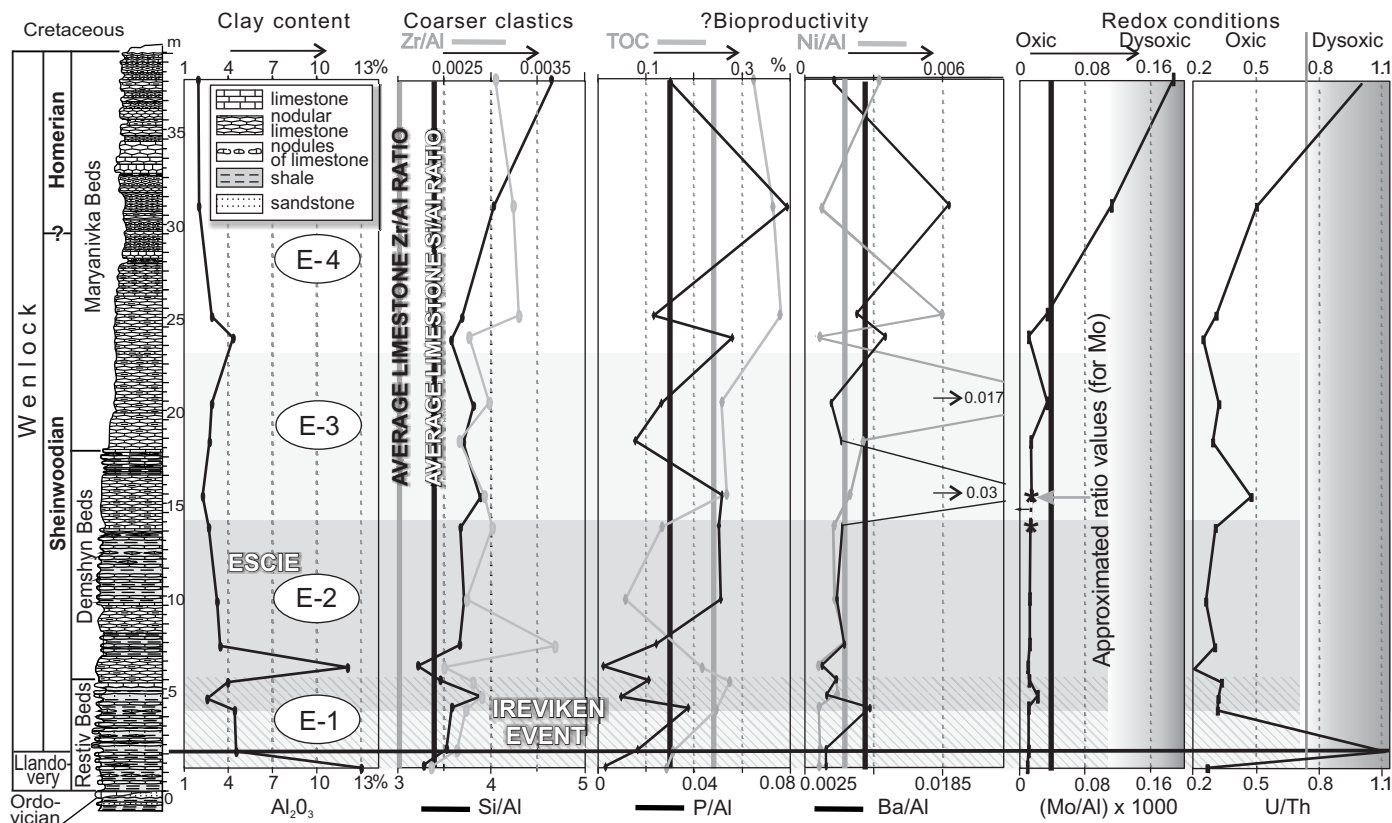
Fig. 7. Stratigraphical distribution of the Al-normalized abundance for selected major and trace elements as well as Al_2O_3 and TOC contents (wt. %) and the U/Th ratio (for redox thresholds see Racka et al. 2010) from the Kytayhorod section (see SOM 2). Thicker vertical lines indicate level of the ratios for average limestone after Wedepohl (1971, 1991). Approximated proxy values, resulted from the content of Mo below the detection levels, are asterisked. Shades of gray denote three slices of the ESCIE.

cated by abruptly increasing Zr/Al and Si/Al ratios, correlated also with the K/Al proxy trend (Fig. 7). Heightened Zr/Al levels are suggestive of some volcaniclastic material in the peak values, even though definite bentonites occur only higher in the Silurian succession of Podolia (Huff et al. 2000).

All presumed bioproductivity tracers show in detail largely dissimilar temporal changes, and are also somewhat questionable because the crucial elements are usually very weakly correlated both with Al and TOC: r = -0.33 and -0.12 for P, respectively, as well as r = 0.12 and -0.52 for Ba, r = 0.99 and -0.24 for Ni, and r = -0.06 and 0.36 for Zn. Thus, their authigenic character is suspected (or organic matter has been differently degraded in the sediments). However, the proxy data analysed collectively exhibit the congruent major increasing-upward trend.

Declining bottom water oxygenation towards at least dysoxic conditions, after the ESCIE (see below), is clearly evidenced by several indices (U/Th, Ni/Co). Normalized Mo contents reveal the most evident chemostratigraphical trend: the long lasting stable low levels are followed by a rapid forty-fold increase during the E-4 timespan (Fig. 7). This tracer is the most reliable as it is unrelated to aluminosilicate phases (r= -0.24 with Al; but r = 0.56 with TOC), by contrast with indices based on V contents (r = 0.97 with Al; but r = -0.41 with TOC). The very high U/Th ratio in transgressive

graptolite-bearing horizon of the Restiv Beds (see below) is known from the one sample only, and contrasts with low Mo/Al and most other redox proxy values. This suggests its link rather to a post-depositional enrichment, even if a higher-resolution sampling is requested.

Geochemical trends across the Klonk Event

Lithofacies variation across the Klonk Event is significant in the Dnistrove section because dark shale set with bioclastic limestone partings (Dnistrove Level; Fig. 4) occurs in the lowermost part of the Khudykivtsi Member, spanning the S–D boundary (Fig. 8). Carbonate content decreased to 22% in the Dnistrove Level (it is largely between 60% and 85%), and this is coupled with SiO_2 values above 45%, and Al_2O_3 concentrations above 12% (Fig. 9). Otherwise, the marly-micritic lithologies (see Fig. 5C, E, F; Nikiforova et al. 1972: figs. 83, 84, and 141) are enriched overall in terrigenous material, as evidenced by irregularly fluctuating Al and Si contents, varying from 1.3% to 5.4% and 6.2% to 20.7%, respectively. Dolomitization is relatively unimportant at this site even where MgO content is as high as 5.3% as this is notably linked with aluminosilicates (r = 0.82 with Al).
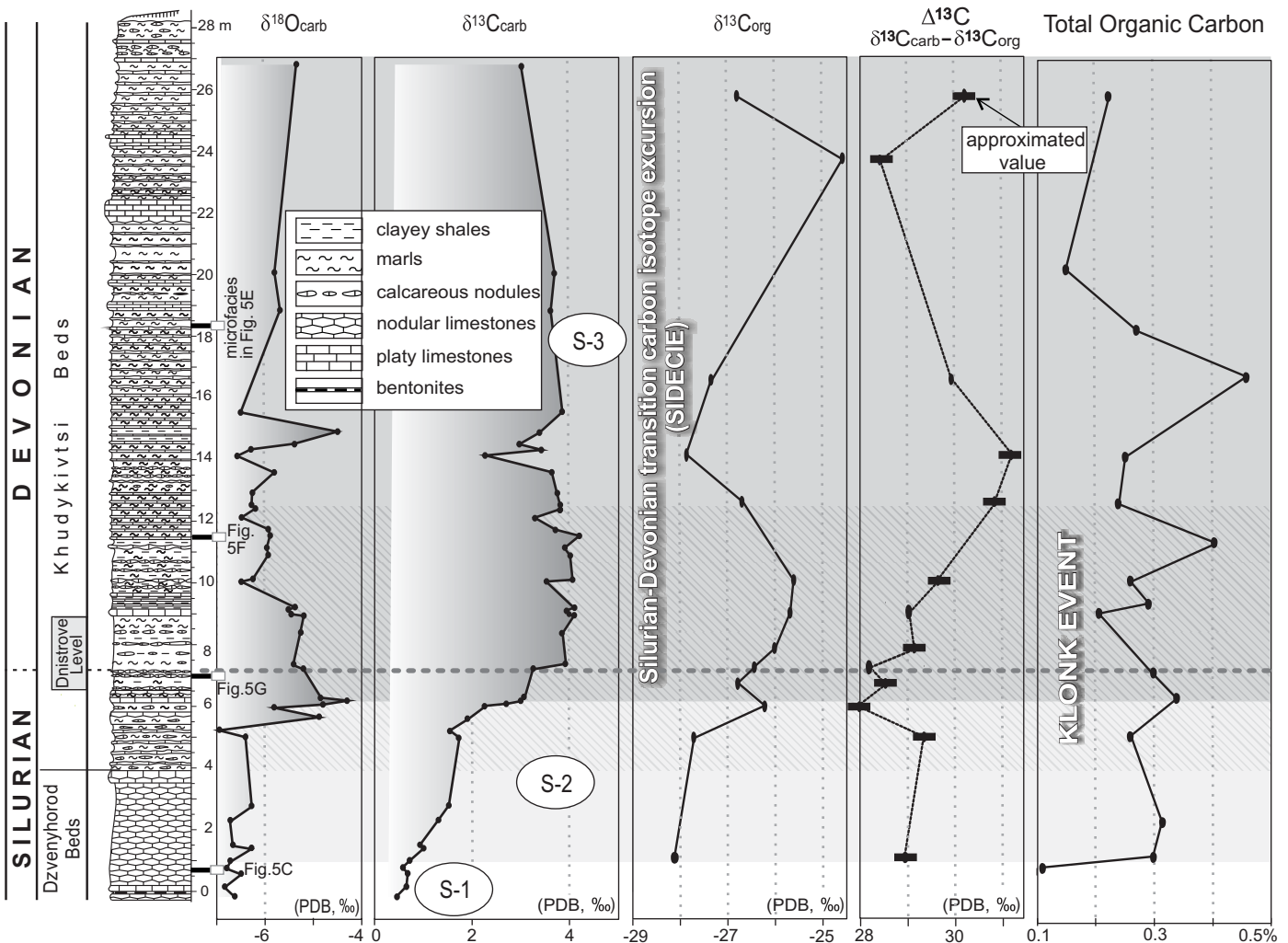
Fig. 8. Secular trends of $\delta^{13}C$ and $\delta^{18}O$ values in carbonate and organic matter, $\Delta^{13}C$ and total organic carbon from section 64 near Dnistrove village (see SOM 3). Two slices S-1 to S-3 (marked by shades of grey) denote of the Silurian–Devonian transition carbon isotope excursion (SIDECIE): the interval S-3 corresponds to the isotopic highstand; S-2 to the increasing curve segment, and S-1 to the regional background. Lithology after Nikiforova et al. (1972: fig. 82), modified. Note that the Klonk biotic event (crossed band) is associated roughly with the final positive shift (S-2) and initial highstand (S-3) $\delta^{13}C$ curve slices; its lower event boundary corresponds to a collapse of carbonate production and chitinozoan crisis near the base of Dnistrove Level, and the upper boundary is questionably placed below an acme level of brachiopod and conodont faunas (see Figs. 4 and 23).

Carbon and oxygen isotopes.—The abrupt and coeval increase of $\delta^{13}C_{carb}$ and $\delta^{18}O_{carb}$ values is thoroughly described by Małkowski et al. (2009; see also Kaljo et al. 2012). The $\delta^{13}C_{carb}$ excursion, with the highest value of 3.8‰ and 4.5‰, is confirmed also in nearby outcrop at Dzvenyhorod and drill core section in the Ternopil area, respectively (Kaljo et al. 2012; see Fig. 2B). The lower part of the S–D excursion (SIDECIE) is recorded in the $\delta^{13}C_{carb}$ data with an amplitude of ca. 4‰ in in the Dnistrove succession (and above 5‰ when considering all the Podolian data).

This trend may be now roughly correlated with a parallel shift in the $\delta^{13}C_{org}$ levels by 3.5‰ (Fig. 8), but this is notably reversed higher in the succession. Thus, more high-resolution data are necessary to constrain this co-variation discrepancy, as well as more irregular $\Delta^{13}C$ secular changes, marked by a distinct increase coeval with the three-point $\delta^{13}C_{org}$

lowstand. The $\Delta^{13}C$ curve instability notably contrasts with a long-lasting isotopic plateau seen in the $\delta^{13}C_{carb}$ values.

Inorganic bulk geochemistry.—As at Kytayhorod, the terrigenous component reveals two somewhat opposing first-order trends. Clay abundance is distinctly lower in the upper half of the section, whilst the grain-size and possible volcaniclastic admixture abruptly increases up to sand fraction in the uppermost part, as recorded in the very high Zr/Al and Si/Al ratios (Fig. 9).

Considering proxies of bioproductivity, similar serious reservations can be expressed as for the Kytayhorod samples. Irregular secular variations suggest pulses of enhanced fertilization/primary production, but recorded largely in the lower part of the succession, including the Dnistrove Level, and conspicuously absent in its middle part. The pattern is certainly partly biased by the dominantly detrital provenance
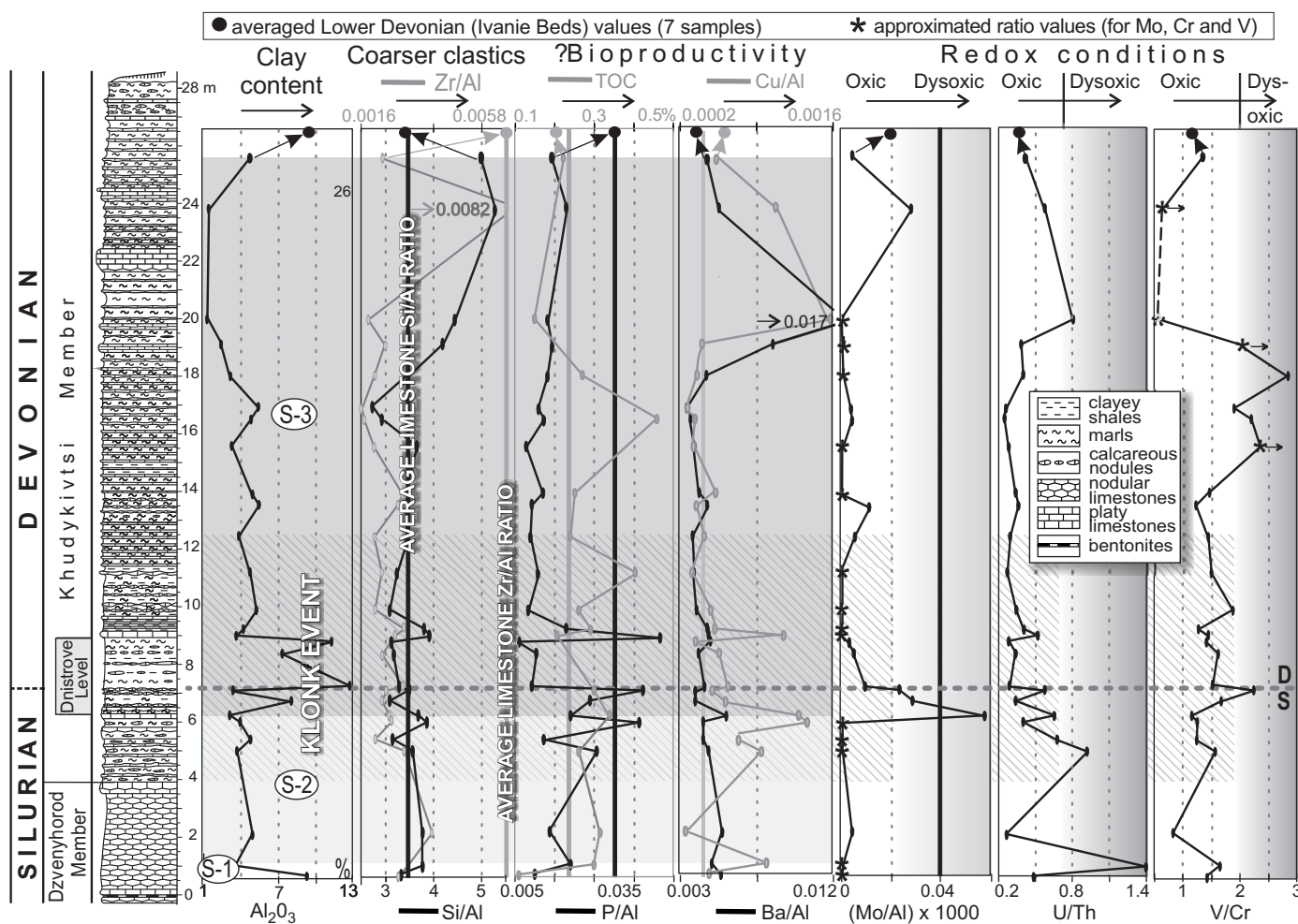
Fig. 9. Stratigraphic distribution of the Al-normalized abundance for selected major and trace elements as well as Al_2O_3 and TOC contents (wt.%) and the U/Th and V/Cr ratios from the Dnistrove section (see SOM 4). Approximated proxy values, resulted from the Mo, V, and Cr content below the detection levels, are asterisked. Averaged data for the higher Lower Devonian strata from Zalishchyky (Ivanie Beds; Małkowski et al. 2009; Fig. 2; see SOM 4) are also shown. Shades of gray denote two slices of the SIDECIE.

of the elements analysed, visible in the adverse relationships between aluminosilicates and organic carbon even for the most trustworthy tracers P (r = 0.39 and -0.10, respectively) and Cu (r = 0.65 and -0.42).

Clearest data are again provided by collective use of redox indicators, because the steady oxic regimes are evidenced exclusively in the middle part of section, just above the S–D boundary, and, at most, dysoxic regimes may be suggested for the remaining SIDECIE portions, marked by fossil-poor, variably bioturbated muddy lithofacies (Fig. 5E, F). Mo is once more predominantly present as an authigenic phase, and therefore the most certain proxy in light of the insignificant correlation with Al, and also with TOC (r = 0.31 and 0.25, respectively).

Organic geochemistry

Organic carbon abundances are invariably low in both sections, as shown by TOC values ranging from 0.06 to 0.38% at Kytayhorod and from 0.11 to 0.46% at Dnistrove (SOM 1 and 3). The organic matter is rather erratically distributed in the latter succession, and an exact association occurs neither with the major $\delta^{13}C_{carb}$ shift nor with black shale lithologies around the S–D boundary (Fig. 8). However, the TOC maxima are notably found in the limestone set related to the SIDECIE plateau. By contrast, organic carbon distribution does not show any link with the ESCIE because this is characterized by an upward increasing trend. What is more, the minimal concentration (0.06%) is found in the $\delta^{13}C_{carb}$ excursion peak (Fig. 6A). Thus, the major secular trends of TOC and inorganic proxies are connected each other at Kytayhorod (Fig. 7), but this correlative link is obscured at Dnistrove, especially in the middle SIDECIE slice (Fig. 9).

Results of the pilot GC-MS study on samples from the Podolian localities (SOM 5) are influenced by thermal maturity: biomarker data indicate at least ca 80–100°C, and of the order of 150°C is indicated by our new observations of the conodont colour alteration (cf. also Drygant 1993 and Huff et al. 2000: 498–499).
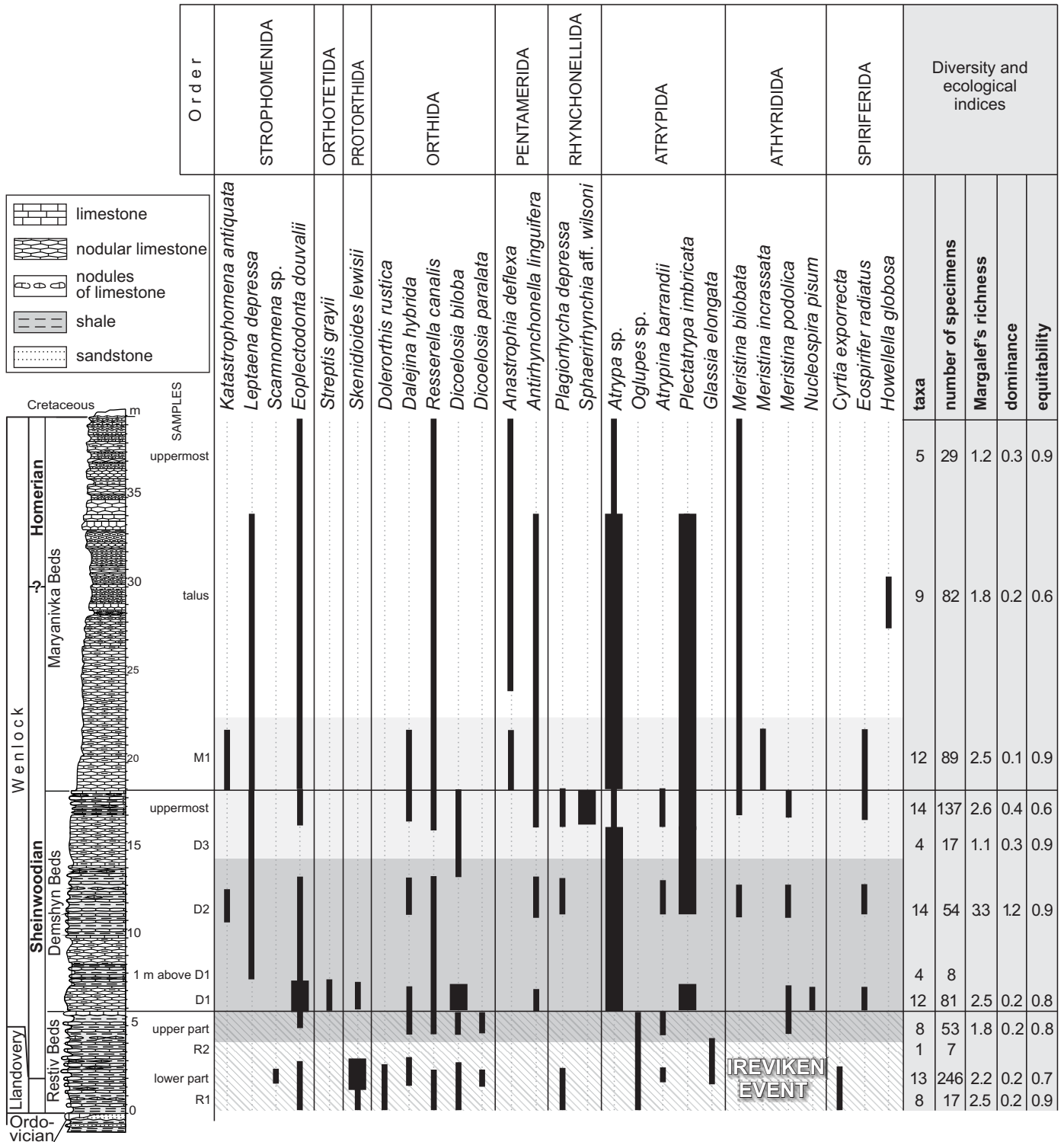
Fig. 10. Distribution of brachiopod species, diversity, and ecological indices through the Kytayhorod Horizon in Kytayhorod section. Dominating species are marked with thicker lines. Shades of gray denote three slices of the ESCIE.

Cyclic biomarkers like steranes or hopanes have not been found or are present as traces. The most frequently encountered organic compounds are relatively stable n-alkanes and polycyclic aromatic hydrocarbons and their alkyl derivatives. Among n-alkanes, the most abundant are short-chain varieties ([nC17 + nC18 + nC19]/[nC27 + nC28 + nC29]) suggestive of prevalent marine organic matter. However, carbon preference indices (CPI and CPI[25–31]) are above 1 (as high as 2.01 for sample LM3 from Dnistrove) in the long-chain n-alkane sets, characteristic for land-derived organic material due to dominating odd-numbered (over even-numbered) carbon chains (e.g., Peters et al. 2005). Thus, a

mixed marine-continental source of organic carbon is supposed for the studied shelf successions, and is confirmed by palynofacies at Dnistrove, also grossly obscured by thermal overprint (see below). Furthermore, predominantly oxic sedimentary regimes are suggested by high pristane to phytane ratios (Didyk et al. 1978).

Faunal dynamics across the Ireviken Event

Quantitative distributional and diversity data on three fossil groups, representing both benthic and most likely largely pelagic biotas, are explored below. The faunal dynamics is considered in the context of environmental variables throughout

the two global isotopic events, interpreted from the above geochemical patterns.

Brachiopods.—The stratigraphically oldest brachiopod fauna of the Restiv Beds (samples R1 to upper part) is quite diverse taxonomically being represented by up to 14 species (Figs. 10, 11). The most characteristic members of the fauna are species of *Skenidioides* and *Dicoelosia* (see also Modzalevskaya 1968). Other genera represented are *Scamnomena*, *Eoplectodonta*, *Dalejina*, *Resserella*, *Plagiorhyncha*, *Oglupes*, *Atrypina*, *Glassia*, *Meristina*, and *Cyrtia* (see Figs. 12–14). These generally well preserved brachiopods are mostly characterized by small shell dimensions and thin-ribbed surface sculpture (see also Modzalevskaya and Nikiforova 1980). They were either (i) fixosessile (see Bassett 1984), staying attached to the substrate with their pedicle during all stages of growth
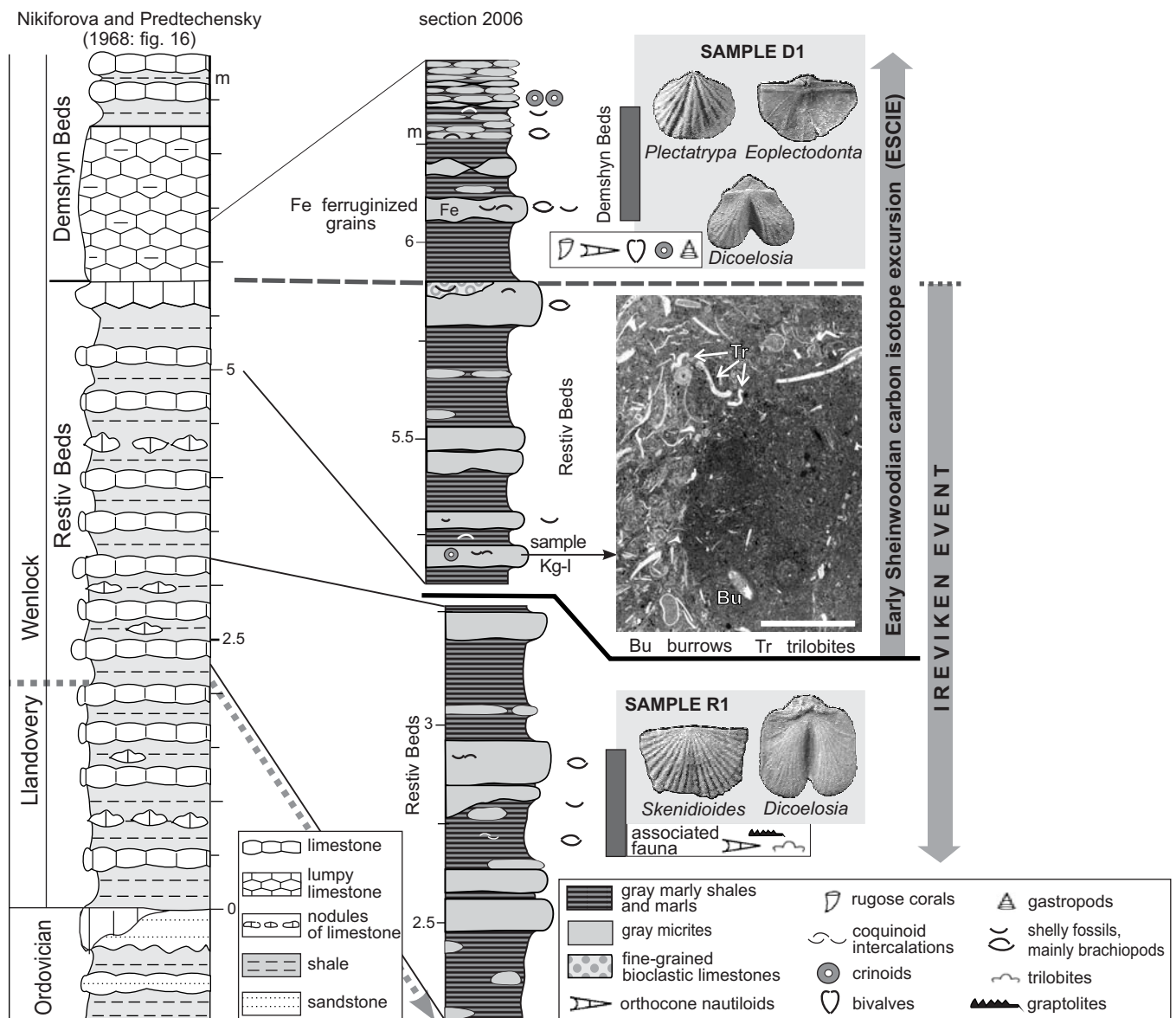

Fig. 11. Lowermost Wenlock lithologic and faunal succession at Kytayhorod, against the key brachiopod assemblages (see Fig. 10) and a representative micritic microfacies of the Restiv Beds, i.e., bioturbated skeletal wackestone to packstone with shelly bioclasts, crinoids, and trilobites (compare Fig. 5). Note onset of the carbon isotope excursion (ESCIE) before the ending of Ireviken Event.

(e.g., *Scamnomena*, *Skenidioides*, *Dicoelosia*, *Dolerorthis*, *Atrypina*, *Glassia*, *Cyrtia*), or (ii) liberosessile, becoming secondarily free-lying after whole or partial atrophy of the pedicle (e.g., *Eoplectodonta*, *Oglupes*). Ambitopic *Eoplectodonta* and *Oglupes* developed different adaptations for stabilisation of the shell on soft muddy bottoms. The adult strophomenide *Eoplectodonta* remained on the surface with the hinge line down partially sunk into the sediment keeping the anterior commissure above a muddy bottom. Dattilo (2004) showed that strophomenid brachiopods were quite mobile and responsive to environmental conditions and that they could live in a convex valve-up position (Lescinsky 1995; Baliński 2010) or assume a near-vertical, semi-infaunal position to escape burial. The adult atrypide *Oglupes*, after atrophy of the pedicle, became recumbent on the soft substrate and was stabilized by flat ventral valve and widely extended frills (see Fig. 13E). This atrypide, which is the largest species in the association, possessed a highly efficient spirolophe lophophore, which enabled it to flourish in deeper-water settings with an impoverished food supply (see Fürsich and Hurst 1974). The overall taxonomic inventory of brachiopods from the Restiv Beds strongly implies that the fauna represents the globally distributed high diversity *Dicoelosia* or *Dicoelosia–Skenidioides* community (see e.g., Boucot 1975, 2005; Gritsenko et al. 1999; Jin and Copper 1999; Watkins et al. 2000; Li and Allen 2008). Both communities have been interpreted as characteristic of outer shelf to slope, deep-water environments indicating a Benthic Assemblage (BA) 4–5 of Boucot (1975). According to Copper (2004), the occurrences of *Glassia* in Britain and Gotland indicate deeper-water settings, probably equivalent of BA 4 or BA 5. *Eoplectodonta*, which is a common brachiopod not only in the Restiv Beds but ranges to the top of the Kytayhorod section, is one of the most characteristic members of the deeper-water *Clorinda* Community (BA 5) during most of the Britain Silurian (Cocks 1970). Johnson (1987; see also Brett et al. 1993; Watkins et al. 2000) estimated the bathymetry of BA 4–5 in the range of 60–120 m. Watkins et al. (2000) demonstrated that brachiopod species diversity of *Dicoelosia* communities remained unchanged from the early Silurian to the early Devonian on a global basis.

The brachiopods of the overlying Demshyn Beds reveal slightly greater taxonomic diversity than the underlying beds. They are represented by 18 species in total of which 8 continue their ranges from the Restiv beds (Fig. 10). Among them *Dicoelosia* occurs to the top of the interval whereas *Skenidioides* was found only in its lowermost part. The brachiopod fauna is dominated by the strophomenide *Eoplectodonta*, atrypides *Atrypa* and *Plectatrypa*, and in the uppermost part of the interval by the mass-occurrence of the rhynchonellide *Sphaerirhynchia*. This genus forms clusters similar to those described by Fürsich and Hurst (1981) for *Sphaerirhynchia*

wilsoni from the Silurian of England and Gotland. *Katastrophomena*, *Leptaena*, *Streptis*, *Antirhynchonella*, *Nucleospira*, *Eospirifer*, and the above-mentioned atrypides appeared in the Demshyn Beds for the first time. Medium- and large-sized forms dominate in this interval. Ambitopic forms with whole or partial atrophy of the pedicle are represented by *Katastrophomena*, *Leptaena*, *Eoplectodonta*, *Antirhynchonella*, *Sphaerirhynchia*, *Atrypa*, and *Meristina*.

In general, the brachiopod fauna from the Demshyn Beds suggests continuity of *Dicoelosia* communities (BA 4–5). This is also supported by the numerous occurrences of *Plectatrypa* which occurs mostly in deeper, shaly, distal shelf facies on Gotland (Copper 2004). Rare findings of *Antirhynchonella*, which represents the same morphological type as *Clorinda*, suggest also some relation to the *Clorinda* Community of Ziegler et al. (1968) correlated with BA 5 (Boucot 1975). Fürsich and Hurst (1981) concluded that *Sphaerirhynchia wilsoni* lived typically semi-infaunally on soft muddy substrates in very calm, low energy settings. Some morphological adaptations of brachiopods from the interval, e.g., strongly sulcate anterior commissure, alate hinge margin, and thin shell, indicate a quiet-water environment (Fürsich and Hurst 1974: fig. 6). The brachiopod fauna from the Demshyn Beds reveals also great similarity to the *Eoplectdonta douvalii* Community described by Hurst (1975) from the Wenlock of Wales and the Welsh Borderland. As many as 78% of the brachiopod species from the Demshyn Beds are also listed by Hurst (1975) in the inventory of the *Eoplectdonta douvalii* Community. Although the brachiopod communities of the Restiv and Demshyn beds indicate similar settings within BA 4–5, the appearance of generally medium- and large-sized brachiopods in latter and dominance of smaller-sized forms in the Restiv Beds suggest some shallowing efect in the section. However, the general faunal changes at that time indicate that sea-level change appears not to have been substantial.

In the Maryanivka Beds 13 brachiopod species in total have been identified during the present investigations. Medium- and large-sized forms predominate while small species have been not found. Several forms do not continue their range from the preceding Demshyn Beds, with the most important loss being of *Dicoelosia*. *Anastrophia*, and *Howellella* are the only genera which appeared new for this interval (Fig. 10). Besides the absence of *Dicoelosia*, the total inventory of brachiopod taxa from the Maryanivka Beds did not changed much in comparison with the preceding Demshyn Beds fauna: 10 genera range through both intervals. Two species from the interval are reported at higher levels in other sections. These are *Leptaena depressa* and *Eospirifer radiatus* which were revealed in the Muksha and Cherche beds, respectively (Nikiforova et al. 1972). Although it seems probable that the brachiopod fauna of the Maryanivka Beds represents more or less

Fig. 12. Silurian brachiopods from the Kytayhorod section. **A**, **M**, **N**. *Eoplectodonta douvalii* (Davidson, 1847). **A**. ZPAL Bp 71/1, almost complete shell in dorsal (A_1), ventral (A_2), lateral (A_3), posterior (A_4), and anterior (A_5) views; Maryanivka beds, sample M1. **M**. ZPAL Bp 71/2, exterior of ventral valve; Demshyn beds. **N**. ZPAL Bp 71/3, interior of dorsal valve; Demshyn beds, sample D2. **B**. *Dicoelosia biloba* (Linnaeus, 1758), ZPAL Bp 71/4, shell in dorsal (B_1), ventral (B_2), lateral (B_3), posterior (B_4), and anterior (B_5) views; Demshyn beds, sample D2. **C**. *Resserella canalis* (Sowerby, 1839), ZPAL Bp →
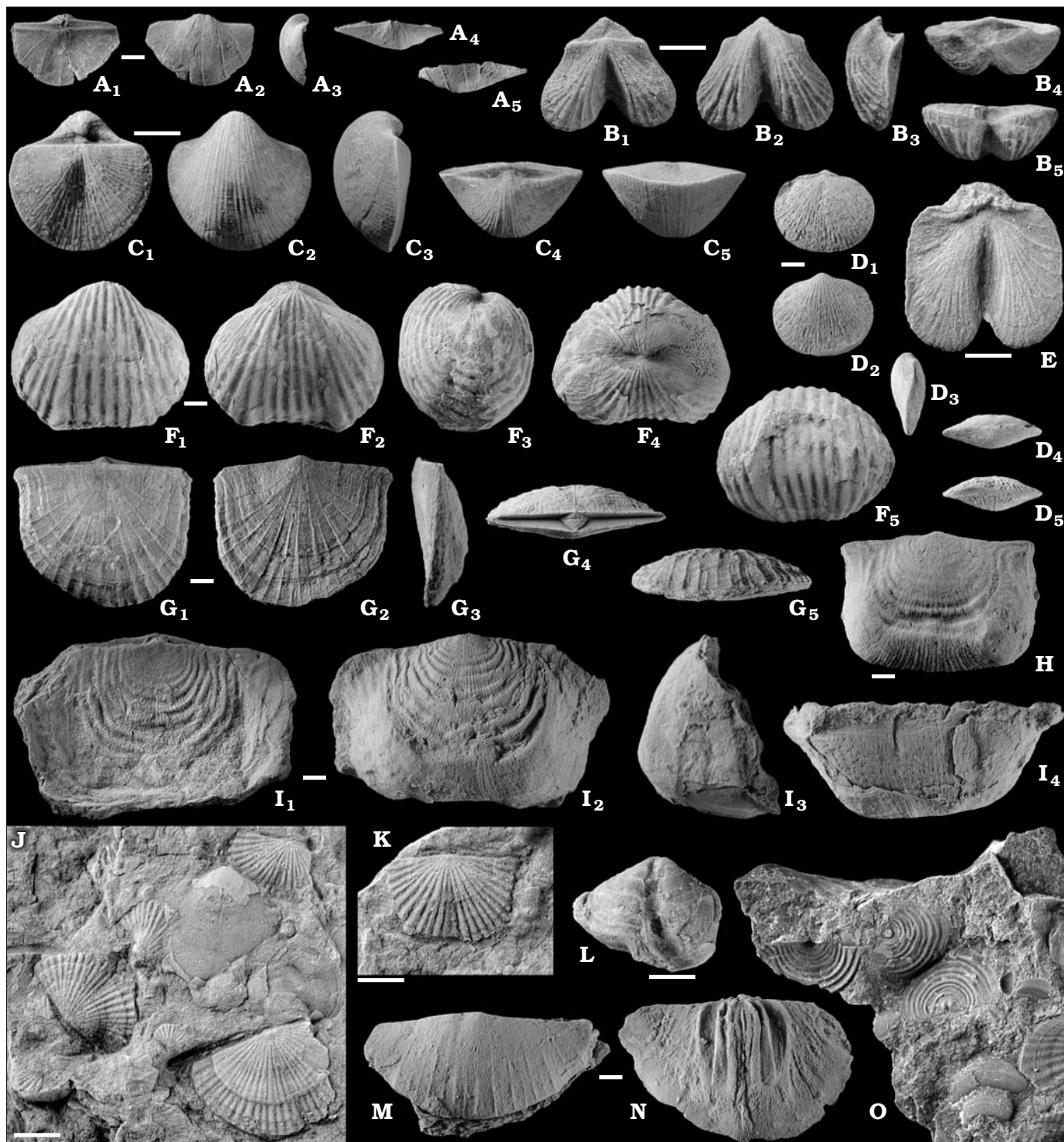
71/5, shell in dorsal (C_1), ventral (C_2), lateral (C_3), posterior (C_4), and anterior (C_5) views; upper part of the Restiv beds. **D**. *Dalejina hybrida* (Sowerby, 1839), ZPAL Bp 71/6, shell in dorsal (D_1), ventral (D_2), lateral (D_3), posterior (D_4), and anterior (D_5) views; Demshyn beds, sample D1. **E**. *Dicoelosia paralata* Bassett, 1972, ZPAL Bp 71/7, slightly damaged shell in dorsal view; Restiv beds, 0.8 m above sample R1. **F**. *Anastrophia deflexa* (Sowerby, 1839), ZPAL Bp 71/8, complete shell in dorsal (F_1), ventral (F_2), lateral (F_3), posterior (F_4), and anterior (F_5) views; lower part of the Maryanivka beds. **G**. *Katastrophomena antiquata* (Sowerby, 1839), ZPAL Bp 71/9, shell in dorsal (G_1), ventral (G_2), lateral (G_3), posterior (G_4), and anterior (G_5) views; Demshyn beds. **H, I**. *Leptaena depressa* (Sowerby, 1824). **H**. ZPAL Bp 71/10, complete shell in ventral view; Demshyn beds, sample D3. **I**. ZPAL Bp 71/11, slightly damaged shell in dorsal (I_1), ventral (I_2), lateral (I_3), posterior (I_4), and anterior (I_5) views; lower part of the Maryanivka beds. **J, K**. *Skenidioides lewisii* (Davidson, 1848). **J**. ZPAL Bp 71/12, slab with three well visible dorsal valves; Restiv beds, 0.8 m above sample R1. **K**. ZPAL Bp 71/13, exterior of dorsal valve; Restiv beds, sample R1. **L**. *Streptis grayii* (Davidson, 1848), ZPAL Bp 71/14, slightly incomplete shell in ventral view; lower part of the Demshyn beds. **O**. *Scamnomena* sp., ZPAL Bp 71/15, slab with three visible specimens; Restiv beds, slightly above sample R1. Scale bars 2 mm.
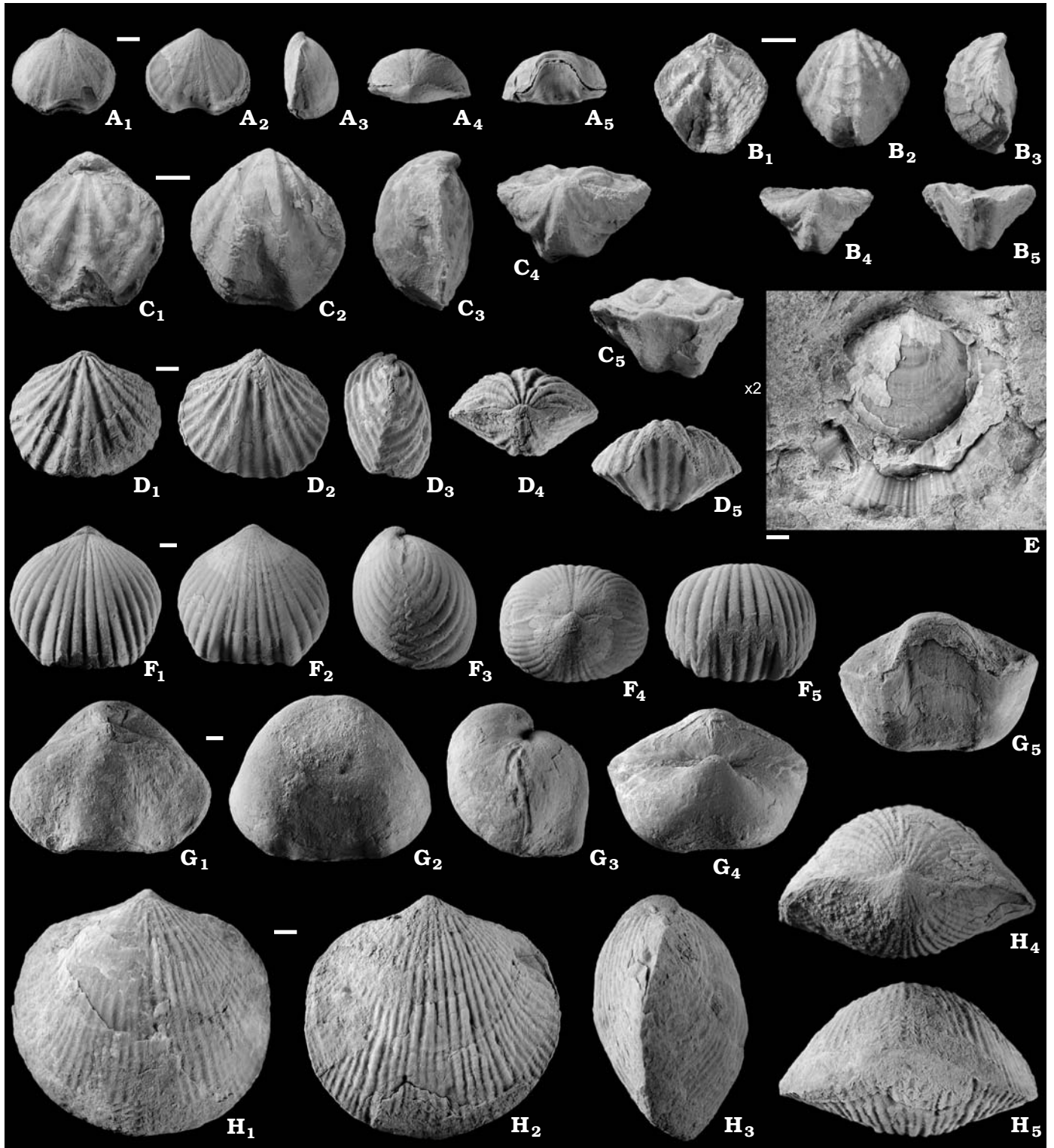
Fig. 13. Silurian brachiopods from the Kytayhorod section. **A**. *Plagiorhycha depressa* (Sowerby, 1839), ZPAL Bp 71/16, shell in dorsal (A_1), ventral (A_2), lateral (A_3), posterior (A_4), and anterior (A_5) views; Restiv beds, sample R1. **B**, **C**. *Atrypina barrandii* (Davidson, 1848), ZPAL Bp 71/17 (**B**), ZPAL Bp 71/18 (**C**), two shells in dorsal (B_1, C_1), ventral (B_2, C_2), lateral (B_3, C_3), posterior (B_4, C_4), and anterior (B_5, C_5) views; upper part of the Restiv beds (B) and upper part of the Demshyn beds (C). **D**. *Plectatrypa imbricata* (Sowerby, 1839), ZPAL Bp 71/19, shell in dorsal (D_1), ventral (D_2), lateral (D_3), posterior (D_4), and anterior (D_5) views; Demshyn beds, sample D1. **E**. *Oglupes* sp., ZPAL Bp 71/20, shell with partially preserved frills in ventral view; Restiv beds, sample R2. **F**. *Sphaerirhynchia* aff. *wilsoni* (Sowerby, 1816), ZPAL Bp 71/21, complete shell in dorsal (F_1), ventral (F_2), lateral (F_3), posterior (F_4), and anterior (F_5) views; Demshyn beds. **G**. *Antirhynchonella linguifera* (Sowerby, 1839), ZPAL Bp 71/22, large shell in dorsal (G_1), ventral (G_2), lateral (G_3), posterior (G_4), and anterior (G_5) views; lower part of the Maryanivka beds. **H**. *Atrypa* sp., ZPAL Bp 71/23, shell in dorsal (H_1), ventral (H_2), lateral (H_3), posterior (H_4), and anterior (H_5) views; Demshyn beds. Scale bars 2 mm.
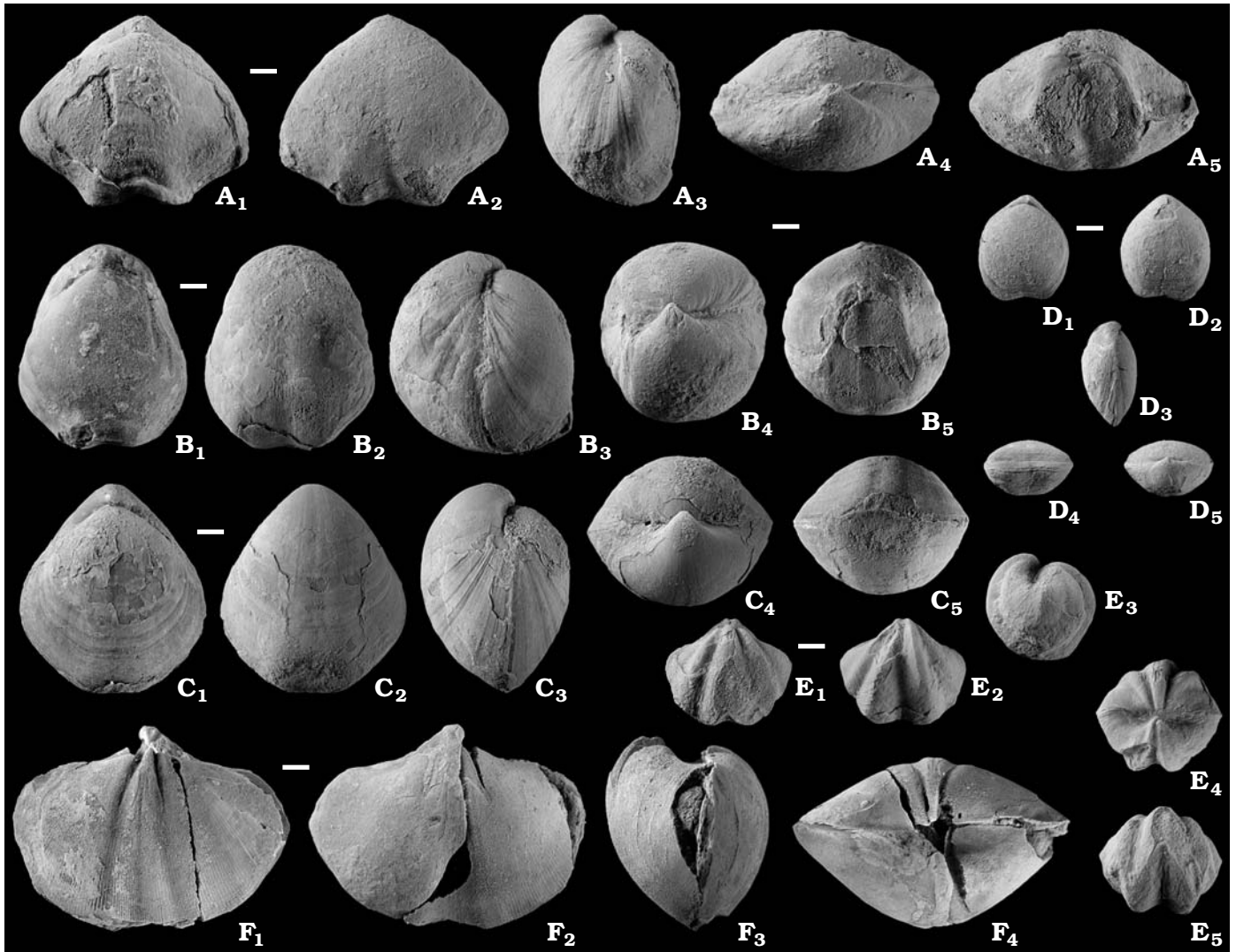
Fig. 14. Silurian brachiopods from the Kytayhorod section. **A**. *Meristina bilobata* Modzalevskaya, 1980, ZPAL Bp 71/24, shell in dorsal (A_1), ventral (A_2), lateral (A_3), posterior (A_4), and anterior (A_5) views; Demshyn beds, sample D2. **B**. *Meristina incrassata* Modzalevskaya, 1980, ZPAL Bp 71/25, shell in dorsal (B_1), ventral (B_2), lateral (B_3), posterior (B_4), and anterior (B_5) views; Maryanivka beds, sample M1. **C**. *Meristina podolica* (Nikiforova, 1954), ZPAL Bp 71/26, shell in dorsal (C_1), ventral (C_2), lateral (C_3), posterior (C_4), and anterior (C_5) views; upper part of the Restiv beds. **D**. *Glassia elongata* Davidson, 1881, ZPAL Bp 71/27, shell in dorsal (D_1), ventral (D_2), lateral (D_3), posterior (D_4), and anterior (D_5) views; Restiv beds, 0.8 m above sample R-1. **E**. *Howellella globosa* Tsegelnyuk, 1976, ZPAL Bp 71/28, in dorsal (E_1), ventral (E_2), lateral (E_3), posterior (E_4), and anterior (E_5) views; lower part of the Maryanivka beds. **F**. *Eospirifer radiatus* (Sowerby, 1834), ZPAL Bp 71/29, slightly incomplete shell in dorsal (F_1), ventral (F_2), lateral (F_3), posterior (F_4), and anterior (F_5) views; Demshyn beds. Scale bars 2 mm.

the same, a slightly impoverished BA 4–5, some changes are noteworthy. Local extinction of the long-lasting *Dicoelosia* combined with first appperance of *Howelella* may be linked to the basin shallowing (the latter spiriferid is a nominative genus for BA 2 in the coeval Appalachian faunas; Brett and Baird 1995; Boucot 2005).

Thus, the succession of the brachiopod fauna in the Kytayhorod section shows rather gradual and minor temporal changes. The most characteristic trend observable in the fauna is a change from stressed assemblages of prevailing small-dimensioned forms in the Restiv Beds (? a reflection of Lilliput effect during the Ireviken crisis; Urbanek 1993) to medium- and large-sized forms in the Demshyn Beds (i.e., during the $\delta^{13}C$ $\delta^{13}C_{carb}$ highstand; Fig. 6A), and, particularly, Marya-

nivka Beds. Also important seems to be disappearance of *Skenidioides* in the lower part of the Demshyn Beds and, successively, *Dicoelosia* at the top of the interval. Thus, contrary to the diversity changes and extinctions during the Ireviken Event which have been observed among shallow-water brachiopod fauna on Gotland (Kaljo et al. 1996; Erlfeldt 2006; see also data on the Lau Event in Gustavsson et al. 2005), Australia (lingulids only; Valentine et al. 2003) and North America (Boucot 1990; Boucot in Kaljo et al. 1996), the brachiopods from the Kytayhorod section do not reveal any substantial perturbation. This is in agreement with observation of Watkins et al. (2000) that deep-water *Dicoelosia* communities showed long-term stability and were apparently unaffected by Silurian global oceanic events.
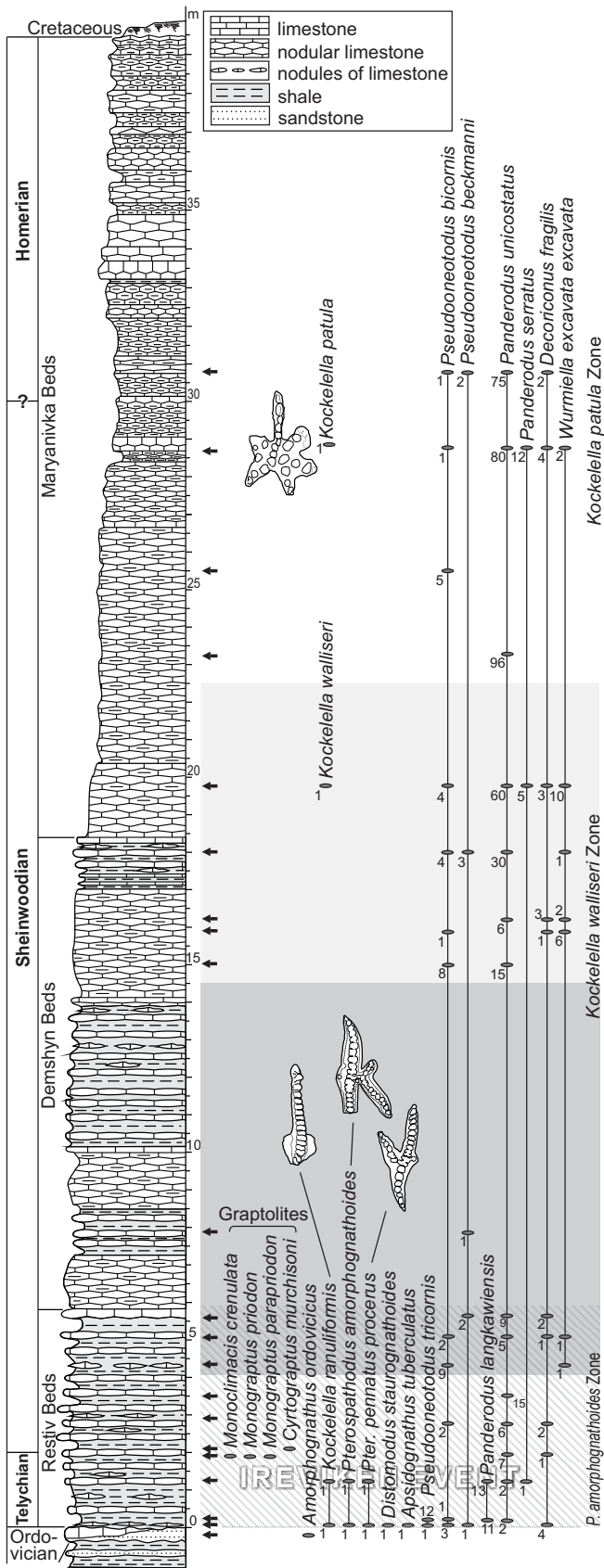
Fig. 15. Conodont and graptolite distribution in the Kytayhorod section. Numbers near the ovals are numbers of specimens in the sample. Shades of gray denote three slices of the ESCIE.

Conodonts.—The conodont assemblages exhibit a two-step distributional pattern, characterized by a low-frequency but relatively high diversity assemblage (up to 9 species) quickly replaced in the succession by a stabilized, but typically species poor (mostly 1–4 species) *Panderodus*-dominated biota of overall increasing abundance (Fig. 15). A similar pattern of abundance was noted for the far richer Estonian assemblages by Hints et al. (2006).

The diverse fauna is limited to two basal samples from the Restiv Beds. The occurrences characterize an initial uppermost Telychian phase of ESCIE, and this regional turnover of the Ireviken Event in the pelagic biota is partly coincident with the oldest "Datum Points" of Jeppsson (1997: fig. 17.2; see also updated data in Cramer et al. 2010). Even if influenced by scarcity of the fauna (mostly single specimens), the First Telychian Datum is clearly suggested by last occurrence of *Pseudooneotodus tricornis* in the second sample (12 specimens), whilst *Panderodus langkawiensis* disappeared in the third sample (13 specimens), ca. 1 m higher; this species is considered by Jeppsson (1997, 1998) and Jeppson et al. (2005) to have become extinct at the Sheinwoodian Datum 3.3. Thus, a condensed nature of the lowermost sampled layers in the Ireviken Event may be assumed, especially that coeval condensed sections are known commonly worldwide (Hints et al. 2006; Haq and Schutter 2008: fig. 2; Kleffner and Barrick 2010; Ray and Butcher 2010). A replacement of the series boundary, downward to a ca. 1 m lower level than accepted by Koren et al. (1989), may be therefore considered.

Moreover, even a cryptic hiatus possibly occurs higher in the Ireviken interval (David Loydell, personal communication 2012; see also Kaljo et al. 2007: 216), if the graptolite species *Monoclimacis crenulata* would be confirmed in the Restiv Beds just below entry of the guide Wenlock species, *Cyrtograptus murchisoni* (Fig. 15); *M. crenulata* is unknown worldwide above the middle Telychian *Oktavites spiralis* Biozone (Fig. 2 in Cramer et al. 2010). So, these taxonomic data of Tsegelnyuk et al. (1983) need revision to confirm the implied biostratigraphical or biogeographic peculiarity.

The more widespread faunas from the Demshyn Beds (i.e., in the E-2 highstand) and lower Maryanivka Beds include well-known species that survive the Ireviken Event, such as *Decoriconus fragilis* and *Pseudooneotodus bicornis*. In addition, the most common species *Panderodus unicostatus* also belongs to the survivors, and this ubiquitous species may have had a wide environmental tolerance, as shown by Zhang and Barnes (2002) for the Llandovery of Anticosti Island, Québec. Single occurrences of the index species for the upper, but not uppermost Sheinwoodian *Kockelella walliseri* Zonal Group, *K. walliseri*, and *K. patula* (see Cramer et al. 2010: fig. 3; Sh2 time slice of Cramer et al. 2011a), were found in the Maryanivka Beds. As inferred by Cramer et al. (2010, 211a), this conodont dating, even though under current revision due to a proved biogeographic differentiation in the first occurrence of the both species, coincides with worldwide end of the ESCIE.
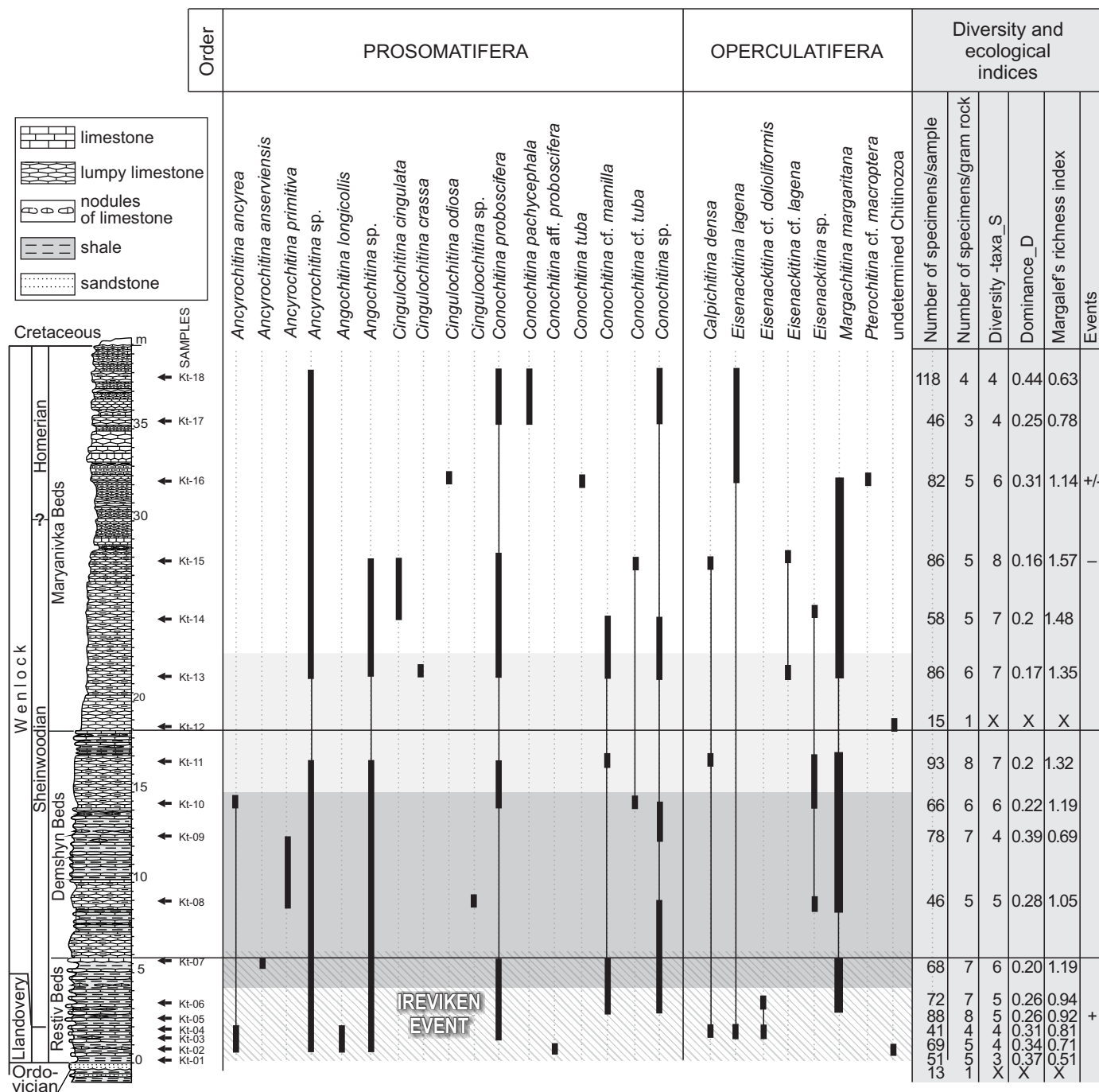
Fig. 16. Distribution of chitinozoans species, diversity, and ecological indices in the Kytayhorod section. Shades of gray denote three slices of the ESCIE.

Chitinozoans.—Chitinozoans are organic-walled microfossils of uncertain biological affinity; it is likely that they represent the egg-capsules of soft-bodied marine animals. Their ecological distribution is rather diverse, however, the wide geographical and facies distribution indicate that the chitinozoan biota (chitinozoophorans) may have been either mostly planktic/nekto-pelagic or much more rarely benthic (Miller 1996; Grahn and Paris 2011). The species with thick-walled and poorly ornamented vesicles have been usually interpreted as possibly benthic, high hydrodynamic energy environment occupants, while thin-walled highly ornamented with long processes vesicles have been suggested as pelagic, similar to graptolites in their mode of distribution in the outer shelf environment (Miller 1996; Grahn and Paris 2011).

Chitinozoans in the Kytayhorod section are characterized by a moderately diverse (up to 13 taxa) *Margachitina*-dominated assemblage (SOM 5; Figs. 16, 17). Although their abundance is partly controlled by the facies, with more abundant assemblages from clay-rich rocks, an impoverishment, in frequency and richness terms, has been observed in the basal and upper parts of the succession. This is not a very strong secular differentiation, however, without any obvious
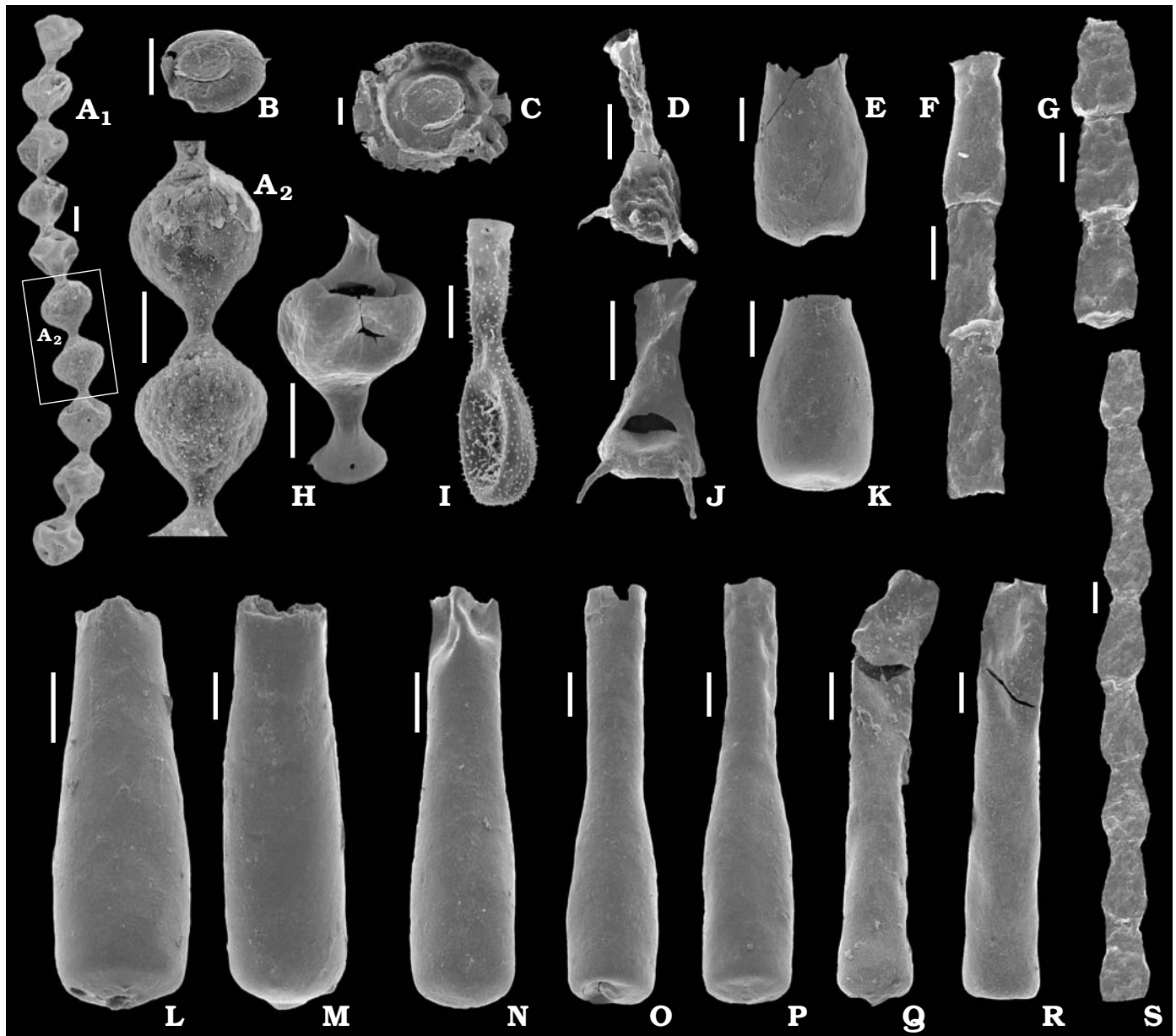
Fig. 17. Stereoscan microphotographs of selected Chitinozoa from the Kytayhorod section. **A, H**. *Margachitina margaritana* (Eisenack, 1937). **A**. ZPAL Ch. 8/170S42, sample Kt 06/03; chain of ten vesicles in lateral view (A$_1$) and detail of the connetcion between the vesicle (A$_2$). **H**. ZPAL Ch. 8/170S32, sample Kt 08/11; fragment of a chain of two slightly deformed vesicles showing how aperture is linked to the succeeding vesicle. **B**. *Calpichitina densa* (Eisenack, 1962), ZPAL Ch 8/176S58, sample Kt 06/15. **C**. *Pterochitina* cf. *macroptera* Eisenack, 1959, ZPAL Ch. 8/156S128, sample Kt 06/16. **D**. *Ancyrochitina* sp., ZPAL Ch 8/176S58, sample Kt 06/06. **E**. *Eisenackitina dolioliformis* Umnova, 1976, ZPAL Ch 8/176S73, sample Kt 06/05. **F**. *Cingulochitina odiosa* (Laufeld, 1974), ZPAL Ch 8/172S46, sample Kt 06/16. **G**. *Cingulochitina crassa* Nestor, 1994, ZPAL Ch 8/172S48, sample Kt 06/13. **I**. *Angochitina longicollis* Eisenack, 1959, ZPAL Ch. 8/157S62, sample Kt 08/10. **J**. *Ancyrochitina primitiva* Eisenack, 1964, ZPAL Ch 8/176S58, sample Kt 06/08. **K**. *Eisenackitina lagena* (Eisenack, 1968), ZPAL Ch 8/176S70, sample Kt 06/03. **L, M**. *Conochitina proboscifera* Eisenack, 1937. **L**. ZPAL Ch 8/176S50, sample Kt 06/17. **M**. ZPAL Ch 8/176S41, sample Kt 06/14. **N**. *Conochitina tuba* Eisenack, 1932, ZPAL Ch 8/176S40, sample Kt 06/16. **O, P**. *Conochitina pachycephala* Eisenack, 1964. **O**. ZPAL Ch 8/176S39, sample Kt 06/18. **P**. ZPAL Ch 8/176S44, sample Kt 06/17. **Q**. *Conochitina* cf. *mamilla* Laufeld, 1974, ZPAL Ch 8/176S27, sample Kt 06/13. **R**. *Conochitina* sp. ZPAL Ch 8/176S29, sample Kt 06/11. **S**. *Cingulochitina cingulata* (Eisenack, 1937), ZPAL Ch 8/172S55, sample Kt 06/15.

link with the $\delta^{13}C$ trends. Two acmes of species representing the genus *Conochitina* were found in the lowermost and topmost samples which were highly-dominated by *C. proboscifera* and *C. pachycephala*, respectively. The chitinozoans suggest a position for the Sheinwoodian–Homerian boundary at ca. 30 m level. This would be above the occurrences of

Cingulochitina cingulata and below the FAD of *Conochitina pachycephala*.

This fairly stabilized dynamics pattern differs from the abrupt changes in chitinozoan faunas at the Llandovery–Wenlock boundary (Nestor et al. 2002; Lehnert et al. 2010), even if partly due to a stratigraphical gap within the *Margachitina*
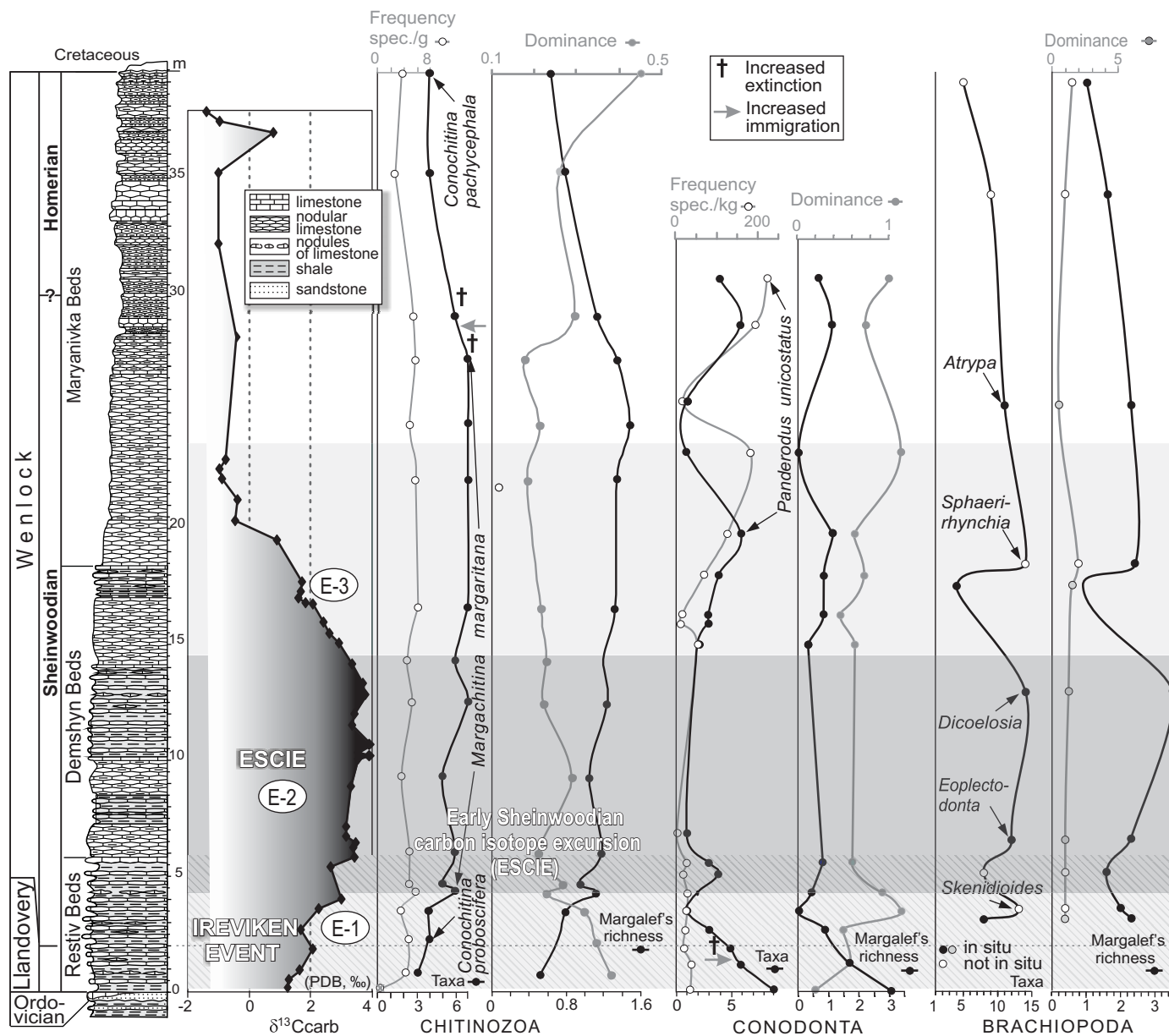
Fig. 18. Faunal dynamics across the Ireviken Event and early Sheinwoodian carbon isotope excursion (ESCIE) in the Kytayhorod section. Shades of gray denote three slices of the ESCIE.

margaritana Zone sensu stricto, recognised from Estonia by Loydell and Nestor (2005) and Hints et al. (2006; see also Sadler 2012: fig. 8). Two identified species, *Angochitina longicollis* and, with reservation, *Eisenackitina dolioliformis*, are quoted by Nestor et al. (2002) among chitinozoan victims of the profound late Ireviken crisis in pelagic domain (= level 8 of these authors; or conodont Datum 6; see also Jeppsson et al. 2005).

Other groups.—Our field observations, as well literature data on other fossil groups (Nikiforova and Predtechensky 1968: fig. 16; Nikiforova et al. 1972) are in a general agreement with the main distribution patterns outlined above (Fig. 18), controlled primarily by oscillating regressive sea-level trend (Koren et al. 1989: fig. 105).

The Restiv Beds are ecologically distinctive because of the unique occurrences of graptolites (rare in a thin 0.2 m level only; Fig. 15) and macroflora (*Pseudosajania)*, and also far more widely distributed benthic groups: crinoids, gastropods, solitary rugose corals (*Orthopaterophyllum*), nautiloids, and trilobites (*Acidaspis*; common in some layers). Also *Tasmanites* (Prasinophyceae, unilocular green algae) was recovered only in the two lowest chitinozoan samples. Assemblages from the lowermost part of the Demshyn Beds include the five above mentioned benthic groups and bivalves, with locally frequent solitary rugose corals (*Orthopaterophyllum*, *Sverigophyllum*), whilst some higher sets (e.g., units 4–6 of Nikiforova et al. 1972) are either unfossiliferous (nodular lithologies) or characterized by infaunal to epifaunal filter-feeding bivalve fauna only, with

Grammysia and *Mytilarca*. The abundant brachiopod fauna of upper Demshyn Beds is accompanied by a rather impoverished assemblage of trilobites, solitary corals (*Stereotactis*), crinoids, and gastropods.

Poor benthos, in terms of diversity and frequency, is known from the thick nodular limestone units of Maryanivka Beds, where in a few layers, besides brachiopods, merely solitary and colonial corals (*Paleofavosites*), gastropods, crinoids, and trilobites (*Bumastus*) have been found. Intensively bioturbated micritic microfacies varieties of this succession (Figs. 5A, B, D, 11) demonstrate the recurrent development of soft-bodied infauna in the muddy bottom sediments. In addition, there is noteworthy rock-forming abundance of dasycladacean green algae (*Rhabdoporella*) in the shallowing basin (Fig. 5B), up to ca. 50 m water depth (Ischenko 1976, 1985). Also, the Wenlock phytoplankton associations are remarkably diverse in Podolian successions, especially these from the Maryanivka Beds (more than 25 species; Le Hérissé et al. 2009: fig. 8).

Faunal dynamics across the Klonk Event

Brachiopods.—The stratigraphically oldest brachiopod found in the trench at Dnistrove is *Dayia bohemica* which occurs in the topmost part of the Dzvenyhorod Beds (see also Kaljo et al. 2012), i.e., about 1.3–1.6 m below the S–D boundary (Fig. 19; see also detailed description of the brachiopod fauna from this section in Baliński 2012). The species occurs mainly in the thin bedded nodular limestone where it forms almost monospecific nest-like clusters of usually articulated shells (Fig. 4). *D. bohemica* is a characteristic species for the uppermost layers of the Pridoli Series of Bohemia, Estonia, Lithuania, and Latvia (Havlíček and Štorch 1990; Rubel 1977). Tucker (1964) noted that *Dayia navicula*, a closely related species to *D. bohemica*, in the Silurian of the Welsh Borderland achieved its widest distribution and greatest abundance in the offshore zones where the sea bottom was below wave base. He also suggested that the incurvature of the ventral umbo in *D. navicula* prohibited emergence of the pedicle and that the majority of mature individuals rested freely on the sea bottom (see also Kozłowski 1929: 180). Boucot (1975) remarked that *Dayia* constituted a low-diversity, single brachiopod genus community in quiet-water settings within BA 3. Havlíček and Štorch (1990) proposed a separate *Dayia bohemica* Subcommunity where the nominate species formed brachiopod banks. Johnson (1987) suggested that BA 3 ranges approximately from 30 to 60 m water depth. However, Martma et al. (2005: fig. 3) showed the Ludlow *Dayia* assemblage in BA4, adjacent to the pelagic biofacies, and this deeper-water position seems to correspond better with the Podolian data (Gritsenko et al. 1999). About 0.3 m above the layer with abundant *Dayia bohemica* there is a few cm thick shale with numerous specimens of the

athyridide *Dnestrina gutta* (Fig. 4). *D. gutta* is a small species, rarely exceeding 6 mm in length, with a plano-convex profile, and open delthyrium. The species is known also from the Pridoli of Moldavia, and Western Europe (Alvarez and Copper 2002). A similar form was described as *D.* cf. *gutta* by Jahnke et al. (1989) from the uppermost Silurian of Yunnan Province, China. The occurrence of *D. gutta* in the Dnistrove Level suggests stressed, impoverished, low diversity, short-ranging assemblages living in somewhat deeper water conditions than *Dayia bohemica*. Besides *D. gutta*, very rare single valves of *D. bohemica* occur in these layers. It seems justified to propose a low diversity, quiet water *Dnestrina gutta* Community which is probably closely analogous to the slightly younger *Gracianella* Community of Boucot (1975) mentioned below.

Although the first appearance of the atrypide *Gracianella* (*Sublepida*) *paulula* at Dnistrove is ca. 20 cm below the S–D boundary, its main occurrence is 40 cm above it. The occurrences are paired with the base of the $\delta^{13}C_{carb}$ plateau (see Figs. 4 and 19). Other brachiopods constitute 9% of the assemblage being represented by small-sized *Resserella elegantuloides*, *Plectodonta* (*Plectodonta*) *mariae pantherae*, *Pseudoprotathyris infantilis*, and *Howellella* (*Howellella*) *latisinuata*. It should be noted that within the range of *G.* (*S.*) *paulula* a layer with the graptolite *Monograptus uniformis angustidens* has also been recovered. The most characteristic brachiopod *G.* (*S.*) *paulula* is characterized by its minute, up to 4 mm long, weakly biconvex, ribbed shell. It seems that this fauna represents the low-diversity high dominance, quiet-water *Gracianella* Community of Boucot (1975) recognised in the Silurian non-reef communities of the Uralian–Cordilleran and North Atlantic Regions. According to Boucot (1975) the community relates mainly to BA 4 and 5 but also partly to BA 3 (see also Johnson et al. 1976; Zhang 2001).

In the succeeding 4 m of rhythmic marls and limestones the brachiopods are either very rare, poorly preserved or absent. However, at about 5.5 m above the S–D boundary (beds 47–48) a fossiliferous ca. 30 cm thick layer appears with a high-diversity, well preserved, and distinctive brachiopod assemblage dominated by medium-sized forms. The most characteristic are *Septatrypa* (*Septatrypa*) *secreta* (27% of the assemblage), *Plectodonta* (*Plectodonta*) *mariae pantherae* (13%), *Sphaerirhynchia gibbosa* (12%), *Clorinda pseudolinguifera* (11%) and *Talentella crassiformis* (7%). Thus, the five most common species constitute 70% of the assemblage whereas the remaining 30% of the assemblage comprises 11 brachiopod species. Only *Sphaerirhynchia gibbosa* occurs more richly higher in the Dnistrove succession. The brachiopod assemblage is represented by a variety of morphological types and ecological adaptations, e.g., small- to large-sized, concavo-convex, biconvex to globose, smooth, ribbed to frilled, with or without functional pedicle (Baliński 2012). The specimens are mostly articulated with the exception of *Clorinda pseudolinguifera* which possessed a mechanically weaker and more prone to disarticulation hinge structure of deltidiodont type. The presence of numer-
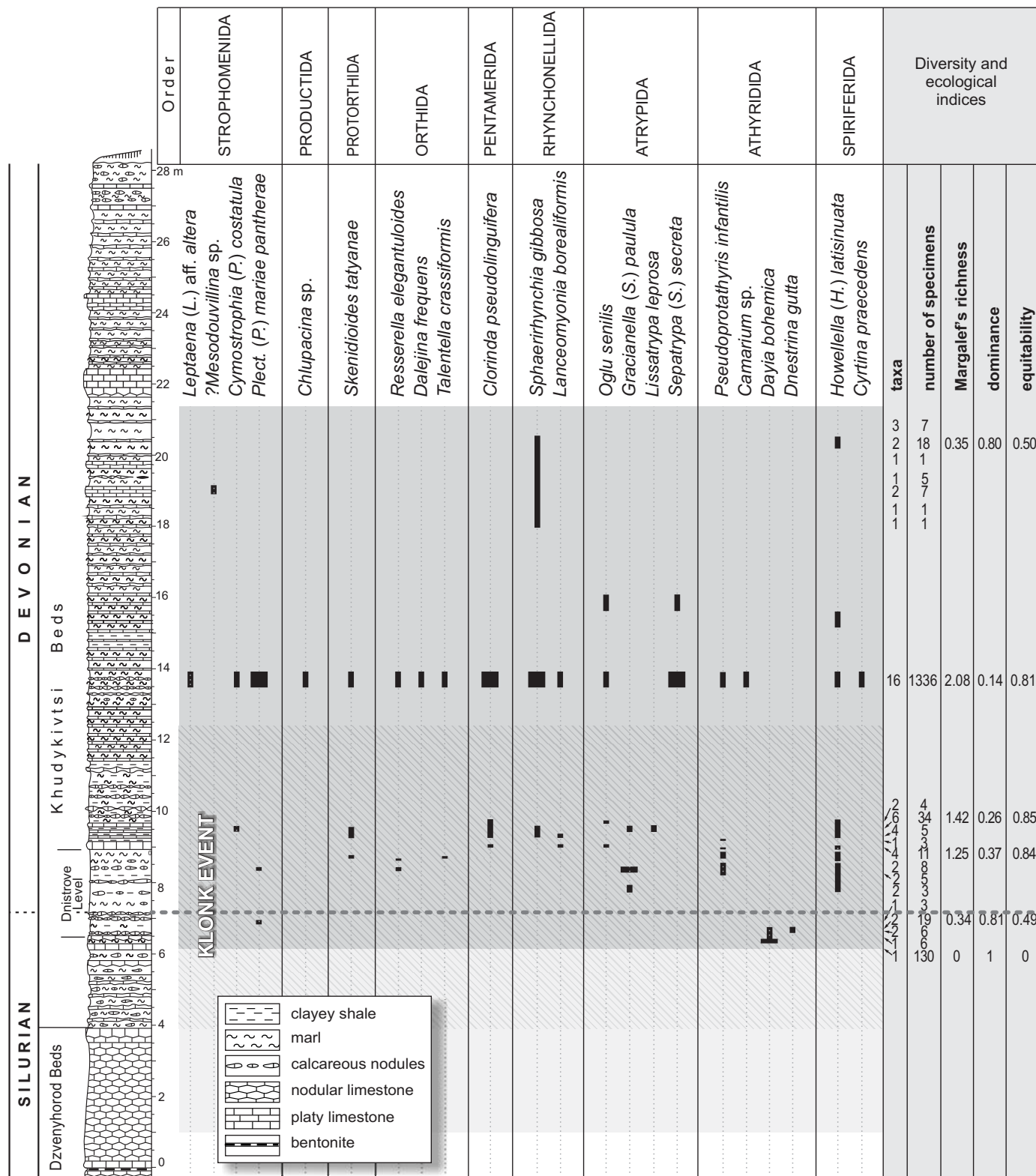
Fig. 19. Distribution of brachiopod species, diversity, and ecological indices through the S–D passage beds at Dnistrove. Dominating species marked with thicker lines. Shades of gray denote two slices of the SIDECIE.

ous strophomenide *P.* (*P.*) *mariae pantherae* in the assemblage is very distinctive due to its colour pattern performing apparently a protective function through disruptive camouflage against visual systems of potential predators (Baliński

2010). This in turn implies that the brachiopods lived within the photic zone.

The presence of numerous *S.* (*S.*) *secreta* in beds 47–48 suggests that the fauna may be compared to the Silurian

non-reef quiet-water *Dubaria* Community of Boucot (1975) which corresponds with BA 3 (the genus *Dubaria* Termier, 1936 is considered a synonym of *Septatrypa* Kozłowski, 1929; see Copper 2002a: 1465). Jones and Hurst (1984) noted, however, that *Dubaria* in the Silurian of North Greenland inhabited quiet water, cryptic habitats associated with reefs. On the other hand, according to Havlíček and Štorch (1990) in the Pridoli of Bohemia the *Dubaria* Community is related to quiet, shallow-water settings at about BA 2–3. Thus, the inventory and character of the brachiopod and associated fauna from beds 47–48 at Dnistrove (see below) indicate probably a setting near the lower (outer) limit of the photic zone equivalent to the BA 3–4 boundary (see Brett at al. 1993).

In summary, the relations between brachiopod faunal distribution and the isotope excursion are rather complex (see Fig. 19), but progressively improved conditions for the sessile shelly faunas are clearly associated with this event in the earliest Devonian. Far more restricted benthos characterizes the rapid increase phase of $\delta^{13}C_{carb}$ values prior to the S–D boundary. Only two species became extinct across the period boundary (compare the diversity data in Talent et al. 1993). Interestingly, monospecific acmes of *Dayia minor* distinguish also specific deeper-water habitats through the large-scale Ludlow carbon cycle disturbance in the Prague Basin (Lehnert et al. 2007b).

Conodonts.—The limestone layers in the Dnistrove succession are mostly rich in conodonts (Figs. 20). Comparatively abundant are: *Ozrkodina typica*, *Parazieglerodina eosteinhornensis*, *Wurmiella excavata*, and *Panderodus unicostatus* (see detailed description of the conodont fauna from this section in Drygant and Szaniawski 2012). Thus, despite somewhat irregular frequency trends, the less abundant faunas occur in the Dnistrove Level and in the uppermost part of the succession (Drygant 2010). In diversity terms, however, more suitable conditions for diverse pelagic biota are found in the Devonian part, i.e., towards the end of the SIDECIE interval (see Fig. 20).

An overturn in the faunas is recognised near the S–D boundary level, when four Silurian-type species have disappeared (e.g., *Delotaxis detorta* and *Parazieglerodina eosteinhornensis*), and a more species-rich Devonian assemblage (up to 6 species), with *Zieglerodina remscheidensis*, *Caudicriodus*, and *Pandorinellina*, suddenly flourished in the shallowing epeiric sea. This succession may be overall correlated with the *Oulodus elegans detortus* to *Icriodus hesperius* (= *Caudicriodus hesperius* after Drygant 2010 and Drygant and Szaniawski 2012) zonal passage, as newly redefined by Corradini and Corriga (2012: fig. 5), paired with a radiation of early icriodontids (see also Slavík et al. 2012). Furthermore, a resemblance to the North American faunal step 3 of Barrick et al. (2005), determined by extinction of *Delotaxis detorta* and approximated with the basal Devonian shift to *Decoriconus*- and *Pseudooneotodus*-rich biofacies with *Zieglerodina remscheidensis*, is noticeable.
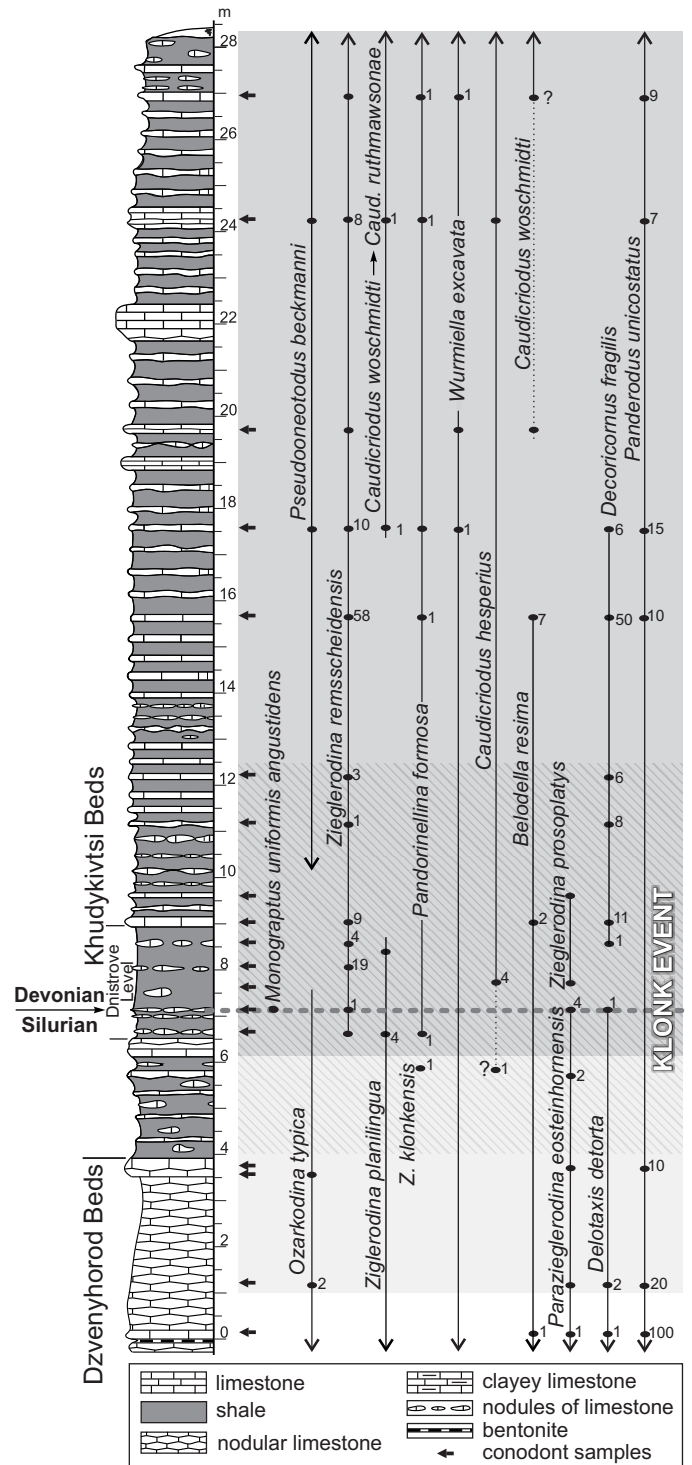

Fig. 20. Conodont and graptolite distribution through the S–D passage beds at Dnistrove. Shades of gray denote two slices of the SIDECIE.

Chitinozoans.—The occurrence of characteristic species such as *Urnochitina urna*, *Eisenackitina bohemica*, *Cingulochitina* ex. gr. *ervensis*, *Calpichitina velata*, *Margachitina catenaria* and *Anthochitina* ex. gr. *superba* represents a clear co-occurrence range zone within the S–D boundary interval at Dnistrove (see SOM 6 and Figs. 21, 22). The high abundance of the thick-walled vesicles of *Urnochitina* (Operculatifera)
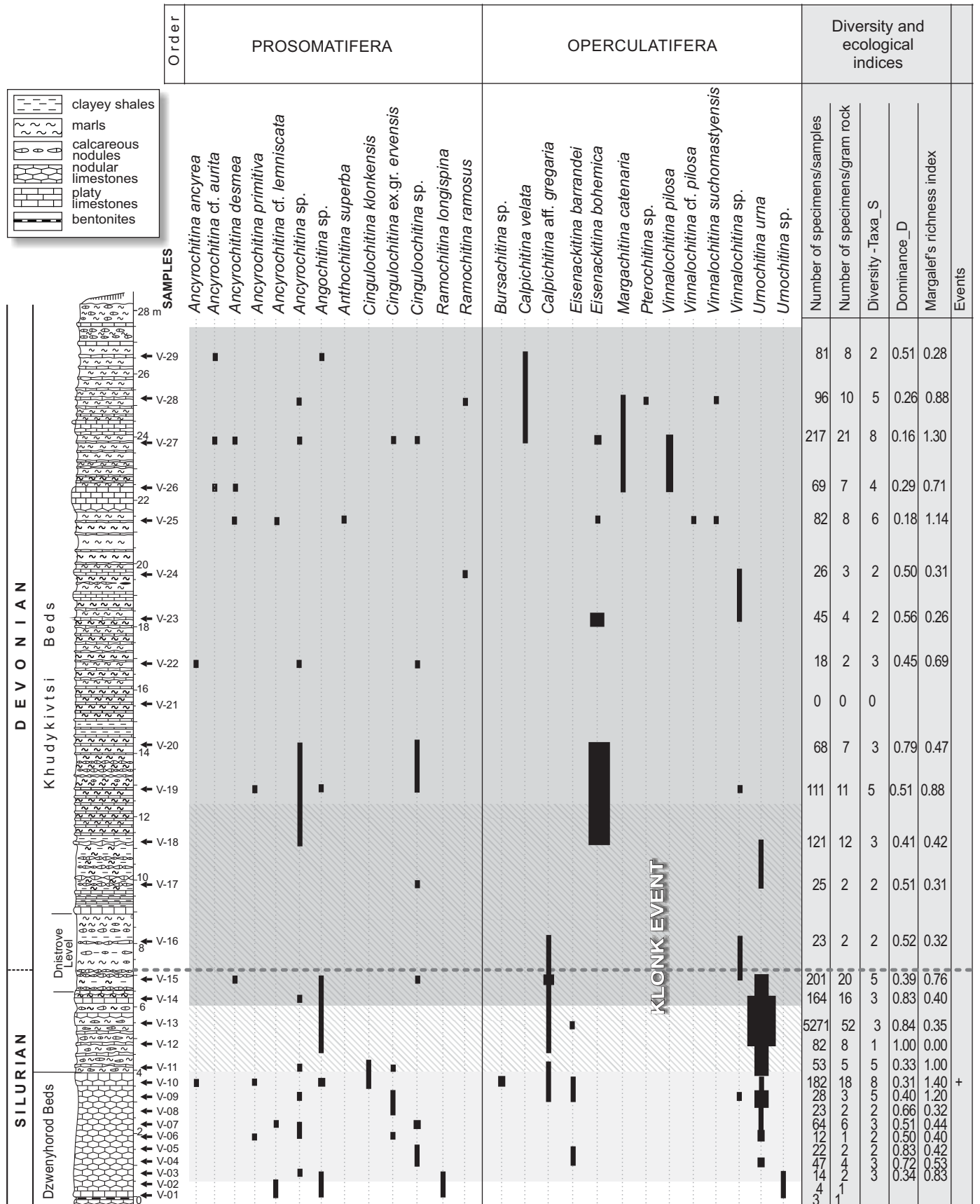
Fig. 21. Distribution of chitinozoans species, diversity, and ecological indices through the S–D boundary beds in the Dnistrove section. Shades of gray denote two slices of the SIDECIE.
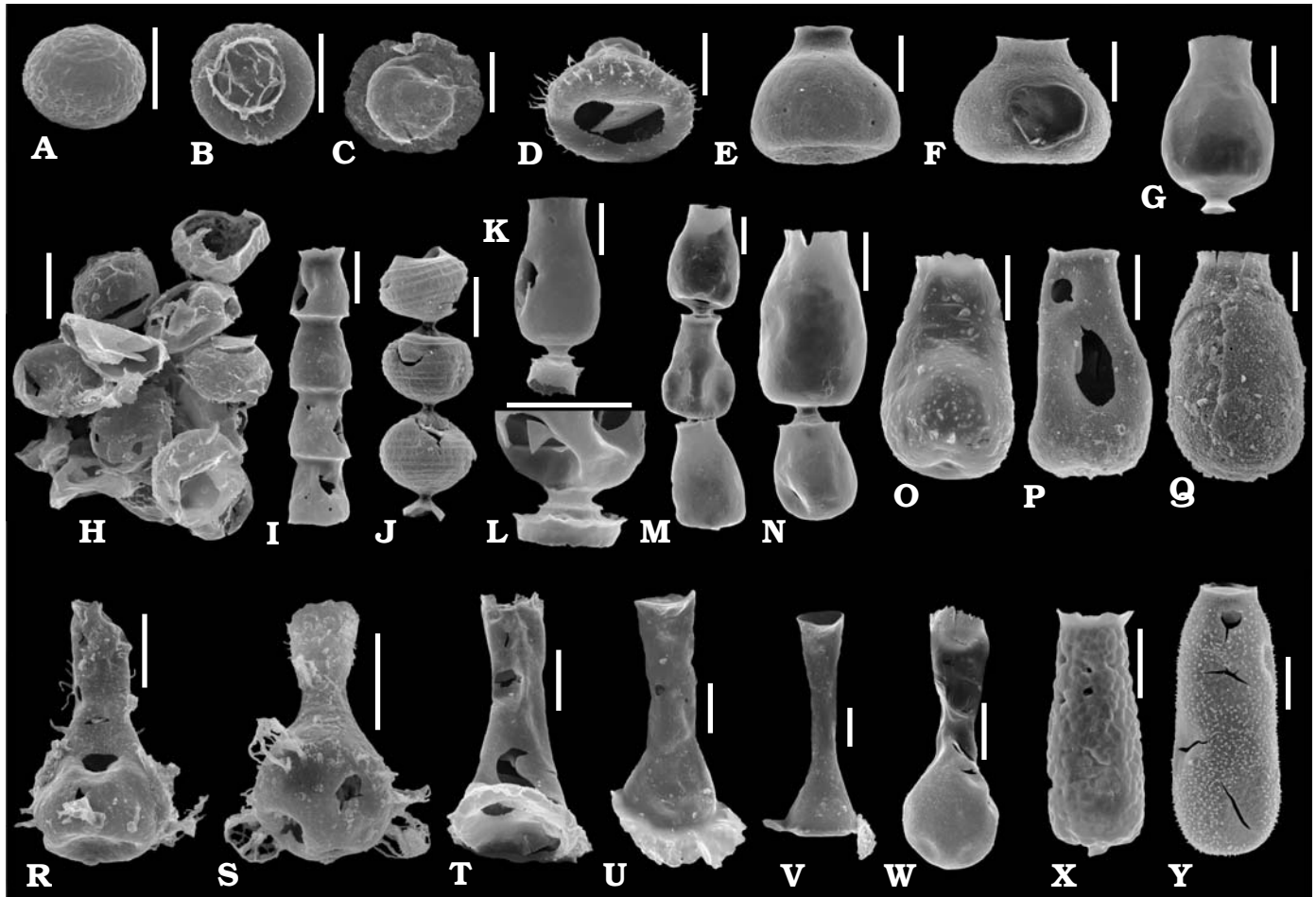
Fig. 22. Stereoscan microphotographs of selected Chitinozoa from the Dnistrove section. **A**, **H**. *Calpichitina* aff. *gregaria* Paris and Křiž, 1984. **A**. Single specimen in oblique lateral view, ZPAL Ch. 8/159S117, sample V-15. **H**. Vesicles aggregated in cluster, ZPAL Ch. 8/161S101, sample V-13. **B**. *Calpichitina velata* (Wrona, 1980), ZPAL Ch 8/160S53, sample V-27. **C**. *Pterochitina* sp., ZPAL Ch. 8/152S099, sample V-28. **D**. *Vinnalochitina pilosa* (Wrona, 1980), ZPAL Ch 8/159S054, sample V-27. **E–F**. *Vinnalochitina* cf. *suchomastyensis* Paris and Laufeld, 1981. **E**. ZPAL Ch 8/152S054, sample V-25. **F**. ZPAL Ch 8/152S107, sample V-27. **G**, **K–N**. *Urnochitina urna* (Eisenack, 1934). **G**. ZPAL Ch 8/160S55, sample V-09. **K**. Specimen with wide copula and operculum attached, ZPAL Ch 8/160S102, sample V-10. **L**. Detail of aboral part showing operculum attachment, ZPAL Ch 8/160S85, sample V-10. **M**. Chain of three closely similar vesicles, ZPAL Ch 8/161S112, sample V-13. **N**. Two marginal vesicles of a chain, showing small terminal vesicle, ZPAL Ch 8/161S104, sample V-15. **I**. *Cingulochitina* ex. gr. *ervensis* (Paris, 1979), Chain of four vesicles, ZPAL Ch 8/159S094, sample V-27. **J**. *Margachitina catenaria* Obut, 1973, Chain of three vesicles, ZPAL Ch 8/159S094, sample V-27. **O–Q**. *Eisenackitina barrandei* Paris and Křiž, 1984. **O**. ZPAL Ch 8/161S001, sample V-04. **P**. ZPAL Ch 8/152S017, sample V-05. **Q**. ZPAL Ch 8/152S058, sample V-13. **R**. *Ramochitina* cf. *longispina* (Wrona, 1980), ZPAL Ch 8/172S077, sample V-03. **S**. *Ancyrochitina* cf. *aurita* Wrona, 1980, ZPAL Ch 8/159Y02, sample V-27. **T–V**. *Anthochitina* ex. gr. *superba* Eisenack, 1971. **T**. ZPAL Ch 8/152S056, sample V-25. **U**. ZPAL Ch 8/159S042, sample V-25. **V**. ZPAL Ch 8/159S082, sample V-25. **W**. *Angochitina* sp., ZPAL Ch 8/159S160, sample V-13. **X**. *Eisenackitina* sp., ZPAL Ch 8/160S54, sample V-03. **Y**. *Eisenackitina bohemica* (Eisenack, 1934), ZPAL Ch 8/159S127, sample V-23. Scale bars 50 μm.

could reflect a cold water environment related to the cooling period preceding the S–D boundary event near the SIDECIE onset (see below, and Figs. 22, 23, and 25), rather than high energy hydrodynamic conditions. The abundant occurrence of the similarly structured vesicles of *Eisenackitina barrandei* and *E. bohemica* higher in the Klonk Event interval could partly have an analogous nature.

In the upper part of the section, in the SIDECIE slice, an abundant and diversified chitinozoan assemblage occurs again, dominated by *Ancyrochitina* and *Angochitina*. These are species of a fundamentally different group of Chitinozoa belonging to Prosomatifera, characterized by thin-walled

highly ornamented vesicles, with spines, ramified processes and vellum. This abundance could be the result of progressive warming during the Lochkovian in the area.

In summary, the distribution of chitinozoans at Dnistrove demonstrates specific dynamics across the major S–D isotopic perturbation (see also Paris and Grahn 1996), comparable only in part with the other pelagic and benthic groups analysed above (Fig. 23).

Other groups.—The S–D transition in Podolia is characterized overall by a slight diversity drop in the impoverished organic-walled microphytoplankton, by contrast with the di-
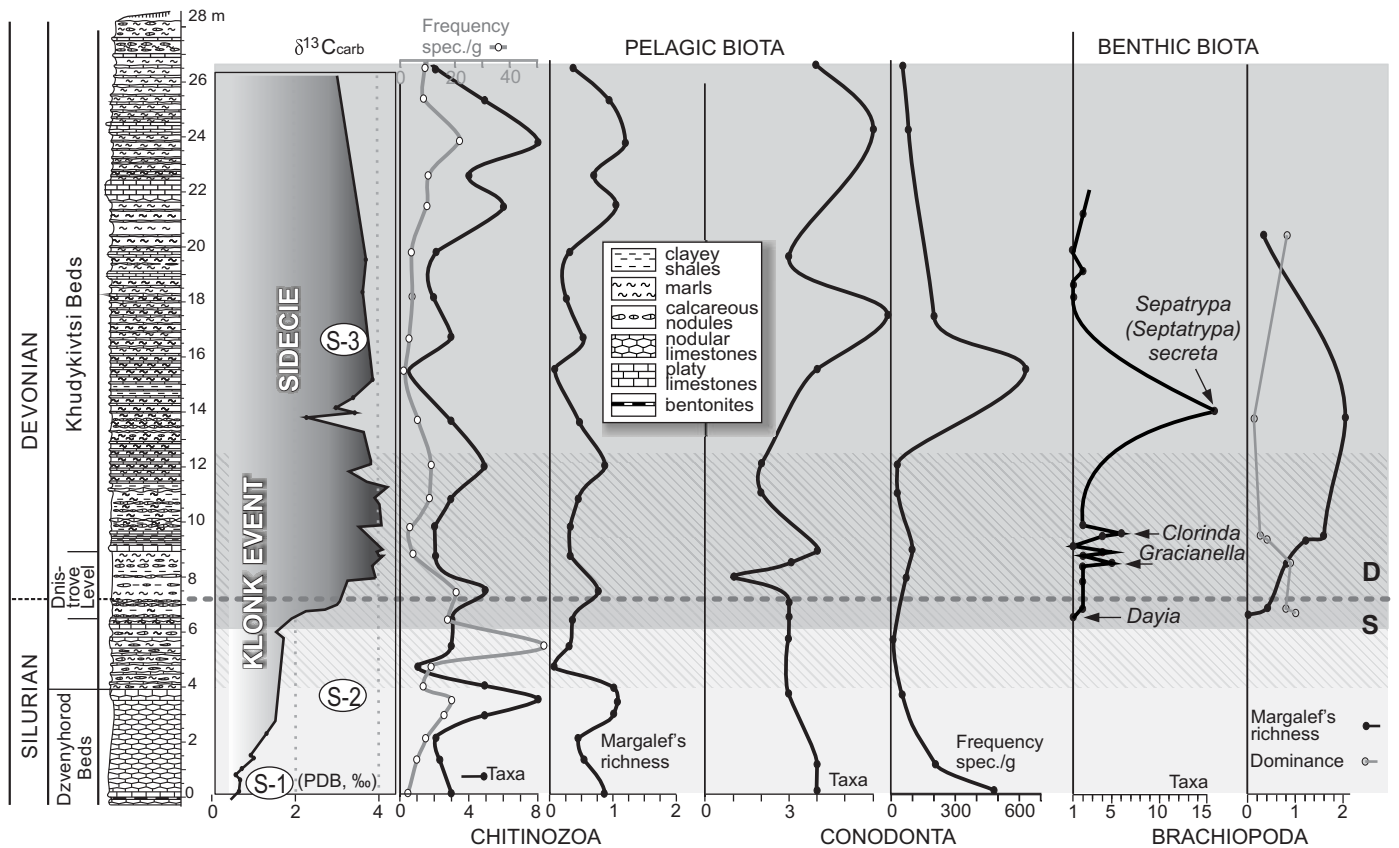
Fig. 23. Faunal dynamics through the Klonk Event and S–D transition carbon isotope excursion (SIDECIE) at Dnistrove. Shades of gray denote two slices of the SIDECIE.

verse older Silurian (Wenlock–Ludlow) acritarch-chlorophyte (prasinophyte) assemblages (see Le Hérissé et al. 2009: fig. 8). In the Dnistrove Level (Fig. 4), palynomorphs in four samples are poorly preserved in dark shaly lithologies due to pervasive oxidation processes, and only the floras from limestone layers are crudely recognizable (Paweł Filipiak, personal communication 2011). Together with infrequent acritarchs, leiospheres and miospores (*Apiculiretusispora*?), tubular remains with pseudo-cellular cuticles of an enigmatic land plant(?) group Nematophytales (*Laevitubuls*? and *Porcatitubulus*) are commonly recovered. The clearly mixed marine-terrestrial character differentiates the Podolian palynofacies from the coeval, more offshore Bohemian assemblage, with acritarchs, leiospheres and mazueloids (Brocke et al. 2006). Large prasinophytes are widespread in both successions (see SOM 6), and probably indicate episodic eutrophic and/or hypoxic conditions, as known e.g., from the Frasnian–Famennian mass extinction boundary beds (Filipiak 2002; see also summary in Le Hérissé et al. 2009).

From a faunal viewpoint, not very frequent trilobites (*Proetus*, *Acaste*, and *Calymene*), brachiopods (atrypids, *Delthyris*, *Isorthis*, *Daya*, and *Zygospiraella*), bivalves and rugosan horn corals are quoted from the uppermost Dzvenyhorod Beds (see lists in Nikiforova and Predtechensky 1968: fig. 29; Nikiforova et al. 1972; Nikiforova 1977; Koren et al. 1989). The topmost 1.6 m of the Silurian at Dnistrove are specifically

characterized by occurrences of crinoids, orthocone nautiloids, fistuliporid bryozoans, trilobites (*Proetus*, *Acastella*), suspension-feeding bivalves (stationary epifaunal *Actinopteria*, facultatively mobile infaunal *Lunulicardium* and *Dualina*), and ostracods (*Libumella*, *Kuresaaria*). In particular, the remnants of the large free-floating crinoid *Scyphocrinites elegans*, including bulb-shaped loboliths, are very common, forming several lenticular and locally graded bioclastic intercalations, up to 10 cm thick (see Fig. 5G). This unique acme horizon is widely recognizable worldwide (e.g., Zhivkovich and Chekhovich 1986; Jahnke et al. 1989; Havlíček and Štorch 1990; Ferretti et al. 1998; Chlupáč and Hladil 2000; Vacek 2007; Lubeseder 2008; Verniers et al. 2008; Donovan and Lewis 2009; Valenzuela-Ríos and Liao 2012). Within the upper Dnistrove Level, a thin black shale horizon with abundant specimens of the guide graptolite *Monograptus uniformis angustidens* was found (Fig. 4; see Nikiforova 1977). Conversely, numerous large shells of nautiloid *Podolicoceras giganteum* are patchy distributed in a ca. 2 m interval thick around the system boundary.

Above the S–D boundary, in addition to common bioturbating infauna (Fig. 5E, F), the brachiopod *Septatrypa*- and *Sphaerirhynchia*-dominated faunas are accompanied by rather rare but ubiquitous crinoid ossicles, trilobites (*Acastella*), nautiloids (*Risoceras*), and occasionally also bivalves (*Actinopteria, Panenka, Mytyliarca*), gastropods (*Platyce-*

ras), corals (*Pachyfavosites*, solitary rugosan *Pseudomicro-plasma*), graptolites (*Linograptus*), bryozoans, ostracods (*Richina*), and tentaculitids.

Discussion

As stressed by many authors, the Silurian global biogeochemical perturbations were regularly associated with stepwise extinction events and restructurings, grouped "at the very beginning or even prior" to the major isotopic event (Munnecke et al. 2010: 301; see also Jeppsson 1997, 1998; Munnecke et al. 2003; Cramer and Saltzman 2007a, b; Loydell 2007; Calner 2008; Lehnert et al. 2010; Melchin et al. 2012: fig. 21.11; Molloy and Simpson 2012; Noble et al. 2012). In particular, Lehnert et al. (2010: 320) stated precisely for the Ireviken Event: "(…) faunal extinctions are connected to time intervals of warming before the establishment of more stable and cooler conditions during the main Sheinwoodian glacial". In fact, since the Jeppsson's (1990, 1997, 1998, 2005) model of oceanic episodes, cooling pulses and, at least in the Early Silurian, expanding ephemeral Gondwanan ice sheets are usually considered responsible for the ecosystem turning points (Lehnert et al. 2007a; Loydell 2007; Calner 2008; Žigaitė et al. 2010; Sadler et al. 2011; Giles 2012; Kozłowski and Sobień 2012; Melchin et al. 2012; Stanley 2012). Conversely, Retallack (2009) interpreted pedostratigraphic spikes (i.e., high-precipitation deep-calcic excursions) as correlative very closely with the Silurian carbon cycle disturbances, and corresponding to greenhouse episodes and sea-level highstands. If so, both the climatic and eustatic driving factors, associated with the biogeochemical signals, were probably quite complex, as shown for the Ireviken Event by Lehnert et al. (2010; see also Stanley 2012). For example, as stressed Kozłowski and Sobień (2012), a combination of glacioeustatic lowstand, gustiness and low-latitude aridity might have been critical for the aeolian Fe-dominated nutrient delivery and cyanobacterial blooming. Also Loydell (2007) regarded that intensified atmospheric circulation during icehouse intervals may have caused increased nutrient input via wind-blown dust, resulting finally in enhanced bioproductivity and benthic oxygen depletion.

Several authors (e.g., Wenzel and Joachimski 1996; Lehnert et al. 2007a; Calner 2008: Fig. 3; Žigaitė et al. 2010) explicitly postulated that the Silurian eustatic cyclicity was glacially driven (see a glacioeustatic scenario of the Lau Event; Fig. 4 in Lehnert et al. 2007a), and this assertion is extended lastly to Early and Middle Devonian (Elrick et al. 2009; see also Miller et al. 2011). However, as noted by Munnecke et al. (2010: 404, 407): "In general there seems to be a clear mismatch between $\delta^{18}O$ data and sea-level reconstructions based on sequence stratigraphy" and "up until now there is no consensus on Silurian climate development, especially for the post-Llandovery". In addition, Nardin et al. (2011) stressed the climatic impact of changes in plate motion and weathering

of fresh volcanic rocks, which resulted in a long-term warming trend from the major late Telychian icehouse (Cancañiri glaciation; Brand et al. 2006) to the Middle Devonian.

On the other hand, the stressed diachroneity of biotic and isotopic signals, influenced by the pattern in the best-known Ireviken Event, is an overestimation as the Silurian paradigma. Sadler (2012: 5) acknowledged clearly that "there is no standard numerical method for picking boundaries and peaks of Silurian isotope excursions". More importantly, as confirmed also by the Podolian record, the extinction steps are largely placed in the rising limb of the $\delta^{13}C$ curves (see Figs. 24, 25), and thus linked to an initial shift in the carbon cycling, but not with its background (= steady) biogeochemical state. There is little doubt that these ecological turning points were driven by an accelerating disequilibrium of fragile habitat parameters and suddenly increasing environmental stress (see e.g., Urbanek 1993), coarsely only mirrored by the measured ^{13}C enrichment trends.

Significance of the Podolian succession.—Both global isotopic events are unquestionably paired with $\delta^{18}O_{carb}$ positive excursions in the Podolian sections (Figs. 5A and 7), confirmed by heavy $\delta^{18}O_{phosp}$ values in Joachimski et al. (2009) and Lehnert et al. (2010), and therefore to largely declining near-surface temperatures in the marine basin (Figs. 24, 25). Rapid climate perturbations, maybe forced by volcanic activity (Lehnert et al. 2010), are also partly supported by the $\Delta^{13}C$ secular patterns, suggestive of cooling episodes promoted by falling levels of atmospheric pCO_2, as recorded in negative $\Delta^{13}C$ shifts. This chemostratigraphical pattern is certainly traced only across the S–D transition. The lower-resolution data for the ESCIE are rather inconclusive but it seems to deny a dominant warming trend, as postulated from the North American $\Delta^{13}C$ record by Cramer and Saltzman (2007a). In fact, correlation of the $\delta^{18}O_{phosp}$ and $\delta^{18}O_{carb}$ value shifts and negative $\Delta^{13}C$ signals is to some extent vague (compare Fig. 6A with Bickert et al. 1997: fig. 3; Heath et al. 1998: fig. 2; Brand et al. 2006: fig. 12; Cramer and Saltzman 2007a: fig. 5; Lehnert et al. 2010: figs. 3, 4; see also Noble et al. 2012: fig. 5), and further studies are warranted.

Furthermore, the predicted environmental changes are expected to affect biota mostly in pelagic habitats (especially conodonts, graptolites, and trilobites; e.g., Kaljo et al. 1996; Lehnert et al. 2007b; Loydell 2007; Calner 2008; Sadler et al. 2011; ?also radiolarians, Noble et al. 2012), during times of oligotrophic photic-zone conditions and reduced primary production. Faunal responses in the both Podolian sections follow the above scenario only in part, as manifested especially by the conodont crisis of the Ireviken Event (?also by ostracod turnover; Abushik 1971), prior to the major isotopic/climatic ESCIE disturbance. This large-scale biotic crisis did not affect the relatively deeper-water brachiopods and chitinozoans (in taxonomic richness terms). Nevertheless, the Lilliput effect sensu Urbanek (1993), known among Gotland brachiopods during the Lau Event (Gustavsson et al. 2005), is a recognizable phenomenon also in the Ireviken-re-
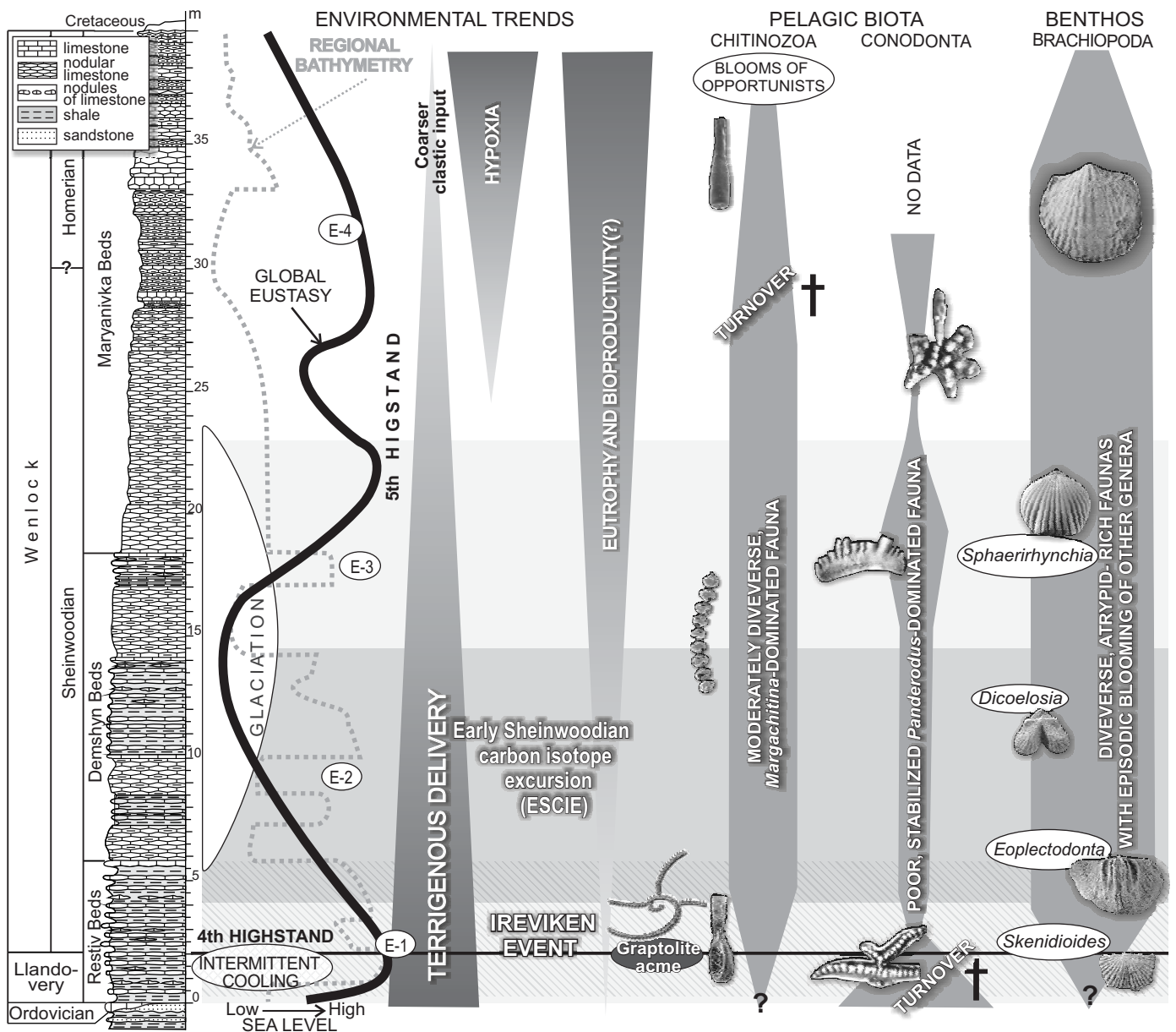
Fig. 24. Scheme of main environmental changes and faunal responses across the Ireviken Event and early Sheinwoodian carbon isotope excursion (ESCIE) in the Kytayhorod succession. Overall eustatic pattern and climatic events compiled from Johnson (2010: fig. 2; see other sea-level curves in Lüning et al. 2000: fig. 9; Cramer and Saltzman 2007: fig. 5; Brett et al. 2009: fig. 20; Ray and Butcher 2010: fig. 1) and Lehnert et al. (2010: figs. 1–3), respectively. Regional bathymetric curve modified from Koren et al. (1989: fig. 1). Note a distinctive discrepancy of the both sea-level patterns in some intervals, probably mostly controlled by regional epeirogenic activity in the Podolian shelf domain. Shades of gray denote three slices of the ESCIE.

lated brachiopod fauna from Kytayhorod. Thus, a regional distinctiveness of the Podolian epeiric domain seems to be manifested, especially in the negligible dynamics of specimen- and species-poor chitinozoan communities across the Ireviken Event and heavy carbon ESCIE interval.

The carbonate ecosystem evolution, from outer shelf toward reefal platform (Koren et al. 1989), was forced mostly by the regional epeirogeny regime paired with a generally regressive eustatic tendency, after the abrupt transgressive onlap inluenced by conspicuous eustatic sea-level rise in late Llandovery (the highstand 4 of Johnson 2006: fig. 1). This

synsedimentary tectonism in the shelf basin located near to the mobile Trans-European Suture is revealed by several discrepancies between global and regional sea-level changes, along with rather weak correlation with glacioeustatic effects, implied from the O-isotopic data (Fig. 24; see above). Remarkably, as revealed by the large-scale increase in the $^{87}Sr/^{86}Sr$ ratio (Brand et al. 2006; Gouldey et al. 2010), the perturbation in long-term carbon cycle and pronounced climatic changes due to increased chemical weathering were likely driven by the initial plate-terrane collisions (Salinic orogeny; see Goodman and Brett 1994; Ettensohn and Brett
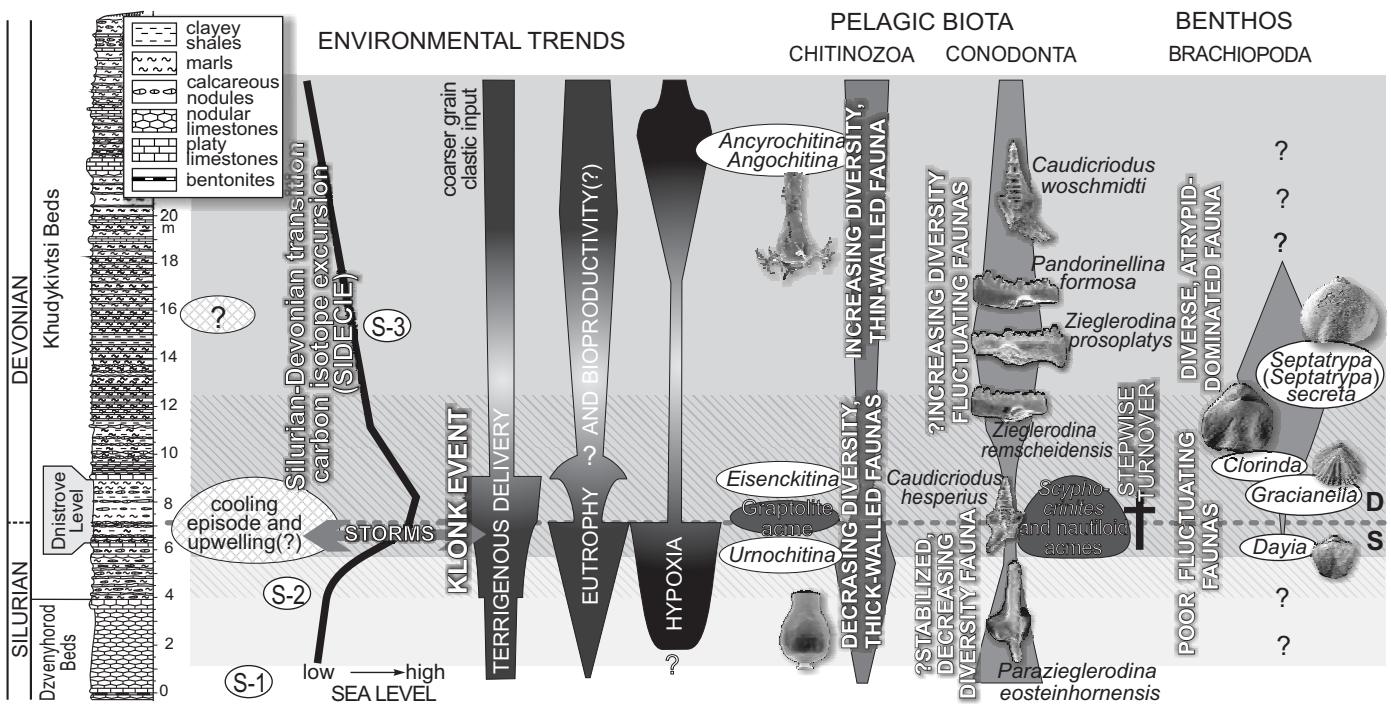
Fig. 25. Scheme of main environmental changes and faunal responses across the Klonk Event and the S–D transition carbon isotope excursion (SIDECIE) in the Dnistrove succession. Sea-level pattern after Walliser (1996: fig. 1; see other sea-level curves in Haq and Schutter 2008: fig. 2; Brett et al. 2009: fig. 20; Johnson 2010: fig. 1; Munnecke et al. 2010: fig. 2); for discussion of differently recorded eustasy, as well as climatic setting see Buggisch and Joachimski (2006) and Małkowski and Racki (2009). Shades of gray denote two slices of the SIDECIE.

1998; Brand et al. 2006; Cramer and Saltzman 2007a; Krawczyk et al. 2008).

The S–D boundary isotopic event appears to be more widely geographically recorded than previously assumed (see Małkowski et al. 2009: fig. 8). The SIDECIE, in various chemostratigraphical variants, in addition to new Laurentian and peri-Gondwanide sites (e.g., Suttner 2007; Kleffner et al. 2009), is recognizable in organic carbon also in the South China, Turkey, and Morocco (amplitude between ca. 3‰ and 8‰; Zhao et al. 2011), as well as in the whole-rock carbonate record in the Canadian Arctic islands (amplitude of ca. 3‰ and 3.5‰ in two sections; Märss et al. 1998), east Baltica (ca. 2‰ only; Kaljo et al. 2012) ; Central Urals (ca. 4‰ in shallow-water facies, but only 2.2‰ in pelagic micrites; Chekhovich et al. 1990), and Subpolar Urals (at least ca. 1.5‰ in shallow-water, coral-rich facies; Yureva et al. 2002).

During this S–D boundary turning point, a moderate faunal changeover, both in benthic and pelagic groups, is recognised in the Podolian epeiric sea exclusively at the very beginning of the prolonged ^{13}C-enriched SIDECIE timespan, possibly due to progressive dysoxia induced via enhanced bioproductivity by a climatic cooling (e.g., Wenzel and Joachimski 1996; Loydell 2007), an echo of the conspicuous mid-Pridoli glacial episode (Žigaitė et al. 2010: fig. 3). In Podolia, the pelagic graptolite acme and clay-dominated deposition of the Dnistrove Level were clearly linked with a deepening pulse across the S–D boundary (Fig. 25; compare Koren et al. 1989: fig. 105; Kaljo et al. 2012), interpreted as a

typical event for the "Bohemian facies" by Walliser (1996; see also Jeppsson 1998; Brett et al. 2009; Vacek et al. 2010, Valenzuela-Ríos and Liao 2012). This sea-level pattern was unexpectedly paired with "regressive" scyphocrinoid tempestite episodes (see Fig. 5G) and nautiloid profusion on the distal hemipelagic shelf that was recurrently punctuated by major storm action (compare Vacek 2007). A similar peculiar facies shift is commonly reported from strata deposited during the Klonk Event (Walliser 1996), e.g., from Central Urals (Zhivkovich and Chekhovich 1986), Sardinia (Ferretti et al. 1998), Bohemia (Hladil and Beroušek 1992; Vacek 2007), China (Jahnke et al. 1989), and Morocco (Lubeseder 2008). As advocated by Vacek et al. (2010: 270): "The facies change close to the S–D boundary and deposition of the *Scyphocrinites* H[orizon] might predominantly result from a biotic event unrelated to sea-level changes and local subsidence, rather than from sea-level rise/drop". In general terms, comparable biotic dynamics were established in many other localities from different continents (e.g., Havlíček and Štorch 1990; Feist et al. 1997; Kříž 1998; Chlupáč and Hladil 2000; Yureva et al. 2002; Barrick et al. 2005; Suttner 2007; Manda and Frýda 2010; Zhao et al. 2011; Valenzuela-Ríos and Liao 2012). In particular, the transient collapse of the Podolian carbonate factory ("carbonate crisis") corresponded to worldwide reef demise (Copper 2002b; Kiessling 2009), but without coeval loss in graptolite diversity (see Sadler et al. 2011).

On the other hand, the possible influence of eustatic sea-

level rise (?and nutrient-rich upwelling currents; Lubeseder 2008; Manda and Frýda 2010; Histon 2012) remains conjectural in spite of contrary, i.e., regressive bathymetric data from different regions (e.g., House and Ziegler 1997; Carrera et al. 2012), as summarized by Buggisch and Joachimski (2006) and Małkowski and Racki (2009). A tectonic control of the sea-level changes, in the collisional geodynamic setting (Acadian orogeny and a final closure of the Iapetus Ocean; see e.g., Goodman and Brett 1994; Copper 2002b; Krawczyk et al. 2008; Małkowski and Racki 2009; Narkiewicz et al. 2011), is expected also in the Klonk Event timespan. As manifested by thicknesses of the Přidoli–Lochkovian open-shelf successions (above 1 km; Nikiforova et al. 1972; Małkowski et al. 2009), a subsidence rate in the peri-Tornquist foreland basin (?due to dextral transtension) was very high (see Drygant 2003; Sliaupa et al. 2006). During the comparatively very warm timespan (Joachimski et al. 2009; Nardin et al. 2011), this regionally effective factor overrode a regressive, allegedly glacioeustatic tendency (see Žigaitė et al. 2010).

After this overall increased stress episode, the Early Devonian carbonate ecosystem quickly recovered in a shallowing setting. Diverse shelly benthos and pelagic communities temporarily flourished in the Podolian shelf domain (see Niki-forova et al. 1972), still being affected by episodic oxygenation and temperature changes.

Concluding remarks and implications

The Ireviken and Klonk biotic crises and related global isotope excursions, identified in Podolian sections, reveal opposite environmental and biotic trends, partly influenced by the later Caledonian geodynamic setting of the TESZ domain:

(i) The major Ireviken Event was marked by well-defined temporal changes in detrital input, redox states and, supposedly, bioproductivity, but without correlative relations with the δ^{13}C pattern (Fig. 24). Thus, the global biogeochemical disturbance was of minor ecosystem significance in the mostly epeirogeny-controlled sedimentary signature of this epeiric sea, as claimed also for other Laurussian sites in many other studies (see review in Cramer and Saltzman 2007a, b; Calner 2008; Munnecke et al. 2010).

(ii) The depositional and ecological signature of the Klonk Event exhibits some temporal links with the abrupt δ^{13}C shift toward the basal Devonian isotopic plateau, although effectively overprinted by the tectonically driven transgressive trend in the crucial interval (Fig. 25). Regardless of specific causes, the isotopic shift is reflected in the carbonate crisis paired with a tendency towards eutrophication, oxygen deficiency and temperature drop at the S–D boundary time. The features collectively point to the uniqueness of the Klonk Event among the Silurian global events, and some similarity already to Devonian transgressive/anoxic episodes (see Walli-

ser 1996; Buggisch and Joachimski 2006; Małkowski and Racki 2009).

(iii) In the light of the above results, advanced multidisciplinary studies to decipher complex interactions between Silurian ecosystems, forced by climatic, eustatic, tectonic and subsequent biogeochemical (i.e., carbon cycling) factors, and quickly evolving marine and terrestrial biospheres, in terms of effects of the accelerated terrestrialization (see Strother et al. 2010), are necessary in other palaeogeographical domains.

Acknowledgements

References

Abushik, A.F. [Abušik, A.F.] 1971. Ostracodes of the Silurian and Lower Devonian key section of Podolia [in Russian]. *In*: V.A. Ivanova (ed.), *Paleozojskie Ostrakody iz Opornyh Razrezov Evropejskoj Časti SSSR*, 7–133. Nauka, Moskva.

Alvarez, F. and Copper, P. 2002. Uncertain. *In*: R.L. Kaesler (ed.), *Treatise on Invertebrate Paleontology, Part H, Brachiopoda, Revised 4*, 1604–1614. Geological Survey of America and University of Kansas Press, Boulder.

Azmy, K., Veizer, J., Bassett, M.G., and Copper, P. 1998. Oxygen and carbon isotopic composition of Silurian brachiopods: implications for coeval seawater and glaciations. *Geological Society of America, Bulletin* 110: 1499–1512.

Baliński, A. 2010. First colour-patterned strophomenide brachiopod from the earliest Devonian of Podolia, Ukraine. *Acta Palaeontologica Polonica* 55: 695–700.

Baliński, A. 2012. The brachiopod succession through the Silurian–Devonian boundary beds at Dnistrove, Podolia, Ukraine. *Acta Palaeontologica Polonica* 57: 897–924.

Barrick, J.E., Meyer, B.D., and Ruppel, S.C. 2005. The Silurian–Devonian boundary and the Klonk Event in the Frame Formation, subsurface West Texas. *In*: J.E Barrick and H.R. Lane (eds.), A standing ovation: Papers on honour of Gilbert Klapper. *Bulletins of American Paleontology* 369: 105–122.

Bassett, M.G. 1984. Life strategies of Silurian brachiopods. *Special Papers in Palaeontology* 32: 237–263.

Berry, W.B.N., Wilde, P., and Quinby-Hunt, M.S. 1989. Paleozoic (Cambrian through Devonian) anoxitropic biotopes. *Palaeogeography, Palaeoclimatology, Palaeoecology* 74: 3–13.

Bickert, T., Pätzold, J., Samtleben, C., and Munnecke, A. 1997. Paleoenvironmental changes in the Silurian indicated by stable isotopes in brachiopod shells from Gotland, Sweden. *Geochimica et Cosmochimica Acta* 61: 2717–2730.

Boucot, A.J. 1975. Evolution and extinction rate controls. *Developments in Palaeontology and Stratigraphy* 1: 1–427.

Boucot, A.J. 1990. Silurian and pre-Upper Devonian bio-events. *In*: E.G. Kauffman and O.H. Walliser (eds.), Extinction events in Earth history. *Lecture Notes in Earth Sciences* 30: 125–132.

Boucot, A.J. 2005. Ecostratigraphy's basis, using Silurian and Devonian examples, with consideration of the biogeographic complication. *In*: E.A.M. Koutsoukos (ed.), *Applied Stratigraphy, Part II. Topics in Geobiology, 1, Vol. 23*, 55–71. Springer-Verlag, Berlin.

Brand, U., Azmy, K., and Veizer, J. 2006. Evaluation of the Salinic I tectonic, Cancañiri glacial and Ireviken biotic events: biochemostratigraphy of the Lower Silurian succession in the Niagara Gorge area, Canada and U.S.A. *Palaeogeography, Palaeoclimatology, Palaeoecology* 241: 192–213.

Brett, C.E. and Baird, G.C. 1995. Coordinated stasis and evolutionary ecology of Silurian to Middle Devonian faunas in the Appalachian Basin. *In*: D.H. Erwin and R.L. Anstey (eds.), *New Approaches to Speciation in the Fossil Record*, 285–315. Columbia University Press, New York.

Brett, C.E., Boucot, A.J., and Jones, B. 1993. Absolute depths of Silurian benthic assemblages. *Lethaia* 26: 25–40.

Brett, C.E., Ferretti, A., Histon, K., and Schönlaub, H.P. 2009. Silurian sequence stratigraphy of the Carnic Alps, Austria. *Palaeogeography, Palaeoclimatology, Palaeoecology* 279: 1–28.

Brocke, R., Fatka, O., and Wilde, V. 2006. Acritarchs and prasinophytes of the Silurian–Devonian GSSP (Klonk, Barrandian area, Czech Republic). *Bulletin of Geosciences* 81: 27–41.

Brumsack, H.J. 2006. The trace metal content of recent organic carbon-rich sediments: implications for Cretaceous black shale formation. *Palaeogeography, Palaeoclimatology, Palaeoecology* 232: 344–361.

Buggisch, W. and Joachimski, M.M. 2006. Carbon isotope stratigraphy of the Devonian of Central and Southern Europe. *Palaeogeography, Palaeoclimatology, Palaeoecology* 240: 68–88.

Calner, M. 2008. Silurian global events—at the tipping point of climate change. *In*: A.M.T. Elewa (ed.), *Mass Extinctions*, 21–58. Springer-Verlag, Heidelberg.

Calvert, S.E. and Pedersen, T.F. 2007. Elemental proxies for palaeoclimatic and palaeoceanographic variability in marine sediments: interpretation and application. *Developments in Marine Geology* 1: 567–644.

Carrera, M.G., Montoya, E., Rustán, J.J., and Halpern, K. 2012. Silurian–Devonian coral associations across a sequence stratigraphical boundary in the Argentine Precordillera. *Geological Journal* (published online).

Chekhovich, P.A., Zhivkovich, A.Y., Medvedovskaya, N.I., and Stepanova, N.A. 1990. Isotope reference points (for isotope chronostratigraphy) in Paleozoic sections of the Urals. *Doklady, Earth Science Sections* 313: 124–126.

Chlupáč, I. and Hladil, J. 2000. The global stratotype section and point of the Silurian–Devonian boundary. *Courier Forschunginstitut Senckenberg* 225: 1–8.

Cocks, L.R.M. 1970. Silurian brachiopods of the superfamily Plectambonitacea. *Bulletin of the British Museum (Natural History) Geology* 19: 139–203.

Copper, P. 2002a. Atrypida. *In*: R.L. Kaesler (ed.), *Treatise on Invertebrate Paleontology, Part H, Brachiopoda, Revised 4*, 1377–1474. Geological Survey of America and University of Kansas Press, Boulder.

Copper, P. 2002b. Silurian and Devonian reefs: 80 million years of greenhouse between two ice ages. *In*: W. Kiessling, E. Fluegel, and J. Golonka (eds.), Phanerozoic Reef Patterns. *SEPM Special Publication* 72: 181–238.

Copper, P. 2004. *Silurian (Late Llandovery–Ludlow) Atrypid Brachiopods from Gotland, Sweden, and the Welsh Borderlands, Great Britain*. 215 pp. NRC Research Press. Ottawa.

Corradini, C. and Corriga, M.G. 2012. A Přídolí–Lochkovian conodont zonation in Sardinia and the Carnic Alps: implications for a global zonation scheme. *Bulletin of Geosciences* 87: 635–650.

Cramer, B.D. and Saltzman, M.R. 2005. Sequestration of ^{12}C in the deep ocean during the early Wenlock (Silurian) positive carbon isotope excursion. *Palaeogeography, Palaeoclimatology, Palaeoecology* 219: 333–349.

Cramer, B.D. and Saltzman, M.R. 2007a. Early Silurian paired $\delta^{13}C_{carb}$ and $\delta^{13}C_{org}$ analyses from the Midcontinent of North America: implications for paleoceanography and paleoclimate. *Palaeogeography, Palaeoclimatology, Palaeoecology* 256: 195–203.

Cramer, B.S. and Saltzman, M.R. 2007b. Fluctuations in epeiric sea carbonate production during Silurian positive carbon isotope excursions: a review of proposed paleoceanographic models. *Palaeogeography, Palaeoceanography, Palaeoclimatology* 245: 37–45.

Cramer, B.D., Loydell, D.K., Samtleben, C., Munnecke, A., Kaljo, D., Männik, P., Martma, T., Jeppsson, L., Kleffner, M.A., Barrick, J.E., Johnson, C.A., Emsbo, P., Joachimski, M.M., Bickert, T., and Saltzman, M.R. 2010. Testing the limits of Paleozoic chronostratigraphical correlation via high-resolution (<500 k.y.) integrated conodont, graptolite, and carbon isotope ($\delta^{13}C_{carb}$) biochemostratigraphy across the Llandovery–Wenlock (Silurian) boundary: is a unified Phanerozoic time scale achievable? *Bulletin of the Geological Society of America* 122: 1700–1716.

Cramer, B.D., Brett, C.E., Melchin, M.J., Männik, P., Kleffner, M.A., Mclaughlin, P.I., Loydell, D.K., Munnecke, A., Jeppsson, L., Corradini, C., Brunton, F.R., and Saltzman, M.R. 2011a. Revised correlation of Silurian Provincial Series of North America with global and regional chronostratigraphical units and $\delta^{13}C_{carb}$ chemostratigraphy. *Lethaia* 44: 185–202.

Cramer, B.D., Munnecke, A., Schofield, D.I., Haase, K.M., and Haase-Schramm, A. 2011b. A revised $^{87}Sr/^{86}Sr$ curve for the Silurian: implications for global ocean chemistry and the Silurian timescale. *Journal of Geology* 119: 335–349.

Dattilo, B.F. 2004. A new angle on strophomenid palaeoecology: trace-fossil evidence of an escape response for the plectambonitid brachiopod *Sowerbyella rugosa* from a tempestite in the upper Ordovician Kope Formation (Edenian) of northern Kentucky. *Palaios* 19: 332–348.

Didyk, B.M., Simoneit, B.R.T., Brassell, S.C., and Eglinton, G. 1978. Organic geochemical indicators of palaeoenvironmental conditions of sedimentation. *Nature* 272: 216–222.

Donovan, S.K. and Lewis, D.N. 2009. The mid-Palaeozoic camerate crinoid *Scyphocrinites* Zenker in southwest England. *Bulletin of the Mizunami Fossil Museum* 35: 97–100.

Drygant, D.M. 1984. *Korrelâciâ i Konodonty Silurijskih-Nižnedevonskih Otloženij Volyno-Podolij*. 192 pp. Naukova Dumka, Kiev.

Drygant, D.M. 1993. Conodont colour as the indicator of the geological processes (Volyn-Podillia) [in Ukrainian with English abstract]. *Paleontologičeskij žurnal* 23: 35–37.

Drygant, D.M. 2000. Lower and Middle Paleozoic of the Volyn'-Podillya margin of the East-European Platform and Carpathian Foredeep [in Ukrainian]. *Naukovi zapysky Deržavnogo pryrodoznavčogo muzeû* 15: 24–129.

Drygant, D.M. 2003. About the problem of correlation and stratigraphical division of Lower Devonian deposits in the Volyn'-Podillya part of the East-European Platform [in Ukrainian with English summary]. *Proceedings of the State Natural History Museum (Naučnye Zapiski Gosudarstvennogo Prirodovedčeskogo Muzeâ)* 18: 195–208.

Drygant, D.M. 2010. *Devonian Conodonts from South-West Margin of the East European Platform (Volyn'-Podolian Ukraine)* [in Ukrainian]. 156 pp. Academperiodyka, Kyiv.

Drygant, D.M. and Szaniawski, H. 2009. Conodonts of the Silurian–Devonian boundary beds in Podolia, Ukraine. *Rendiconti della Societa Paleontologica Italiana* 3: 281–282.

Drygant, D.M. and Szaniawski H. 2012. Lochkovian conodonts from Podolia, Ukraine and their stratigraphic significance. *Acta Palaeontologica Polonica* 57: 833–861.

Elrick, M., Berkyová, S., Klapper, G., Sharp, Z., Joachimski, M., and Frýda, J. 2009. Stratigraphic and oxygen isotope evidence for My-scale glaciation driving eustasy in the Early–Middle Devonian greenhouse world. *Palaeogeography, Palaeoclimatology, Palaeoecology* 276: 170–181.

Erlfeldt, Å. 2006: Brachiopod faunal dynamics during the Silurian Ireviken

Event, Gotland, Sweden. *Examensarbete i geologi vid Lunds universitet* 199: 1–22.

Eriksson, M.E., Nilsson, E.K., and Jeppsson, L. 2009. Vertebrate extinctions and reorganizations during the Late Silurian Lau Event. *Geology* 37: 739–742.

Ettensohn, F.R. and Brett, C.E. 1998. Early Silurian condensed intervals, ironstones, and sequence stratigraphy in the Appalachian foreland basin. *In*: E. Landing and M.E. Johnson (eds.), Silurian Cycles—Linkages of Dynamic Stratigraphy with Atmospheric, Oceanic and Tectonic Changes. *New York State Museum Bulletin* 491: 89–143.

Fatka, O., Brocke, R., and Wilde, V. 2003. Organic-walled microfossils at the Silurian/Devonian boundary stratotype (Klonk near Suchomasty, Barrandian area, Czech Republic). *INSUGEO, Serie Correlación Geológica* 18: 125–128.

Feist, R., Ivanov, K.S., Sapelnikov, V.P., Ancigin, N.Y.Y., Ivanov, S.N., Mizens, L.I., Bikbayev, A.Z., and Lubov, L.V. 1997. Correlations between the evolution of benthic faunal communities and convergent movements of lithospheric blocks from the Silurian to the Late Devonian in the mid-Palaeozoic Uralian basin. *Tectonophysics* 276: 301–311.

Ferretti, A., Corradini, C., and Serpagli E. 1998. The Silurian and Devonian sequence in SW Sardinia. *In*: E. Serpagli (ed.), Sardinia Guide-book, ECOS VII. *Giornale di Geologia* 60 (Special Issue): 57–61.

Filipiak, P. 2002. Palynofacies around the Frasnian/Famennian boundary in the Holy Cross Mountains, southern Poland. *Palaeogeography, Palaeoclimatology, Palaeoecology* 181: 313–324.

Fürsich, F.T. and Hurst, J.M. 1974. Environmental factors determining the distributions of brachiopods. *Palaeontology* 17: 879–900.

Fürsich, F.T. and Hurst, J.M. 1981. Autecology of the Silurian brachiopod *Sphaerirhynchia wilsoni. Journal of Paleontology* 55: 805–809.

Gelsthorpe, D.N. 2004. Microplankton changes through the early Silurian Ireviken extinction event on Gotland, Sweden. *Review of Palaeobotany and Palynology* 130: 89–103.

Giles, P.S. 2012. Low-latitude Ordovician to Triassic brachiopod habitat temperatures (BHTs) determined from $\delta^{18}O$ [brachiopod calcite]: a cold hard look at ice-house tropical oceans. *Palaeogeography, Palaeoclimatology, Palaeoecology* 317–318: 134–152.

Goodman, W.M. and Brett, C.E. 1994. Roles of eustasy and tectonics in development of Silurian stratigraphic architecfure of the Appalachian foreland basin. *In*: J.M. Dennison and F.R. Ettensohn (eds.), Tectonic and Eustatic Controls on Sedimentary Cycles. *Society for Sedimentary Geology, Concepts in Sedimentology and Paleontology* 4: 147–169.

Gouldey, J.C., Saltzman, M.R., Young, S.A., and Kaljo, D. 2010. Strontium and carbon isotope stratigraphy of the Llandovery (Early Silurian): implications for tectonics and weathering. *Palaeogeography, Palaeoclimatology, Palaeoecology* 296: 264–275.

Grahn, Y. and Paris, F. 2011. Emergence, biodiversification and extinction of the chitinozoan grup. *Geological Magazine* 148: 226–236.

Gritsenko, V.P., Istchenko, A.A., Konstantinenko, L.I., and Tsegelnjuk, P.D. 1999. Animal and plant communities of Podolia. *In:* A.J. Boucot and J.D. Lawson (eds.), *Paleocommunities—A Case Study from the Silurian and Lower Devonian*, 462–487. Cambridge University Press, Cambridge.

Gustavsson, L., Calner, M., and Jeppsson, L. 2005. Brachiopod biodiversity changes during the Late Silurian Lau Event, Gotland, Sweden: *In*: D.A.T. Harper, S.L. Long, and M. McCorry (eds.), *Fifth International Brachiopod Congress, 2005, Abstracts*, 40. University of Copenhagen, Copenhagen.

Haq, B.U. and Schutter, S.R. 2008. A chronology of Paleozoic sea-level changes. *Science* 322: 64–68.

Hammer, Ø., Harper, D.A.T., and Ryan, P.D. 2001. PAST: Paleontological statistics software package for education and data analysis. *Palaeontologia Electronica* 4: 1–9.

Havlíček, V. and Štorch, P. 1990. Silurian brachiopods and benthic communities in the Prague Basin (Czechoslovakia). *Rozpravy Ústředniho ústavu geologického* 48: 1–275.

Heath, R.J., Brenchley, P.J., and Marshall, J.D. 1998. Early Silurian carbon and oxygen stable-isotope stratigraphy of Estonia: implications for climatic change. *In*: E. Landing and M.E. Johnson (eds.), Silurian Cycles—Linkages of Dynamic Stratigraphy with Atmospheric, Oceanic and Tectonic Changes. *New York State Museum Bulletin* 491: 313–327.

Hints, O., Killing, M., Männik, P., and Nestor, V. 2006. Frequency patterns of chitinozoans, scolecodonts, and conodonts in the upper Llandovery and lower Wenlock of the Paatsalu core, western Estonia. *Proceedings of the Estonian Academy of Sciences* 55: 128–155.

Histon, K. 2012. Paleoenvironmental and temporal significance of variably colored Paleozoic orthoconic nautiloid cephalopod accumulations. *Palaeogeography, Palaeoclimatology, Palaeoecology* 367–368: 193–208.

Hladil, J. and Beroušek, P. 1992. Taphonomy and primary biotic associations of the Silurian–Devonian boundary stratotype: Klonk, Central Bohemia. *Scripta Facultatis Scientarium Naturalium Universitatis Masarykinae Brunensis, Geologica* 22: 87–96.

House, M.R. and Ziegler, W. (eds.) 1997. On sea-level fluctuations in the Devonian. *Courier Forchungsinstitut Senkenberg* 199: 1–146.

Huff, W.D., Bergström, S.M., and Kolata, D.R. 2000. Silurian K-bentonites of the Dnestr Basin, Podolia, Ukraine. *Journal of the Geological Society, London* 157: 493–504.

Hurst, J.M. 1975. Wenlock carbonate, level bottom, brachiopod-dominated communities from Wales and the Welsh Borderland. *Palaeogeography, Palaeoclimatology, Palaeoecology* 17: 227–255.

Ischenko, A.A. [Iŝenko, A.A.] 1976. Paleoecological characteristic of Silurian and Early Devonian floras of Podolia [in Ukrainian]. *Geologičnij žurnal* 36: 126–130.

Ischenko, A.A. [Iŝenko, A.A.] 1985. *Silurijskie Vodorosli Podolii*. 116 pp. Naukova Dumka, Kiev.

Jahnke, H., Shi, Y., and Haude, R. 1989. The Silurian–Devonian boundary strata and the Early Devonian of the Shidian–Baoshan area (W. Yunnan, China). *Courier Forschungsinstitut Senckenberg* 110: 137–193.

Jenkyns, H.C. 2010. Geochemistry of oceanic anoxic events. *Geochemistry Geophysics Geosystems* 11: Q03004.

Jeppsson, L. 1990. An oceanic model for lithological and faunal changes tested on the Silurian record. *Journal of the Geological Society, London* 147: 663–667.

Jeppsson, L. 1997. The anatomy of the Mid–Early Silurian Ireviken Event and a scenario for P–S events. *In:* C.E Brett and G.C. Baird (eds.), *Paleontological Events: Stratigraphical, Ecological, and Evolutionary Implications*, 451–492. Columbia University Press, New York.

Jeppsson, L. 1998. Silurian oceanic events: summary of general characteristics. *In*: E. Landing and M.E. Johnson (eds.), Silurian Cycles—Linkages of Dynamic Stratigraphy with Atmospheric, Oceanic and Tectonic Changes. *New York State Museum Bulletin* 491: 239–257.

Jeppsson, L. 2005. Oceanic and climatic cycles. *In*: M.E. Eriksson and M. Calner (eds.), The Dynamic Silurian Earth, Subcommision on Silurian Stratigraphy Field Meeting 2005, Field Guide and Abstracts. *Sveriges Geologiska Undersökning, Rapporter och Meddelanden* 121: 17–20.

Jeppsson, L., Calner, M., and Eriksson, M.E. 2005. Locality descriptions. *In*: M.E. Eriksson and M. Calner (eds.), The Dynamic Silurian Earth, Subcommision on Silurian Stratigraphy Field Meeting 2005, Field Guide and Abstracts. *Sveriges Geologiska Undersökning, Rapporter och Meddelanden* 121: 22–56.

Jin, J. and Copper, P. 1999. The deep-water brachiopod *Dicoelosia* King, 1850, from the Early Silurian tropical carbonate shelf of Anticosti Island, eastern Canada. *Journal of Paleontology* 73: 1042–1055.

Joachimski, M.M., Breisig, S., Buggisch, W., Talent, J.A., Mawson, R., Gereke, M., Morrow, J.R., Day, J., and Weddige, K. 2009. Devonian climate and reef evolution: insights from oxygen isotopes in apatite. *Earth and Planetary Science Letters* 284: 599–609.

Johnson, J.G., Boucot, A.J., and Murphy, M.A. 1976. Wenlockian and Ludlovian age brachiopods from the Roberts Mountains Formation of Central Nevada. *University of California Publications in Geological Sciences* 115: 1–102.

Johnson, M.E. 1987. Extent and bathymetry of North American platform seas in the Early Silurian. *Paleoceanography* 2: 185–211.

Johnson, M.E. 2006. Relationship of Silurian sea-level fluctuations to oceanic episodes and events. *GFF* 128: 115–121.

Johnson, M.E. 2010. Tracking Silurian eustasy: alignment of empirical evidence or pursuit of deductive reasoning? *Palaeogeography, Palaeoclimatology, Palaeoecology* 296: 276–284.

Jones, B. and Hurst, J.M. 1984. Autecology and distribution of Silurian brachiopod *Dubaria*. *Palaeontology* 27: 699–706.

Kaljo, D., Boucot, A.J., Corfield, R.M., Le Herisse, A., Koren'n, T.N., Kříž, J., Männik, P., Märss, T., Nestor, V., Shaver, R.H., Siveter, D.J., and Viira, V. 1996. Silurian bioevents. *In:* O.H. Walliser (ed.), *Global Events and Event Stratigraphy in the Phanerozoic*, 173–224. Springer-Verlag, Berlin.

Kaljo, D., Grytsenko, V., Martma, T., and Mõtus, M.A. 2007. Three global carbon isotope shifts in the Silurian of Podolia (Ukraine): stratigraphical implications. *Estonian Journal of Earth Sciences* 56: 205–220.

Kaljo, D., Martma, T., Grytsenko, V., Brazauskas, A., and Kaminskas, D. 2012. Přídolí carbon isotope trend and upper Silurian to lowermost Devonian chemostratigraphy based on sections in Podolia (Ukraine) and the East Baltic area. *Estonian Journal of Earth Sciences* 61: 162–180.

Kiessling, W. 2009. Geologic and biologic controls on the evolution of reefs. *Annual Review of Ecology, Evolution, and Systematics* 40: 173–192.

Kiipli, T., Kiipli, E., and Kaljo, D. 2010. Silurian sea level variations estimated using $SiO_2/A1_2O_3$ and $K_2O/A1_2O_3$ ratios in the Priekule drill core section, Latvia. *Bollettino della Societa Paleontologica Italiana* 49: 55–63.

Kleffner, M.A. and Barrick, J.E. 2010. Telychian–early Sheinwoodian (early Silurian) conodont-, graptolite-, chitinozoan- and event-based chronostratigraphy developed using the graphic correlation method. *Memoirs of the Association of Australasian Palaeontologists* 39: 191–210.

Kleffner, M.A., Barrick, J.E., Ebert, J.R., Matteson, D.K., and Karlsson, H.R. 2009. Conodont biostratigraphy, $\delta^{13}C$ chemostratigraphy, and recognition of Silurian/Devonian boundary in the Cherry Valley, New York region of the Appalachian Basin. *In:* D.J. Over (ed.), Conodont studies commemorating the 150th anniversary of the first conodont paper (Pander 1856) and the 40th anniversary of the Pander Society. *Palaeontographica Americana* 62: 57–73.

Koren, T.N., Abushik, A.F., Modzalevskaya, T.L., and Predtechensky, N.N. 1989. Podolia. *In:* C.H. Holland and M.G. Bassett (eds.), A global standard for the Silurian System. *National Museum of Wales, Geological Series* 9: 141–149.

Kozłowski, R. 1929. Les Brachiopodes gothlandiens de la Podolie Polonaise. *Palaeontologia Polonica* 1: 1–254.

Kozłowski, W. and Sobień, K. 2012. Mid-Ludfordian coeval carbon isotope, natural gamma ray and magnetic susceptibility excursions in the Mielnik IG-1 borehole (Eastern Poland)—dustiness as a possible link between global climate and the Silurian carbon isotope record. *Palaeogeography, Palaeoclimatology, Palaeoecology* 339–341: 74–97.

Krawczyk, C.M., McCann, T., Cocks, L.R.M., England, R., McBride, J., and Wybraniec, S. 2008. Caledonian tectonics. *In:* T. McCann (ed.), *The Geology of Central Europe. Volume 1: Precambrian and Palaeozoic*, 303–381. Geological Society, London.

Krzemiński, W., Krzemińska, E., and Wojciechowski, D. 2010. Silurian synziphosurine horseshoe crab Pasternakevia revisited. *Acta Palaeontologica Polonica* 55: 133–139

Kříž, J. 1998. Recurrent Silurian–Lowest Devonian cephalopod limestones of Gondwanan Europe and Perunica. *In:* E. Landing and M.E. Johnson (eds.), Silurian Cycles—Linkages of Dynamic Stratigraphy with Atmospheric, Oceanic and Tectonic Changes. *New York State Museum Bulletin* 491: 183–198.

Kump, L.R. and Arthur, M.A. 1999. Interpreting carbon-isotope excursions: carbonates and organic matter. *Chemical Geology* 161: 181–198.

Kump, L.R., Arthur, M.A., Patzkowsky, M.E., Gibbs, M.T., Pinkus, D.S., and Sheehan, P.M. 1999. A weathering hypothesis for glaciation at high atmospheric pCO$_2$ during the Late Ordovician. *Palaeogeography, Palaeoclimatology, Palaeoecology* 152: 173–187.

Le Hérissé, A., Dorning, K.J., Mullins, G.L., and Wicander, R. 2009. Global patterns of organic-walled phytoplankton biodiversity during the late Silurian to earliest Devonian. *Palynology* 33: 25–75.

Lehnert, O., Eriksson, M.J., Calner, M., Joachimski, M., and Buggisch, W. 2007a. Concurrent sedimentary and isotopic indications for global climatic cooling in the Late Silurian. *Acta Palaeontologica Sinica* 46 (Supplement): 249–255.

Lehnert, O., Frýda, J., Buggisch, W., Munnecke, A., Nützel, A., Kříž, J., and Manda, Š. 2007b. $\delta^{13}C$ record across the Ludlow Lau Event: new data from mid palaeolatitudes of northern peri-Gondwana (Prague Basin, Czech Republic). *Palaeogeography, Palaeoclimatology, Palaeoecology* 245: 227–244.

Lehnert, O., Männik, P., Joachimski, M.M., Calner, M., and Frýda, J. 2010. Palaeoclimate perturbations before the Sheinwoodian glaciation: a trigger for extinctions during the "Ireviken Event". *Palaeogeography, Palaeoclimatology, Palaeoecology* 296: 320–331.

Lescinsky, H. 1995. The life orientation of concavo-convex brachiopods: overturning the paradigm. *Paleobiology* 21: 520–551.

Li, R.-Y. and Allen, T. 2008. Llandovery (Early Silurian) orthide brachiopod associations from Anticosti Island, eastern Canada. *Canadian Journal of Earth Sciences* 45: 189–201.

Loydell, D.K. 2007. Early Silurian positive $\delta^{13}C$ excursions and their relationship to glaciations, sea-level changes and extinction events. *Geological Journal* 42: 531–46.

Loydell, D.K. and Frýda, J. 2007. Carbon isotope stratigraphy of the upper Telychian and lower Sheinwoodian (Llandovery–Wenlock, Silurian) of the Banwy River section, Wales. *Geological Magazine* 144: 1015–1019.

Loydell, D.K. and Nestor, V. 2005. Integrated graptolite and chitinozoan biostratigraphy of the upper Telychian (Llandovery, Silurian) of the Ventspils D-3 core, Latvia. *Geological Magazine* 142: 369–376.

Lubeseder, S. 2008. Palaeozoic low-oxygen, high-latitude carbonates: Silurian and Lower Devonian nautiloid and scyphocrinoid limestones of the Anti-Atlas (Morocco). *Palaeogeography, Palaeoclimatology, Palaeoecology* 264: 195–209.

Lüning, S., Craig, J., Loydell, D.K., Storch, P., and Fitches, B. 2000. Lower Silurian "hot shales" in North Africa and Arabia: regional distribution and depositional model. *Earth-Science Reviews* 49: 121–200.

Łuczyński, P., Skompski, S., and Kozłowski, W. 2009. Sedimentary history of Upper Silurian biostromes of Podolia (Ukraine) based on stromatoporoid morphometry. *Palaeogeography, Palaeoclimatology, Palaeoecology* 271: 225–239.

Małkowski, K. and Racki, G. 2009. A global biogeochemical perturbation across the Silurian–Devonian boundary: ocean-continent-biosphere feedbacks. *Palaeogeography, Palaeoclimatology, Palaeoecology* 276: 244–254.

Małkowski, K., Racki, G., Drygant, D., and Szaniawski, H. 2009. Carbon isotope stratigraphy across the Silurian–Devonian transition in Podolia, Ukraine: evidence for a global biogeochemical perturbation. *Geological Magazine* 146: 674–689.

Manda, Š. and Frýda, J. 2010. Silurian–Devonian boundary events and their influence on cephalopod evolution: evolutionary significance of cephalopod egg size during mass extinctions. *Bulletin of Geosciences* 85: 513–540.

Manda, Š., Štorch, P., Slavík, L., Frýda, J., Kříž, J., and Tasáryová, Z. 2012. The graptolite, conodont and sedimentary record through the late Ludlow Kozlowskii Event (Silurian) in the shale-dominated succession of Bohemia. *Geological Magazine* 149: 507–531.

Märss, T., Caldwell, M., Gagnier, P.-Y., Goujet, D., Männik, P., Martma, T., and Wilson, M. 1998. Distribution of Silurian and Lower Devonian vertebrate microremains and conodonts in the Baillie-Hamilton and Cornwallis Island sections, Canadian Arctic. *Proceedings of the Estonian Academy of Sciences, Geology* 47: 51–76.

Martma, T., Brazauskas, A., Kaljo, D., Kaminskas, D., and Musteikis, P. 2005. The Wenlock–Ludlow carbon isotope trend in the Vidukle core, Lithuania, and its relations with oceanic events. *Geological Quarterly* 49: 223–234.

Mashkova, T.V. 1971. Zonal conodont assemblages from boundary beds of the Silurian and Devonian of Podolia [in Russian]. *In:* D.V. Nalivkin (ed.), *Granica Silura i Dievona i Biostratigrafâ Silura. Trudy III Mieždunarodnogo Simpozûma, t. I*, 157–164. Izdatielstvo Nauka, Leningrad.

Melchin, M.J. Sadler, P.M., Cramer, B.D., Cooper, R.A., Gradstein, F.M., and Hammer, O. 2012. The Silurian Period. *In:* F.M Gradstein, J.G.

Ogg, M. Schmitz, and G. Ogg (eds.), *The Geologic Time Scale 2012*, 525–558. Elsevier, Amsterdam.

Miller, K.G., Mountain, G.S., Wright, J.D., and Browning, J.V. 2011. A 180-million-year record of sea level and ice volume variations from continental margin and deep-sea isotopic records. *Oceanography* 24: 40–53.

Miller, M.A. 1996. Chitinozoa. *In*: J. Jansonius and D.C. MacGregor (eds.), *Palynology: Principles and Applications* 1: 307–336. American Association of Stratigraphical Palynologists Foundation, Salt Lake City.

Modzalevskaya, T.L. [Modzalevskaâ, T.L.] 1968. *Third International Symposium on Silurian–Devonian Bundary and Lower and Middle Devonian Stratigraphy. Atlas of Silurian and Early Devonian Fauna of Podolia* (appendix to the guide). 37 pls. Ministry of Geology of the USSR, All-Union Scientific-Research Geological Institute (VSEGEI), Leningrad.

Modzalevskaya, T.L. [Modzalevskaâ, T.L.] and Nikiforova, O.I. 1980. Ecologic-taphonomic analysis of the Wenclockian brachiopods of Podolia [in Russian]. *Ežegodnik Vsesoûznogo Paleontologičeskogo Obŝestva* 23: 159–169.

Molloy, P.D. and Simpson, A.J. 2012. An analysis of the Ireviken Event in the Boree Creek Formation, New South Wales, Australia. *In*: J.A. Talent (ed.), *Earth and Life, Part III, Global Biodiversity, Extinction Intervals and Biogeographic Perturbations Through Time*, 615–630. Springer-Verlag, Berlin.

Munnecke, A., Samtleben, C., and Bickert, T. 2003. The Ireviken Event in the lower Silurian of Gotland, Sweden—relation to similar Palaeozoic and Proterozoic events. *Palaeogeography, Palaeoclimatology, Palaeoecology* 195: 99–124.

Munnecke, A., Calner, M., Harper, D.A.T., and Servais, T. 2010. Ordovician and Silurian sea-water chemistry, sea level, and climate: a synopsis. *Palaeogeography, Palaeoclimatology, Palaeoecology* 296: 389–413.

Munnecke, A., Delabroye, A., Servais, T., Vandenbroucke, T.R.A., and Vecoli, M. 2012. Systematic occurrences of malformed (teratological) acritarchs in the run-up of Early Palaeozoic δ^{13}C isotope excursions. *Palaeogeography, Palaeoclimatology, Palaeoecology* 367–368: 137–146.

Nardin, E., Goddéris, Y., Donnadieu, Y., Le Hir, G., Blakey, R.C., Pucéat, E., and Aretz, M. 2011. Modeling the early Paleozoic long-term climatic trend. *Geological Society of America Bulletin* 123: 1181–1192.

Narkiewicz. M., Grad, M., Guterch. A., and Janik, T. 2011. Crustal seismic velocity structure of southern Poland: preserved memory of a pre-Devonian terrane accretion at the East European Platform margin. *Geological Magazine* 148: 191–210.

Nestor, V. 1994. Early Silurian chitinozoans of Estonia and North Latvia. *Academia* 4: 1–163.

Nestor, V., Einasto, R., and Loydell, D.K. 2002. Chitinozoan biostratigraphy and lithological characteristics of the Lower and Upper Visby boundary beds in the Ireviken 3 section, Northwest Gotland. *Proceedings of the Estonian Academy of Sciences, Geology* 51: 215–226.

Nikiforova, O.I. 1977. Podolia. *In*: A. Martinsson (ed.), The Silurian–Devonian Boundary. *IUGS Publication, Series A* 5: 52–64.

Nikiforova, O.I. and Predtechensky, N.N. 1968. *A Guide to the Geological Excursion on Silurian and Lower Devonian Deposits oof Podolia (Middle Dnestr River). Third Interenational Symposium On Silurian–Devonian Boundary and Lower and Middle Devonian Stratigraphy*. 58 pp. Ministry of Geology of the USSR, Leningrad.

Nikiforova, O.I., Predtechensky, N.N. [Predtečenskij, N.N], Abushik, A.F. [Abušik, A.F.], Ignatovich, M.M. [Ignatovič, M.M], Modzalevskaya, T.L. [Modzalevskaâ, T.L.], Berger, A.Y. [Berger, A.Â], Novoselova, L.S., and Burkov, Y.K [Burkov, Û.K.]. 1972. *Opornyj razrez Silura i nižnego Devona Podolii*. 258 pp. Izdatiel'stvo "Nauka", Leningrad.

Noble, P.J., Lenz, A.C., Holmden, C., Masiak, M., Zimmerman, M.K., Poulson, S.R., and Kozłowska, A. 2012. Isotope geochemistry and plankton response to the Ireviken (earliest Wenlock) and *Cyrtograptus lundgreni* events, Cape Phillips Formation, Arctic Canada. *In*: J.A. Talent (ed.), *Earth and Life, Part III, Global Biodiversity, Extinction Intervals and Biogeographic Perturbations Through Time*, 631–652. Springer-Verlag, Berlin.

Paleobiology Database 2012. Accessed on 10.07.2012. http://paleodb.org

Paris, F. and Grahn, Y. 1996. Chitinozoa of the Silurian–Devonian boundary sections in Podolia, Ukraine. *Palaeontology* 39: 629–649.

Paris, F., Winchester-Seeto, T., Boumendjel, K., and Grahn, Y. 2000. Toward a global biozonation of Devonian chitinozoans. *Courier Forschungsinstitut Senckenberg* 220: 39–55.

Peters, K.E., Walters, C.C., and Moldowan, J.M. 2005. *The Biomarker Guide. Biomarkers and Isotopes in Petroleum Exploration and Earth History. 2nd edition*. 1155 pp. Cambridge University Press, New York.

Porębska, E. 2005. Organic carbon isotope record and the state of mid-Palaeozoic ocean—example from the Gory Bardzkie (Sudetes, Gondwanan Europe). *In*: M.E. Eriksson and M. Calner (eds.), The Dynamic Silurian Earth, Subcommision on Silurian Stratigraphy Field Meeting 2005, Field Guide and Abstracts. *Sveriges Geologiska Undersökning, Rapporter och Meddelanden* 121: 87.

Porębska, E., Kozłowska-Dawidziuk, A., and Masiak, M. 2004. The *lundgreni* event in the Silurian of the East European Platform, Poland. *Palaeogeography, Palaeoclimatology, Palaeoecology* 213: 271–294.

Pujol, F., Berner, Z., and Stüben, D. 2006. Palaeoenvironmental changes at the Frasnian/Famennian boundary in key European sections: chemostratigraphical constraints. *Palaeogeography, Palaeoclimatology, Palaeoecology* 240: 120–145.

Ray, D. and Butcher, A. 2010. Sequence stratigraphy of the type Wenlock area (Silurian), England. *Bollettino della Società Paleontologica Italiana* 49: 47–54.

Racka, M., Marynowski, L., Filipiak, P., Sobstel, M., Pisarzowska, A., and Bond, D.P. 2010, Anoxic Annulata Events in the Late Famennian of the Holy Cross Mountains (Southern Poland): geochemical and palaeontological record: *Palaeogeography Palaeoclimatology Palaeoecology* 297: 549–575.

Retallack, G.J. 2009. Cambrian, Ordovician and Silurian pedostratigraphy and global events in Australia. *Australian Journal of Earth Sciences* 56: 571–586.

Ruban, D.A. 2011. Taxonomic diversity structure of Silurian crinoids: stability versus dynamism. *Annales de Paléontologie* 97: 87–98.

Rubel, M.P. 1977. Revision of Silurian Dayiacea (Brach.) from the North-East Baltic [in Russian]. *Eesti NSV Teaduste Akadeemia Toimetised (Keemia Geoloogia)* 26: 211–220.

Sadler, P.M. 2012. Integrating carbon isotope excursions into automated stratigraphic correlation: an example from the Silurian of Baltica. *Bulletin of Geosciences* 87: 681–694.

Sadler, P.M., Cooper, R.A., and Melchin, M.J. 2011. Sequencing the graptoloid clade: building a global diversity curve from local range charts, regional composites and global time-lines. *Proceedings of the Yorkshire Geological Society* 58: 329–343.

Sageman, B.B., Murphy, A.E., Werne, J.P., Ver Straeten, C.A., Hollander, D.J., and Lyons, T.W. 2003. A tale of shales: the relative roles of production, decomposition, and dilution in the accumulation of organic-rich strata, Middle–Upper Devonian, Appalachian basin. *Chemical Geology* 195: 229–273.

Saltzman, M.R. 2005. Phosphorus, nitrogen, and the redox evolution of the Paleozoic oceans. *Geology* 33: 573–576.

Schröder, S. and Grotzinger, J.P. 2007. Evidence for anoxia at the Ediacaran–Cambrian boundary: the record of redox-sensitive trace elements and rare earth elements in Oman. *Journal of the Geological Society, London* 164: 175–187.

Sindern, S, Warnsloh, J., Trautwein-Bruns, U., Chatziliadou, M., Becker, S., Yüceer, S., Hilgers, C., and Kramm, U. 2008. Geochemical composition of sedimentary rocks and imprint of hydrothermal fluid flow at the Variscan front—an example from the RWTH-1 well (Germany). *Zeitschrift der Deutschen Gesellschaft für Geowissenschaften* 159: 623–640.

Skompski, S., Łuczyński, P., Drygant, D., and Kozłowski, W. 2008. High-energy sedimentary events in lagoonal successions of the Upper Silurian of Podolia, Ukraine. *Facies* 54: 277–296.

Slavík, L., Carls, P., Hladil, J., and Koptíková, L. 2012. Subdivision of the

Lochkovian Stage based on conodont faunas from the stratotype area (Prague Synform, Czech Republic). *Geological Journal*: 47: 616–631.

Sliaupa, S., Fokin, P., Lazauskiene, J., and Stephenson, R.A. 2006. The Vendian–early Paleozoic sedimentary basins of the East European Craton. *In*: D.G. Gee and R.A Stephenson (eds.), European Lithosphere Dynamics. *Geological Society of London Memoirs* 32: 449–462.

Śliwiński, M.G., Whalen, M.T., Meyer, F.J., and Majs, F. 2012. Constraining clastic input controls on magnetic susceptibility and trace element anomalies during the Late Devonian *punctata* Event in the Western Canada Sedimentary Basin. *Terra Nova* 24: 301–309.

Stanley, S.M. 2012. Geobiology of the Phanerozoic. *In*: A.H. Knoll, D.E. Canfield, and K.O. Konhauser (eds.), *Fundamentals of Geobiology*, 403–424. Wiley-Blackwell, Oxford.

Štorch, P. 1995. Biotic crises and post-crisis recoveries recorded by graptolite faunas of the Barrandian area, Czech Republic. *Geolines* 3: 59–70.

Stricanne, L., Munnecke, A., and Pross, J. 2006. Assessing mechanisms of environmental change: palynological signals across the late Ludlow (Silurian) positive isotope excursion (δ^{13}C, δ^{18}O) on Gotland, Sweden. *Palaeogeography, Palaeoclimatology, Palaeoecology* 230: 1–31.

Strother, P.K., Servais, T., and Vecoli, M. 2010. The effects of terrestrialization on marine ecosystems: the fall of CO_2. *In*: M. Vecoli, G. Clément, and B. Meyer-Berthaud (eds.), The Terrestrialization Process: Modelling Complex Interactions at the Biosphere-Geosphere Interface. *Geological Society, London, Special Publications* 339: 37–48.

Suttner, T.J. 2007. Conodont stratigraphy, facies-related distribution patterns and stable isotopes (carbon and oxygen) of the Uppermost Silurian to Lower Devonian Seewarte section (Carnic Alps, Carinthia, Austria). *Abhandlungen der Geologischen Bundesanstalt* 59: 1–111.

Talent, J.A., Mawson, R., Andrew, A.S., Hamilton, P.J., and Whitford, D.J. 1993. Middle Palaeozoic extinction events; faunal and isotopic data. *Palaeogeography, Palaeoclimatology, Palaeoecology* 104: 139–152.

Taylor, S.R. and McLennan, S.M. 1985. *The Continental Crust: Its Composition and Evolution*. 312 pp. Blackwell, Oxford.

Tribovillard, N., Algeo, T.J., Lyons, T., and Riboulleau, A. 2006. Trace metals as paleoredox and paleoproductivity proxies: an update. *Chemical Geology* 232: 12–32.

Tsegelnyuk, P. 1976. Some Ordovician and Early Silurian graptolites of Podolia. *In*: D.L. Kaljo and T.N. Koren (eds.), *Graptolites and Stratigraphy*, 234–244. Academy of Sciences of Estonian SSR, Institute of Geology, Tallinn.

Tsegelnyuk, P., Gritsenko, V., Konstantinenko, L., Ishchenko, A., Abushik, A., Kadlets, N., Bogoyavlenskaya, Drygant, D., Zaika-Novatsky, K., Kadlets, N., Kiselev, G., and Sytova, V. 1983. *The Silurian of Podolia. The Guide to Excursion*. 224 pp. Naukova Dumka, Kiev.

Tucker, E.V. 1964. The ecology of the brachiopod *Dayia navicula* (J. de C. Sowerby). *Annals and Magazine of Natural History, Series 13* 7: 339–345.

Uchman, A., Drygant, D., Paszkowski, M., Porębski, S.J., and Turnau, E. 2004. Early Devonian trace fossils in marine to non-marine redbeds in Podolia, Ukraine: palaeoenvironmental implications. *Palaeogeography, Palaeoclimatology, Palaeoecology* 214: 67–83.

Urbanek, A. 1993. Biotic crises in the history of upper Silurian graptoloids: a palaeobiological model. *Historical Biology* 7: 29–50.

Vacek, F. 2007. Carbonate microfacies and depositional environments of the Silurian–Devonian boundary strata in the Barrandian area (Czech Republic). *Geologica Carpathica* 58: 497–510.

Vacek, F., Hladil, J., and Schnabl, P. 2010. Stratigraphic correlation potential of magnetic susceptibility and gamma-ray spectrometric variations in calciturbiditic facies (Silurian–Devonian boundary, Prague Synclinorium, Czech Republic). *Geologica Carpathica* 61: 257–272.

Valentine, J.L., Brock, G.A., and Molloy, P.D. 2003. Linguliformean brachiopod faunal turnover across the Ireviken Event (Silurian) at Boree Creek, central-western New South Wales, Australia. *Courier Forschungsinstitut Senckenberg* 242: 301–327.

Valenzuela-Ríos, J.I. and Liao, J.C. 2012. Color/facies changes and Global Events, a hoax? A case study from the Lochkovian (Lower Devonian) in the Spanish Central Pyrenees. *Palaeogeography, Palaeoclimatology, Palaeoecology* 367–368: 219–230.

Vecoli, M., Riboulleau, A., and Versteegh, G.J.M. 2009. Palynology, organic geochemistry and carbon isotope analysis of a latest Ordovician through Silurian clastic succession from borehole Tt1, Ghadamis Basin, southern Tunisia, North Africa: palaeoenvironmental interpretation. *Palaeogeography, Palaeoclimatology, Palaeoecology* 273: 378–394.

Verniers, J., Maletz, J., Kříž, J., Žigaitė, Ž., Paris, F., Schönlaub, H.P., and Wrona, R. 2008. Silurian: *In*: T. McCann (ed.), *The Geology of Central Europe. Volume 1: Precambrian and Palaeozoic*, 249–302. Geological Society, London.

Ver Straeten, C.A., Brett, C.E., and Sageman, B.B. 2011. Mudrock sequence stratigraphy: a multi-proxy (sedimentological, paleobiological and geochemical) approach, Devonian Appalachian Basin. *Palaeogeography, Palaeoclimatology, Palaeoecology* 304: 54–73.

Walliser, O.H. 1964. Conodonten des Silurs. *Abhandlungen des Hessisches Landesamtes für Bodenforschung* 41: 1–106.

Walliser, O.H. 1996. Global events in the Devonian and Carboniferous. *In*: O.H. Walliser (ed.), *Global Events and Event Stratigraphy in the Phanerozoic*, 225–250. Springer-Verlag, Berlin.

Watkins, R., Coorough, P.J., and Mayeret, P.S. 2000. The Silurian *Dicoelosia* communities: temporal stability within an Ecologic Evolutionary Unit. *Palaeogeography, Palaeoclimatology, Palaeoecology* 162: 225–237.

Wedepohl, K.H. 1970. Geochemische Daten von sedimentären Karbonaten und Karbonatgesteinen in ihrem faziellen und petrogenetischen Aussagewert. *Verhandlungen der geologischen Bundesanstalt* 4: 692–705.

Wedepohl, K.H. 1971. Environmental influences on the chemical composition of shales and clays. *In*: L.H. Ahrens, F. Press, S.K. Runcorn, and H.C. Urey (eds.), *Physics and Chemistry of the Earth*, 307–331. Pergamon Press, Oxford.

Wedepohl, K.H. 1991. The composition of the upper earth's crust and the natural cycles of selected metals. Metals in natural raw materials. Natural Resources. *In*: E. Merian (ed.), *Metals and Their Compounds in the Environment*, 3–17. Verlag Chemie (VCH), Weinheim.

Wenzel, B. and Joachimski, M.M. 1996. Carbon and oxygen isotopic composition of Silurian brachiopods (Gotland/Sweden): paleoceanographic implications. *Palaeogeography, Palaeoclimatology, Palaeoecology* 122: 143–166.

Wrona, R. 1980. Upper Silurian–Lower Devonian Chitinozoa from subsurface of southeastern Poland. *Palaeontologia Polonica* 41: 103–165.

Yureva, Z.P., Deulin Y.V., Beznosova, T.M., Tsyganko, V.S., Männik, P., and Martma, T. 2002. Calcareous sequences in the Silurian–Devonian boundary beds in the Timan-northern Ural region. *In*: N.P. Yushkin, V.S. Tsyganko, and P. Männik (eds.), *Geology of the Devonian System, Proceedings of the International Simposium, Syktyvkar, Komi Republic*, 321–324. Geoprint, Syktyvkar.

Zhang, N. 2001. Paleoecology and paleobiogeography of Wenlockian (Silurian) brachiopods of the Cape Phillips Formation from Baillie Hamilton Island, Arctic Canada. *Journal of the Czech Geological Society* 46: 95–104.

Zhang, S. and Barnes, C.R. 2002. Paleoecology of Llandovery conodonts, Anticosti Island, Quebec. *Palaeogeography, Palaeoclimatology, Palaeoecology* 180: 33–55.

Zhao, W.J., Wang, N.Z., Zhu, M., Mann, U., Herten, U., and Lücke, A. 2011. Geochemical stratigraphy and microvertebrate assemblage sequences across the Silurian/Devonian transition in South China. *Acta Geologica Sinica* 85: 340–353.

Zhivkovich, A.E. and Chekhovich, P.A. 1986. Carbonate turbidites in the base of the Devonian in central Urals. *Izvestiâ-Akademiâ Nauk SSSR, Seriâ Geologičeskaâ* 5: 72–80.

Ziegler, A.M., Cocks, L.R.M., and Bambach, R.K. 1968. The composition and structure of Lower Silurian marine communities. *Lethaia* 1: 1–27.

Žigaitė, Ž., Joachimski, M.M., Lehnert, O., and Brazauskas, A. 2010. δ^{18}O composition of conodont apatite indicates climatic cooling during the Middle Pridoli. *Palaeogeography, Palaeoclimatology, Palaeoecology* 294: 242–247.